IMMUNOREGULATION OF THE CENTRAL RESPONSE TO PERIPHERAL NERVE INJURY: MOTONEURON SURVIVAL AND RELEVANCE TO ALS

Deborah Olmstead Setter

Submitted to the faculty of the University Graduate School
in partial fulfillment of the requirements
for the degree
Doctor of Philosophy
in the Department of Anatomy and Cell Biology,
Indiana University

April 2017

Accepted by the Graduate Faculty, Indiana University, in partial fulfillment of the requirements for the degree of Doctor of Philosophy.

Kathryn J Jones, Ph.D., Chair

Michelle L. Block, Ph.D.

Doctoral Committee

Virginia M. Sanders, Ph.D.

March 8, 2017

Dale R. Sengelaub, Ph.D.

Xiao-Ming Xu, M.D., Ph.D.

DEDICATION

I dedicate this work to my parents, Patrick and Julia Olmstead, my sister, Jessica Olmstead, and my husband, Andrew Setter. Your love and support made this work possible.

ACKNOWLEDGEMENTS

I am grateful to all of the people who have helped me throughout my graduate education. First, I sincerely thank Dr. Kathryn Jones for being my mentor. I admire her zeal for science and devotion to education. I am most thankful for her helping me grow into a critical thinker and teaching the skills needed to become a successful scientist. I thank Dr. Virginia Sanders, our collaborator, for sharing her expertise in immunology and mentoring me throughout my training. I thank my advisory and research committee members Drs. Michelle Block, Dale Sengelaub, Fletcher White, and Xiao-Ming Xu, for their assistance with this project. I am grateful for their help with experimental design and their encouragement to think broadly about the significance of my work. I also thank the faculty and staff of the Anatomy and Cell Biology department, specifically, Drs. Joseph Bidwell and James Williams, and Kate McMillan, Marthe Augustin, and Tracy McWilliams.

I extend a special thank you to the people who got me started in the laboratory, Drs. Melissa Haulcomb, Rena Meadows, and Todd Brown, and Kate McMillan and Dick Batka. Dick and Melissa helped me overcome a steep learning curve to master facial nerve injury and many other scientific techniques. I thank Dr. Chandler Walker for his advice, guidance, and the time he has spent helping me. I sincerely thank Elizabeth Runge for her contributions to this work, especially in tackling the final leg of this journey. I thank Whitney Miller and Felicia Kennedy for their instrumental work in generating transgenic mice. I also thank Dr. Abhi Iyer in helping advance the neuroimmunological techniques in this study. I thank our research technicians Nicole Schartz, Brandon Brown, Kishan Shah, MeKenzie Hilsmeyer, Jessica Muldoon, Haley

Welch, and Malavika Rajasekharan for all of their contributions to this project. I also thank the LARC staff for doing an excellent job caring for the animals in this work.

I sincerely appreciate the help and guidance from the Medical Scientist Training Program, including Drs. Maureen Harrington, Raghu Mirmira, Rebecca Chan, Wade Clapp, and Jan Receveur. They have always encouraged me to dream big and never limit myself. I am grateful for their support on this career path. I also am deeply appreciative of the friendships I have made in the program, especially with Drs. Daniel Sassoon and Sherri Huang, and Donna Cerabona, Abass Conteh, Nick Race, Stefan Tarnawsky, and James Wodicka. I thank all of the past and present MSTP students for their mentorship and constant reminder of the bright future ahead.

I am endlessly grateful for my family, whose support and love for me made this work possible. I credit my parents, Patrick and Julia Olmstead, for making me who I am today. They taught me the value of hard work, but to also make time for fun along the way. I also thank my sister, Jessica Olmstead, who has always stood by my side. I am thankful for my wonderful grandparents, Pat and Patty Olmstead; spending time with them is a very special break from my studies. I also thank my husband, Andrew Setter, who has been my best friend throughout medical and graduate school. His cheerful attitude and support has helped me achieve my dreams.

Deborah Olmstead Setter

IMMUNOREGULATION OF THE CENTRAL RESPONSE TO PERIPHERAL NERVE INJURY: MOTONEURON SURVIVAL AND RELEVANCE TO ALS

Facial nerve axotomy (FNA) in immunodeficient mice causes significantly more facial motoneuron (FMN) loss relative to wild type (WT), indicating that the immune system is neuroprotective. Further studies reveal that both CD4+ T cells and interleukin-10 (IL-10) act centrally to promote neuronal survival after injury. This study first investigated the roles of IL-10 and CD4+ T cells in neuroprotection after axotomy.

CD4+ T cell-mediated neuroprotection requires centrally-produced IL-10, but the source of IL-10 is unknown. Using FNA on IL-10 reporter mice, immunohistochemistry was employed to identify the IL-10 source. Unexpectedly, axotomy induced astrocyte production of IL-10. To test if microglia- or astrocyte-specific IL-10 is needed for neuroprotection, cell-specific conditional knockout mice were generated. Neither knockout scenario affected FMN survival after FNA, suggesting that coordinated IL-10 production by both glia contributes to neuroprotection.

The effect of immune status on the post-FNA molecular response was studied to characterize CD4+ T cell-mediated neuroprotection. In the recombinase-activating gene-2 knockout (RAG-$2^{-/-}$) mouse model of immunodeficiency, glial microenvironment responses were significantly impaired. Reconstitution with CD4+ T cells restored glial activation to normal levels. Motoneuron regeneration responses remained unaffected by immune status. These findings indicate that CD4+ T cell-mediated neuroprotection after injury occurs indirectly via microenvironment regulation.

Immunodysregulation is evident in amyotrophic lateral sclerosis (ALS), and FMN survival after FNA is worse in the mutant superoxide dismutase (mSOD1) mouse model of ALS. Further experiments reveal that mSOD1 CD4+ T cells are neuroprotective in RAG-$2^{-/-}$ mice, whereas mSOD1 whole splenocytes (WS) are not. The third aim examined if the mSOD1 WS environment inhibits mSOD1 CD4+ T cell glial regulation after axotomy. Unexpectedly, both treatments were equally effective in promoting glial activation. Instead, mSOD1 WS treatment induced a motoneuron-specific death mechanism prevalent in ALS.

In conclusion, the peripheral immune system regulates the central glial microenvironment utilizing IL-10 to promote neuronal survival after axotomy. Astrocytes, specifically, may be responsible for transducing peripheral immune signals into microenvironment regulation. Additionally, the immune system in ALS may directly participate in disease pathology.

Kathryn J. Jones, Ph.D., Chair

TABLE OF CONTENTS

LIST OF TABLES

LIST OF FIGURES

LIST OF ABBREVIATIONS

ALDH1L1	Aldehyde dehydrogenase 1 family member L1
ALS	Amyotrophic lateral sclerosis
AMPA	α-amino-3-hydroxy-5-methyl-4-isoxazolepropionic acid
APCs	Antigen-presenting cells
APP	Amyloid precursor protein
Arg1	Arginase 1
Ask1	Apoptosis signal-regulating kinase 1
ATP	Adenosine triphosphate
Ax	Axotomized facial motor nucleus
BBB	Blood brain barrier
Bcl	B-cell lymphoma
BDNF	Brain-derived neurotrophic factor
C	Control facial motor nucleus
C3	Complement protein 3
C3R	Complement 3 receptor
CCL	C-C motif chemokine ligand
CCR	Chemokine receptor
CD	Cluster of differentiation
CNS	Central nervous system
CRISPR/Cas9	Clustered regularly interspaced short palindromic repeats/CRISPR-associated protein-9 nuclease
CSF	Cerebrospinal fluid
CX3CR1	CX3C chemokine receptor 1
DAPI	4',6-diamidino-2-phenylindole
Daxx	Death-associated protein 6
DISC	Death-induced signaling complex
DNA	Deoxyribose nucleic acid
doa	Days of age
dpo	Days post-operation
EAE	Experimental autoimmune encephalitis
EtOH	Ethanol
F	Forward
Fadd	Fas-associated protein with death domain
fALS	Familial amyotrophic lateral sclerosis
FasL	Fas ligand
FDH	10-formyltetrahydrofolate dehydrogenase
FITC	Fluorescein isothiocyanate
fl	Flox
FMN	Facial motoneuron
FMNuc	Facial motor nucleus
FNA	Facial nerve axotomy
Gap-43	Growth associated protein-43
Gapdh	Glyceraldehyde 3-phosphate dehydrogenase

GDNF	Glial cell-derived neurotrophic factor
GFAP	Glial fibrillary acidic protein
GFP	Green fluorescent protein
HIV	Human immunodeficiency virus
hpo	Hours post-operation
IFNγ	Interferon γ
IgG	Immunoglobulin G
IHC	Immunohistochemistry
IL	Interleukin
IL-6R	IL-6 receptor
iNOS	Inducible nitric oxide synthase
iPSCs	Induced pluripotent stem cells
IRF-8	Interferon-recognition factor 8
JAK	Janus kinase
LMN	Lower motoneuron
LPS	Lipopolysaccharide
MAC	Membrane attack complex
MCSF	Macrophage colony stimulating factor
MHCI	Major histocompatibility complex class I
MHCII	Major histocompatibility complex class II
miR	MicroRNA
MN	Motoneuron
MND	Motoneuron disease
mRNA	Messenger RNA
mSOD1	Mutant superoxide dismutase 1
NeuN	Neuronal nuclei
NF-κB	Nuclear factor kappa-light-chain-enhancer of activated B cells
NMJ	Neuromuscular junctions
nNos	Neuronal nitric oxide synthase
NO	Nitric oxide
P2X7	P2X purinoreceptor 7
P2Y1R	P2Y1 receptor
PACAP	Pituitary adenylate cyclase-activating polypeptide
PBS	Phosphate buffered saline
PBS-T	PBS with 0.1% Triton X-100
PCR	Polymerase chain reaction
PFA	Paraformaldehyde
PLP	Paraformaldehyde-lysine-periodate
PNS	Peripheral nervous system
PS1	Presenilin 1
Ptpn1	Protein tyrosine phosphatase, non-receptor type 1
qPCR	Quantitative polymerase chain reaction
R	Reverse
RAG	Recombinase activating gene
RER	Rough endoplasmic reticulum

RNA	Ribonucleic acid
RNA-seq	RNA-sequencing
RT	Room temperature
sALS	Spontaneous amyotrophic lateral sclerosis
scid	Severe combined immunodeficient
SEM	Standard error of the mean
siRNA	Silencing RNA
SOCS3	Suppressor of cytokine signaling 3
STAT	Signal transducer and activator of transcription
TAE	Tris-acetic acid-ethylenediaminetetraacetic acid
TCR	T cell receptor
Teffs	Effector T cells
TGFβ	Transforming growth factor β
Th	T helper
TLR	Toll-like receptor
TNFR	Tumor necrosis factor α receptor
TNFα	Tumor necrosis factor α
Tradd	Tumor necrosis factor receptor type 1-associated death domain
Traf2	TNF receptor-associated factor 2
Tregs	Regulatory T cells
UMN	Upper motoneuron
VL	Ventrolateral subnucleus of the facial motor nucleus
VM	Ventromedial subnucleus of the facial motor nucleus
wpo	Weeks post-operation
WS	Whole splenocytes
WT	Wild type

CHAPTER 1: INTRODUCTION

Approximately 20 million people in the United States suffer an impaired quality of life due to peripheral nerve injury or disease-induced peripheral neuropathy (Noble et al., 1998; Campbell, 2008; Ciaramitaro et al, 2010; Brannagan, 2012). Veterans, especially those who have served in the Middle East, have a higher incidence of traumatic peripheral nerve injury because body armor technology improvements have increased survivability of formerly lethal traumatic events (Campbell, 2008). Although the peripheral nervous system has robust regenerative capabilities, functional recovery after peripheral nerve injury is frequently suboptimal and presents a significant clinical problem (Campbell, 2008; Houdek & Shin, 2015). Therefore, studying factors that enhance peripheral nerve regeneration may reveal new therapeutic strategies that will improve functional outcomes and quality of life for patients with peripheral nerve injury and neuropathy.

Using the facial nerve axotomy (FNA) model, our laboratory discovered that the adaptive arm of the immune system is necessary for both preserving facial motoneuron (FMN) survival and promoting axon regeneration to target musculature (Serpe et al., 1999; Beahrs et al., 2010). Restoration of the immune system by adoptively transferring whole splenocytes into immunodeficient mice prior to FNA rescues FMN survival. This neuroprotection is specifically mediated by CD4+ T cells belonging to the interleukin-4-producing T helper 2 (Th2) subclass, which is associated with tissue repair and regeneration processes (Byram et al., 2003; Serpe et al., 2003; Wainwright et al., 2008; Kwon et al., 2014; Sadtler et al., 2016). The generation of neuroprotective CD4+ T cells requires two instances of antigen presentation, first by peripheral antigen presenting cells,

then by microglia in the central nervous system (Byram et al., 2004). In addition, reactive astrocytes produce chemokines that further attract T cells to the injured facial motor nucleus (Wainwright et al., 2009b; Wainwright et al., 2009c). Centrally-derived interleukin-10 (IL-10), an anti-inflammatory cytokine, is also necessary for CD4+ T cell-mediate neuroprotection (Xin et al., 2011). On the molecular level, motoneurons upregulate regeneration-associated gene expression, and robust glial activation occurs (Mesnard et al., 2010). Altogether, an orchestrated series of events is involved in CD4+ T cell-mediated neuroprotection, and this study seeks to further elucidate the mechanisms behind this process.

A form of peripheral neuropathy also occurs in amyotrophic lateral sclerosis (ALS), a fatal motoneuron (MN) disease. In ALS, disease pathology first results in loss of the neuromuscular junction, and subsequent axonal die-back leads to death of the MN cell body. Peripheral nerve transection mimics this target disconnection-induced MN death. When FNA is superimposed on the mutant superoxide dismutase 1 (mSOD1) mouse model of ALS, significantly greater FMN loss is observed relative to wild type (WT) (Mesnard et al., 2011). On the gene expression level, the MN regeneration response is intact, but glial activation is dysregulated, and promotion of a MN-specific cell death pathway is also evident (Mesnard et al., 2011; Haulcomb et al., 2014). Significant abnormalities in the immune system are observed in both ALS patients and the mSOD1 mouse model, leading our research group to suspect that immunodysregulation in ALS may contribute to disease pathology. To test this hypothesis, immunodeficient animals received adoptive transfer of either mSOD1 whole splenocytes (WS) or isolated mSOD1 CD4+ T cells and then were subjected to FNA. While neuroprotection was observed in

mSOD1 CD4+ T cell recipients, this rescue was not observed in mSOD1 WS recipients (Mesnard-Hoaglin et al., 2014). This finding suggests that a factor within the mSOD1 whole splenocyte milieu inhibits the neuroprotective effects of mSOD1 CD4+ T cells. A closer study of immune-mediated neuroprotection is warranted to determine how the mSOD1 immune system blocks CD4+ T cell neuroprotection, with the ultimate goal of finding a factor that can therapeutically manipulated to treat motoneuron disease.

To accomplish this goal, it is necessary to first gain a better understanding of both whole splenocyte and CD4+ T cell immune-mediated neuroprotection mechanisms within a normally functioning system, and then to use this information to characterize abnormalities within the ALS immune system. It is also necessary to identify the cellular source and kinetics of IL-10 production after FNA, as neuroprotection requires centrally-produced IL-10. *The central hypothesis of this work is that after nerve injury, activated CD4+ T cells induce microglia to produce IL-10, which orchestrates the generation of an anti-inflammatory, pro-repair microenvironment that ultimately promotes FMN survival, and these events are inhibited within the ALS peripheral immune system environment.*

This hypothesis was tested by the following aims:

Aim 1: Determine the source of neuroprotective IL-10 in the axotomized facial motor nucleus. *The hypothesis for this aim is that microglia are the source of neuroprotective IL-10 after FNA.* To test this hypothesis, a reporter mouse stain was used to identify histologically which cell types within the FMN produce IL-10, and cre/lox mouse strains were used to knockdown IL-10 production in a cell-specific manner. The histological analysis concluded that axotomy induced IL-10 expression in astrocytes, and neurons constitutively produce IL-10. IL-10 knockdown in microglia or astrocytes had no

detrimental effects on FMN survival after FNA. These findings suggest that neuroprotective IL-10 production after FNA comes from either a combined glial effort or neurons.

Aim 2: Characterize gene expression profile changes after facial nerve axotomy in immunodeficient and WT CD4+ T cell-reconstituted mice. *The hypothesis for this aim is that immunodeficiency will result in a dysregulated glial microenvironment response to FNA, and adoptive transfer of WT CD4+ T cells will restore microenvironment responses to normal levels*. qPCR analysis of the laser-captured facial motor nucleus after FNA from both immunodeficient and CD4+ T cell-reconstituted mice was performed. Overall, astrocyte, microglia, and inflammatory cytokine production after FNA was significantly impaired in immunodeficient mice, and adoptive transfer of CD4+ T cells rescued these responses to normal levels. These results lead us to conclude that CD4+ T cell-mediated neuroprotection occurs indirectly via regulation of the glial response to injury, not by direct actions on the motoneurons.

Aim 3: Analyze gene expression profile changes after facial nerve axotomy in mice immunoreconstituted with mSOD1 whole splenocytes or mSOD1 CD4+ T cells. *The hypothesis for this aim is that adoptive transfer of mSOD1 WS will result in a dysregulated glial microenvironment response to FNA, and adoptive transfer of mSOD1 CD4+ T cells will result in regulation of glial microenvironment responses to normal levels*. After adoptive transfer of lymphocytes and FNA, qPCR of the facial motor nucleus from the treatment groups was performed to compare gene expression profiles, similar to Aim 2. A WT WS recipient group was added as an additional control. Both mSOD1 WS and mSOD1 CD4+ T cell recipient groups exhibited comparable

microenvironment regulation responses, however, the mSOD1 WS treatment resulted in significantly greater expression of a MN-specific cell death pathway. These results suggest that the lack of neuroprotection by mSOD1 WS could be due to induction of MN death mechanisms or an alternative glial activation phenotype that is neurotoxic.

CHAPTER 2: LITERATURE REVIEW

2.1. Peripheral nerve injury

The nervous system is divided into central and peripheral components, with the central nervous system (CNS) including the brain, cerebellum, and spinal cord, and the peripheral nervous system (PNS) including the nerves and ganglia. Nerves can convey autonomic, sensory, and motor information to and from the CNS. MN within the CNS are specifically responsible for controlling skeletal muscle contractions.

MN can be subdivided into upper and lower motoneurons (UMN and LMN, respectively). UMN reside in the motor cortex of the brain and their axonal projections synapse on the dendrites and soma of LMN in the brainstem and spinal cord. The axons of LMN exit the CNS and are bundled into the cranial or spinal nerves of the PNS as they follow course to their target musculature.

Cutting of axons ("axotomy") can occur in both the CNS and PNS, and different injury responses are observed after axotomy in these two environments. Following CNS axotomy, such as in spinal cord injury, a suppressive microenvironment prevents axon regeneration and reconnection to target. Oligodendrocytes contribute to this suppression by secreting myelin-associated inhibitors of axonal growth. Additionally, astrocytes generate a glial scar composed of chondroitin sulfate proteoglycans that is a barrier to axonal growth (Huebner & Strittmatter, 2009). For these reasons, there is little functional recovery after CNS trauma. Conversely, the PNS has a robust regeneration response to axotomy. Wallerian degeneration, a process by which Schwann cells and peripheral monocytes clear the distal axonal debris, creates a conduit for the growing daughter axon. Robust activation of regeneration-associated genes is also observed after peripheral nerve

injury, not CNS injury (Bomze et al., 2001; Huebner & Strittmatter, 2009). Therefore, studying PNS regeneration processes will facilitate discovery of novel therapeutic strategies for patients suffering from nerve injury.

Full regeneration after a peripheral nerve injury depends on the survival of the cell body, regrowth of the axon, and reconnection to target. Axotomies can be classified by the severity of the damage administered, ranging from a crush injury (axonotmesis), after which full recovery is detected in a matter of days, to a complete transection injury (neurotmesis), in which no functional recovery is observed (Seddon, 1942; Sunderland, 1951). For the purposes of this study, a neurotmesis-grade axotomy was used. This model was selected because it elicits the greatest amount of MN death, facilitating study of factors that promote or inhibit MN survival after injury.

2.2. Facial nerve axotomy model

The mouse facial motor nucleus (FMNuc) is located in the ventral pons and is comprised of six subnuclei that form a horseshoe-like shape (Ashwell, 1982). Axon projections from FMN wrap dorsomedially around the abducens nucleus (forming a structure called the “genu”) before ventrolaterally exiting the brainstem as the facial nerve rostral to the facial motor nucleus. The facial nerve courses through the internal acoustic meatus and tympanic bulla bone, within which, the nerve to the stapedius muscle branches off, and the remainder of the nerve exits the stylomastoid foramen. The facial nerve then divides into its major branches: temporal, zygomatic, buccal, marginal mandibular, cervical, and posterior auricular. These branches innervate the facial, auricular, and platysma muscles of the head and neck.

The superficial nature and ease of access to the facial nerve as it exits the stylomastoid foramen permits selective injury to the nerve with minimal damage to adjacent tissues. Additionally, examination of the FMN responses is simplified given that they are grouped in the FMNuc. Unlike the spinal cord, interneurons and γ-MN do not reside in the FMNuc, and this distinction allows for exclusive study of α-MN responses. Because of the highly symmetrical nature of the nervous system and lack of crosstalk between the right and left FMNuc, the uninjured FMNuc can be used as a paired internal control for experiments (Isokawa-Akesson & Komisaruk, 1987; Hurley, 2003). Monocytes do not infiltrate into the FMNuc following FNA, and the blood-brain barrier (BBB) remains intact, resulting in a sterile nerve injury (Raivich et al., 1998; Hurley, 2003; Bottcher et al., 2013). Therefore, the resulting responses of the FMN and the surrounding microenvironment are purely consequential to the FNA.

Following FNA, paralysis of vibrissae and loss of the eye blink reflex is immediately observed. With a facial nerve crush (axonotmesis) injury, complete recovery is observed in approximately 10 days post-operation (dpo) (Serpe et al., 2002). With a complete facial nerve transection, no functional recovery is observed, even at 6 months post injury (unpublished data from our laboratory).

Additionally, the rodent model of peripheral nerve injury reproduces the human response to nerve injury. These similarities allow for translation of findings from mouse and rat models to human clinical trials (Campbell, 2008; Wang et al., 2013; Gordon & Borschel, 2016). Regarding facial nerve injury specifically, autopsy examination of the human FMNuc three months post injury reveals morphological changes also observed in

rodent models, validating the use of mouse FNA as a translational scientific technique (Graeber et al., 1993).

2.3. Changes in the facial motor nucleus after facial nerve axotomy

Comprehensive reviews exist detailing the changes in the FMNuc after FNA (Lieberman, 1971; Grafstein, 1975; Moran & Graeber, 2004). Findings most relevant to this dissertation are described in this introductory section.

2.3.1. Motoneuron response

After the axon is severed, the soma of the MN undergoes significant changes in morphology and function as it transitions from a homeostatic to a regenerative phenotype. One of the most distinct manifestations of this transition is chromatolysis, a phenomenon first described by Franz Nissl in 1894. Nissl discovered that basic dyes (e.g., thionin) stain neuronal cytoplasm, and he described the thionin-bound structures in neurons as "Nissl substance." Nissl substance was later discovered to be rough endoplasmic reticulum (RER), and the thionin was binding to the acidic ribosomal RNA studding RER membranes. Neurons have abundant RER within their cytoplasm because they manufacture significantly more protein than other cell types in the brain. Following axotomy, labeling of basophilic structures diminishes, resulting in "chromatolysis" (Greek: *chroma*- color, *lysis*- loosen). Electron microscopy reveals that chromatolysis results from the neuronal RER converting from long, parallel cisternae to disordered, short segments within the cytoplasm, disrupting the color resolution of the thionin stain (Torvik & Skjorten, 1971).

In addition to chromatolysis, the nucleus and nucleolus both swell and migrate eccentrically after FNA (Cammermeyer, 1963; Lieberman, 1971; Guntinas-Lichius et al., 1997). This increased nuclear and nucleolar size results from increased demand placed on the MN to generate necessary cytoskeletal proteins for constructing the regrowing axon. Specifically, actin, tubulin, and growth-associated protein (Gap-43) mRNA and protein synthesis are increased (Lieberman, 1971; Tetzlaff et al., 1988a; Bisby & Tetzlaff, 1992). Conversely, neurofilament production decreases after axotomy, likely due to its role in radial, not longitudinal axon growth (Lieberman, 1971; Tetzlaff et al., 1988a; Bisby & Tetzlaff, 1992). Acetylcholine esterase expression is decreased after axotomy as well, corresponding with the shift in neuronal phenotype away from signal transmission and towards regeneration (Lieberman, 1971).

The exact trigger for the MN cell body response to axotomy is not known; however, evidence suggests that depolarization of the MN cell membrane immediately after axotomy leads to a change in membrane potential that lasts for hours after injury (Cragg, 1970; Berdan et al., 1993). Other theories propose that loss of action potentials, depletion of retrogradely transported materials, or loss of peripheral trophic factors may induce MN changes (Cragg, 1970; Grafstein, 1975; Olsson et al., 1978).

To summarize, the motoneuron responds to the severing of its axon by undergoing a dramatic change in its phenotype from homeostatic signal transduction to a pro-regenerative program with the goal of restoring axonal reconnection to target musculature. Accompanying this phenotypic shift is morphological restructuring of its organelles to meet the increased demand for cytoskeletal protein synthesis.

2.3.2. Microglia response

Following peripheral nerve injury, microglia proliferate and their morphology changes from a small cell body with long, branching processes to a swollen cell body with shortened processes (Graeber et al., 1988; Almolda et al., 2014). Expression of complement 3 receptor (C3R; also known as Mac-1, CD11b, and OX-42) and Iba1 both increase and are useful markers of microglia activation (Ito et al., 1998; Byram et al., 2004). Time-lapse video of FMNuc-containing brainstem slices from neonatal rats at 6-9 dpo reveal microglia migrating along neuronal processes and forming pseudopod and lamellopod processes after FNA (Schiefer et al., 1999) . These findings indicate that microglia respond to axotomy by changing their morphology, motility, and expression of activation markers.

2.3.3. Astrocyte response

In response to axotomy, astrocytes switch from a protoplasmic, GFAP-negative (glial fibrillary acidic protein) phenotype to a fibrous, GFAP-positive phenotype (Tetzlaff et al., 1988b). Astrocyte activation is proportional to the severity of the nerve injury administered, demonstrating their sensitivity to the damage inflicted to the MN (Laskawi & Wolff, 1996). The mouse background strain can alter the astrocyte response to injury, the exact mechanisms of which are unknown (Lidman et al., 2002).

2.3.4. Synaptic stripping

The synaptic inputs on LMN from UMN are ensheathed by astrocytes to maintain the synaptic connection (Castellano et al., 2016). After axotomy, these synaptic inputs are

displaced by microglia in a process called “synaptic stripping” (Blinzinger & Kreutzberg, 1968). Removal of afferent inputs benefits the MN by allowing it to devote its energy towards regeneration and away from signal processing (Jinno & Yamada, 2011; Castellano et al., 2016). Additionally, removal of excitatory inputs prevent excitoxicity (Mentis et al., 1993). Later studies discovered that microglia displaced these synapses in the early phase after axotomy, and between 2-3 weeks post-operation (wpo), astrocytes processes replace the microglia in surrounding the MN soma (Moran & Graeber, 2004).

To initiate synaptic stripping, purines released by the injured MN bind to purine receptors on microglia processes, inducing the microglia to wrap around the MN and aid in separation of synaptic contacts. Microglia sense the types and levels of purines released by the injured MN, and this information initiates pro- or anti-phagocytic responses (Castellano et al., 2016). Interferon-recognition factor 8 (IRF8) is also a key signaling protein for microglia wrapping around axotomized FMN (Masuda et al., 2012; Xie et al., 2014). In summary, synaptic stripping is an important process for promoting MN survival after axotomy and occurs as a result of glia reacting to injury signals from the axotomized MN.

2.4. The immune system and facial nerve axotomy

2.4.1. Consequences of immunodeficiency

To determine if the immune system was beneficial or harmful after nerve injury, FNA was performed on severe combined immunodeficient (scid) mice and FMN survival was quantified at 28 dpo. Scid mice possess a mutation that blocks the maturation of B and T cells, resulting in loss of the adaptive arm of the immune system. More FMN die

after FNA in scid mice relative to WT mice, suggesting that the adaptive arm of the immune system serves a neuroprotective role after FNA. This hypothesis is confirmed when adoptive transfer of WT whole splenocytes into scid mice prior to FNA rescued FMN survival after axotomy to WT levels (Serpe et al., 1999; Serpe et al., 2000). These findings were reaffirmed in the recombinase activating gene-2 knockout (RAG-$2^{-/-}$) mouse, in which B and T cells fail to mature, resulting in a lack of the adaptive arm of the immune system (Serpe et al., 2003). Immunodeficiency also slows functional recovery after facial nerve crush (Serpe et al., 2002; Beahrs et al., 2010). Administration of dexamethasone, a corticosteroid that decreases the number of lymphocytes in the blood, also results in delayed functional recovery and greater neuronal death after FNA (Lieberman et al., 2011).

To identify which immune cell in the adaptive arm of the immune system was neuroprotective, FMN survival after FNA was examined in immune cell knockout mice. In mice deficient in CD4+ T cells, significant FMN loss after FNA occurred. In contrast, mice deficient in CD8+ T cells or B cells had FMN survival comparable to WT after FNA, signifying that only CD4+ T cells are relevant to immune-mediated neuroprotection. These results were verified by adoptive transfer of CD4+ T cells into either $CD4^{-/-}$ or RAG-$2^{-/-}$ mice, and FMN survival was rescued to WT levels, whereas adoptive transfer of CD8+ T or B cells had no effect on FMN survival (Serpe et al., 2003). As new lymphocyte subtypes were discovered, their role in FMN survival after injury was also assessed. Thus far, natural killer cells and regulatory CD4+CD25+ T cells have been ruled out of having neuroprotective effects for injured motoneurons (Byram et al., 2003; DeBoy et al., 2006a).

2.4.2. T cells and neuroprotection

For T cells to execute neuroprotective actions, they require both peripheral and central antigen presentation via major histocompatibility complex class II (MHCII) expressed on antigen-presenting cells (APCs) (Byram et al., 2004). Activated T cells capable of recognizing only ovalbumin by their T cell receptors are not neuroprotective, indicating that antigen-specific activation of T cells is necessary (Byram et al., 2006). After axotomy, antigens from the injured FMN drain into cervical lymph nodes, and APCs in the lymph node activate naïve T cells. These activated T cells circulate and re-encounter target antigen expressed on MHCII in the CNS, inducing a secondary activation that results in effector T cell activity. Microglia are the predominant expressers of MHCII in the CNS and activate T cells with high efficiency relative to astrocytes and other CNS APCs (Male et al., 1987; Pryce et al., 1989; Aloisi et al., 1998; Aloisi et al., 1999; Hurley, 2003).

All CD4+ T cell subsets expand in the draining cervical lymph nodes after FNA, peaking in number at 7 dpo, then declining at 9 dpo as the cells migrate into the peripheral blood (Xin et al., 2008). This timecourse is supported by evidence of T cell infiltration into the injured FMNuc peaking at 14 dpo (Raivich et al., 1998; Ankeny & Popovich, 2007; Ha et al., 2007b). To identify which T cell subset was specifically responsible for neuroprotection, signal transducer and activator of transcription (STAT) and interleukin knockout experiments were performed. These experiments revealed that IL-4 and STAT-6, which promote T cell differentiation towards the Th2 subset, are necessary for neuroprotection.

Facial nerve re-injury experiments provide additional evidence for CD4+ T cell-mediated neuroprotection. An augmented T cell-infiltration response and accelerated functional recovery are observed in animals receiving a second FNA ten weeks following their first FNA. This finding suggests that immune memory from the first FNA leads to a stronger immune response when the injury reoccurs (Ha et al., 2007b; Ha et al., 2008).

2.4.3. IL-10 and other cytokines relevant to neuroprotection

Astrocytes, microglia, and neurons express multiple cytokines and their receptors at homeostasis and after injury, and ongoing studies continue to assess the role these proteins play in neuroprotection.

IL-10 is an anti-inflammatory cytokine that promotes neuroprotection after CNS injury (Kiyota et al., 2012; Joniec-Maciejak et al., 2014; Gravel et al., 2016; Zhou et al., 2016). IL-10 deficiency results in greater FMN loss after FNA. WT CD4+ T cells do not rescue FMN survival after FNA in IL-$10^{-/-}$ mice, indicating that neuroprotective IL-10 does not derive from CD4+ T cells. Furthermore, IL-$10^{-/-}$ CD4+ T cells are capable of neuroprotection in RAG-$2^{-/-}$ mice, ruling out the adaptive arm of the immune system as the IL-10 source (Xin et al., 2011). IL-10 is incapable of crossing the BBB, therefore, neuroprotective IL-10 must derive from the CNS parenchyma (Kastin et al., 2003). IL-10 mRNA and protein levels remain unchanged after FNA in WT mice. In RAG-$2^{-/-}$ mice, however, there is a decrease in IL-10 protein levels at 7 dpo, suggesting that the immune system maintains IL-10 expression after FNA (Xin et al., 2011). IL-10 receptor (IL-10R) is constitutively expressed by neurons, and axotomy induces IL-10R expression exclusively on astrocytes. There was no detectable IL-10R expression on microglia

before or after axotomy. The expression of IL-10R on neurons after FNA is unknown because conventional MN markers, such as choline acetyltransferase, are not expressed by injured MN (Xin et al., 2011). In a transgenic mouse with astrocytic overexpression of IL-10, FMN survival after FNA is increased. Few changes are observed between WT and transgenic IL-10 overproducing mice, except for differential expression of phagocytosis-related proteins in microglia after axotomy (Villacampa et al., 2015). To summarize, IL-10 is an important factor in CD4+ T cell-mediated neuroprotection.

Cytokine expression microarrays of the FMNuc at 7 days post-FNA reveals that Th2-related cytokines are strongly induced, whereas Th1-associated cytokines are undetectable. Of these cytokines, CCL11 expression is the most highly expressed, and its expression peaks at 14 dpo (Wainwright et al., 2009c). A colocalization study identified that FMN express CCL11 constitutively in the uninjured FMNuc. After axotomy, neuronal expression is no longer detectable, and astrocyte expression of CCL11 is induced. At 30 dpo, when the post-axotomy responses return to baseline levels, neuronal CCL11 expression is regained and astrocyte expression of CCL11 is not detectable (Wainwright et al., 2009a). CCL11 binds multiples chemokine receptors (CCR), one of which is CCR3 on T cells. $CCR3^{-/-}$ mice have increased FMN loss after FNA, and adoptive transfer of $CCR3^{-/-}$ CD4+ T cells into $RAG\text{-}2^{-/-}$ mice does not restore FMN survival (Wainwright et al., 2009b). Collectively, these studies indicate that axotomy induces astrocytic production of CCL11 which recruits T cells to the injured FMN.

Tumor necrosis factor-alpha (TNFα) is a pro-inflammatory cytokine that has both neuroprotective and neurotoxic effects in the CNS after injury (Terrado et al., 2000; Liu et al., 2017). TNFα mRNA expression has been described in both early (1-2 dpo) and late

(14 dpo) timepoints post-FNA (Raivich et al., 1998; Streit et al., 1998; Streit et al., 2000). Neutralization of TNFα by overexpression of soluble TNFR1 modestly increases FMN survival after injury (Terrado et al., 2000). TNFα has two receptors, TNFR1 and TNFR2, and they have differential effects on the cellular response. FNA was performed on transgenic mice in which either TNFR1 or TNFR2 was knocked out to determine which receptor was relevant for FMN survival after FNA. No changes in FMN survival or microglia activation were observed in these two mouse models. When both TNFR1 and TNFR2 are simultaneously knocked out, FMN survival is significantly increased (Raivich, 2002). This combined deletion of TNFR1&2 also results in a significant decrease in MHCI expression by microglia (Bohatschek et al., 2004a). MHCI is an important antigen presenting protein for cells and also is necessary for the pruning of synapses during neurodevelopment (Corriveau et al., 1998; Huh et al., 2000). In addition, decreased expression of microglial B7.2, a costimulatory molecule for antigen presentation, is observed in TNFR1&2$^{-/-}$ mice (Bohatschek et al., 2004b). Microglia antigen presentation may play an important role in the synaptic stripping process after axotomy. These data collectively suggest that TNFα is a significant regulator of microglia activity after axotomy, and inhibition of these processes promotes FMN survival.

IL-6 is a pleotropic cytokine with immunoregulatory effects that can promote inflammation or tissue repair (Almolda et al., 2014). mRNA expression is increased within 24 hours post-operation (hpo), and expression of IL-6 receptors (IL-6R) is induced on both astrocytes and neurons after FNA (Klein et al., 1997). Evidence suggests that IL-6 is primarily produced by axotomized FMN (Streit et al., 2000). Knocking out IL-6 prevents axotomy-induced expression of GFAP by astrocytes, a process mediated by IL-6

activation of STAT-3 (Klein et al., 1997; Tyzack et al., 2014). Loss of IL-6 also reduces microglia proliferation after FNA, most likely due to loss of astrocyte production of macrophage colony stimulating factor (MCSF) (Klein et al., 1997). MCSF acts on microglia to induce proliferation and facilitate microglia wrapping around injured FMN (Raivich et al., 1994; Kalla et al., 2001). When adult and neonatal rat responses to FNA are compared, there is significantly less FMN survival in neonatal rats. A lack of IL-6 expression is also observed in neonatal rats after FNA, whereas adult rats have robust IL-6 expression after axotomy (Streit et al., 2000). In an FNA study in which astrocytes constitutively overexpress IL-6, a small increase in FMN death is observed, and the microglia activation response to FNA is significantly altered. Specifically, expression of CD11b peaks at an earlier timepoint post-FNA, and decreased microglia apposition around axotomized FMN is observed (Almolda et al., 2014). These data collectively suggest that a "Goldilocks zone" exists for IL-6 after FNA, outside of which both insufficient and excessive IL-6 can result in neuronal death. To summarize the role of IL-6 in the post-axotomy response, IL-6 expression by neurons after injury stimulates surrounding astrocytes to adopt a pro-regenerative phenotype that promotes proliferation and perineuronal apposition of microglia via MCSF.

Pituitary adenylate cyclase-activating polypeptide (PACAP) can act as a neuroimmune modulator, and its expression by MN is strongly induced as early as 6 hpo (Zhou et al., 1999; Mesnard et al., 2010; Mesnard et al., 2011). Although knocking out PACAP does not impact FMN survival, it does result in significant increases in cytokine expression and microglia activation, suggesting that PACAP regulates the glial microenvironment response to FNA (Armstrong et al., 2008). PACAP promotes

microglia production of Th2-differentiation signaling chemokines, specifically C-C motif chemokine ligand 11 (CCL11) (Wainwright et al., 2008). PACAP gene expression increases after injury in the FMNuc.

2.4.4. Molecular response of cells within the facial motor nucleus to axotomy

When FMN loss after FNA is quantified for each subnucleus of the FMNuc, the ventromedial (VM) subnucleus has the most FMN death, and the ventrolateral (VL) subnucleus has virtually no FMN death. In RAG-2$^{-/-}$ mice, there is no disproportionate effect of immunodeficiency on the distribution of FMN death across the FMNuc, and adoptive transfer of CD4+ T cells does not affect this either (Canh et al., 2006). These findings suggest that a factor within the VM and VL subnuclei determines neuronal fate after injury.

Using laser-capture microdissection, the VM and VL subnuclei were isolated for gene expression analysis to identify what factors promote neuronal survival or death. Unexpectedly, the VL subnucleus had a comparable motoneuron regeneration response. Conversely, significant differences in proinflammatory gene expression and glial activation were observed. When neurons and neuropil were laser-captured separately, the proinflammatory gene expression was only detectable in neuropil samples. Together, these findings indicate that the differences in inflammatory responses in the microenvironment, not neuroregenerative responses, are responsible for mediating neuronal survival after injury.

2.5. Introduction to ALS

ALS is a lethal paralytic disease characterized by progressive loss of motor function with sensory and cognitive sparing (Wijesekera & Leigh, 2009). The prevalence of ALS in the United States is 3.9/100,000 people (Mehta et al., 2014). Males are slightly more affected, and smoking and military service are risk factors associated with ALS (Bryan et al., 2016). Approximately 5-10% of ALS cases are linked to familial heritable gene defects (fALS), and the remaining 90% of cases are classified as spontaneous ALS (sALS) (Calvo et al., 2014). ALS etiology remains unknown, and over 20 genes have been associated with fALS, with a wide range of physiological impacts. These discoveries have led to generation of the cell autonomous and non-cell autonomous theories of MN death in ALS. According to the cell autonomous theory, genetic mutation disrupt vital processes within MN that ultimately leads to MN death. These disruptions can cause MN death via multiple pathways, and theories include excitotoxicity, endoplasmic reticulum stress, protein degradation pathway stress, oxidative stress, mitochondrial dysfunction, altered axonal transport, and synaptic vesicle defects (Ilieva et al., 2009; Pandya et al., 2013). Almost all therapies targeting these abnormalities have failed to improve prognosis, with the exception of riluzole (Turner et al., 2001; Orrell, 2010; Pandya et al., 2013). Riluzole alleviates glutamate-mediated excitotoxicity and extends patient survival by an average of 2-3 months (Meissner et al., 2010).

The non-cell autonomous theory is that ALS genetic mutations negatively affect the microenvironment surrounding the MN, thereby inducing MN death. Neuroinflammatory damage, BBB leakiness, and extracellular accumulations of mSOD1

are all contributors to disease pathology, and many research groups are examining these factors as causative agents for disease (Ilieva et al., 2009; Pandya et al., 2013).

In humans, it is nearly impossible to identify determinants of MN death in ALS because ALS is a clinical disease, meaning that the diagnosis is based on motor deficit progression with all other possible diseases ruled out. Given the hardiness of the CNS motor systems, significant motoneuron death must occur before clinical abnormalities are detected. An additional obstacle in studying ALS is that tissue acquired from a living patient is restricted to either peripheral blood or cerebrospinal fluid (CSF), given that nervous system tissue collection is only permitted at autopsy. Altogether, assessing the sequence of events that leads to MN death in ALS is largely limited to use of rodent models and iPSCs.

2.6. mSOD1 mouse model of ALS

Mutations in SOD1 are the most common genetic cause of ALS (Cirulli et al., 2015). SOD1 is a protein that has been highly conserved throughout evolution and is ubiquitously expressed. SOD1 comprises 1-2% of total soluble protein in the CNS. The primary function of SOD1 is to convert superoxide to hydrogen peroxide (Bunton-Stasyshyn et al., 2015). Knocking out SOD does not result in motoneuron disease (MND) symptoms in mice, suggesting that loss-of-function deficits are not causative for ALS. Instead, studies suggest that either a toxic gain-of-function or prion-like behavior of misfolded SOD protein contribute to MND.

The first mouse model of ALS that recapitulated the human disease was published in 1994 (Gurney et al., 1994). When the human mutated $SOD1^{G93A}$ (mSOD1) gene is

inserted into a B6/SJL mouse, motor deficits can be observed at 120 days of age (doa). The motor deficits first manifest in hindlimb muscles, then progress to forelimbs, and animal death occurs between 150-160 doa. In this mouse model, the first detectable pathology of ALS is the loss of neuromuscular junctions (NMJs) in the hindlimb muscles at 47 doa. At roughly 80 doa, axon loss is evident in the ventral roots, and at 100 doa, MN death is first detected in the lumbar spinal cord, suggesting a progressive die-back of the MN (Gurney et al., 1994; Fischer et al., 2004). This axonal die-back suggests that some disease factor induces target disconnection, which, in turn, leads to MN death (Dadon-Nachum et al., 2011).

2.6.1. Motoneuron-specific mSOD1 and MND

With the discovery of SOD1 mutations causing MND, the next question was whether the mSOD1 mutation isolated to MN alone would induce MN death. Surprisingly, in two mouse models where mSOD1 was expressed solely in MN, no motor deficits or MN pathology were observed, even with doubling of the expression of mSOD1 in MN (Pramatarova et al., 2001; Lino et al., 2002). A later study was successful in recapitulating MND with a Thy1/mSOD1 mouse model, primarily because this genetic model produced about 5-fold more mSOD1 than previously reported models (Jaarsma et al., 2008). Interestingly, the average endstage of disease in this mouse model is between 600-700 doa, suggesting that MN are highly resilient to toxicity from SOD1 mutations. This MN resilience supports the non-cell autonomous hypothesis for ALS.

2.6.2. Microglia-specific mSOD1 and MND

To identify if microglia played a role in mSOD1 MND, a CD11b-cre/mSOD1^{G37R}-flox mouse model was employed. When mSOD1 expression is knocked down in microglia, survival is increased by approximately 100 days relative to control (Boillee et al., 2006). This dramatic effect suggests that mSOD1 expression in microglia significantly contributes to disease progression and MN death. Further characterization of microglia activation in mSOD1 rats determined that in the early presymptomatic phase, monocytes infiltrate the sciatic nerve, while in the late presymptomatic phase, myeloid activation is evident in the spinal cord. This suggests that myeloid cell activation acts in parallel with axonal die-back, but it is unknown if this is causative or reactionary (Graber et al., 2010).

Microglia-mediated neurotoxicity could be consequential to an alteration in the cell's phenotypic polarization after injury or disease. Activated microglia can be roughly divided into M1 and M2 phenotypes, characterized by expression of either pro-inflammatory markers, such as TNFα and inducible nitric oxide synthase (iNOS), and pro-repair markers, such as arginase 1 (Arg1) and IL-10, respectively. Assessment of M1 and M2 markers in mSOD1 mouse spinal cord at multiple timepoints reveals that both cell types increase throughout disease. A significantly higher proportion of activated microglia are Arg1+ than iNOS+, indicating that the majority of microglia are behaving in an M2 pro-repair, anti-inflammatory fashion (Lewis et al., 2014). Inhibition of microglia proliferation or downstream cytokine signaling via janus kinase 2 (JAK2) confers no therapeutic benefit to mSOD1 mice (Tada et al., 2014; Martinez-Muriana et

al., 2016). However, this inhibition strategy affects both M1 and M2 microglia, which could cancel out any neuroprotective effects.

To better understand the inflammatory reaction in mSOD1 mice, a nuclear factor kappa-light-chain-enhancer of activated B cells (NF-κB)/GFP (green fluorescent protein) reporter mouse was crossed with the mSOD1 mouse. NF-κB/GFP was most highly expressed in microglia. Time-lapse videos of MN and microglia co-culture systems reveal that mSOD1 microglia phagocytize both synapses and MN, leading to increased MN death. Inhibiting NF-κB in microglia, not astrocytes, results in significant increases in MN survival in co-culture experiments. NF-κB inhibition in mSOD1 mice also extends survival. Conversely, reducing inhibition of NF-κB results in increased inflammatory cytokine expression and accelerated disease progression, further linking microglia-mediated neuroinflammation and MN death (Frakes et al., 2014). In summary, a growing body of evidence suggests that SOD1 mutations in microglia result in a proinflammatory, hyperphagocytic microglia response that is toxic to MN (Brites & Vaz, 2014).

2.6.3. Astrocyte-specific mSOD1 and MND

In vitro experiments in which mouse mSOD1 astrocytes are co-cultured with normal MN reveal that these astrocytes are highly neurotoxic, suggesting that astrocytes also contribute to non-cell autonomous pathways of MN death (Di Giorgio et al., 2007). Silencing mSOD1 in astrocytes restores MN survival to WT levels (Haidet-Phillips et al., 2011). The use of astrocytes derived from induced pluripotent stem cells (iPSCs) from human fALS and sALS patients yield similar results (Haidet-Phillips et al., 2011). When the cre/lox system is used to knockdown mSOD1 in astrocytes in mSOD1 mice, animal

survival is increased by about 60 days, further supporting this hypothesis. Human ALS iPSC astrocytes injected into the spinal cord of scid mice can engraft into the CNS, and over time motor deficits are observed comparable to mSOD1 mouse deficits (Chen et al., 2015a). In summary, mSOD1 in astrocytes also have demonstrable neurotoxic effects on MN.

2.7. Immune dysregulation in human patients with ALS

The role of the immune system at endstage in ALS has been characterized from analysis of autopsy tissue. In diseased CNS tissue, potent glial activation is observed surrounding MN cell bodies in the CNS. Increased microglia activation correlates with rapidity of disease progression (Brettschneider et al., 2012). Assessment of innate immune activators also reveals significant increases in expression of toll-like receptors (TLR) and their accompanying downstream mediators (Casula et al., 2011). Additionally, complement (C) proteins, C1q and C3d, accumulate in deposits within the spinal cord (Sta et al., 2011). A study analyzing the immune response in ALS muscle tissue also found complement proteins on motor end plates, especially C1q and the membrane attack complex (MAC) (Bahia El Idrissi et al., 2016). This evidence of immune activation at both the peripheral terminal and central soma of the MN suggests that the immune system plays a role in ALS disease pathology.

To characterize inflammatory and immune changes before death in ALS patients, measures of cytokines and white blood cell counts have been reported in multiple studies. The majority of these studies yield conflicting results, most likely a result of their small sample size (8-20 patients) and the heterogeneity of this disease (sALS v fALS,

variability of disease progression rate, gender, age, etc.) (Holmoy et al., 2006; Kuhle et al., 2009; Saleh et al., 2009; Hovden et al., 2013; Ehrhart et al., 2015). For these reasons, I choose to restrict my assessment of immune system alterations in ALS to the highest powered clinical publications. In the Chen et al. 2014 publication, peripheral blood samples were collected from 284 patients with ALS. This study identified that both men and women with ALS had significantly decreased proportions of CD4+ T cells relative to controls, as well as increased circulating immune complexes (Chen et al., 2014). In women, significantly higher C3 levels were also detected in peripheral blood. In Lu et al. 2016, plasma cytokine levels were measured in 98 ALS patients at regular intervals for up to 4 years. This study identified significantly higher levels of 11 inflammatory markers in peripheral blood, including TNFα, pro-inflammatory interleukins (IL-1β and IL-2), and anti-inflammatory interleukins (IL-4 and IL-10). IL-6 was the only cytokine to increase with disease progression (Lu et al., 2016).

T cells may play a special role in ALS disease. Published case studies describe MND-like symptoms in patients infected with human immunodeficiency virus (HIV), an infection that selectively kills CD4+ T cells. With anti-retroviral therapy, these symptoms are eliminated, suggesting a connection between T cells and MN function (Moulignier et al., 2001; Alfahad & Nath, 2013). There have also been reports of ALS development in patients with myasthenia gravis, an autoimmune disease in which antibodies target acetylcholine receptors, leading to elimination of NMJs. These cases further imply an involvement of aberrant immune system activity in ALS disease pathology (Staff & Appel, 2016).

Overall, these studies reveal a dysregulated immune profile in patients with ALS. The involvement of the immune system links the axonal die back and non-cell autonomous theories of ALS etiology because the immune system is an important presence in both the PNS and CNS. Multiple clinical trials using immunosuppression have failed to benefit ALS patients (Kelemen et al., 1983; Brown et al., 1986; Werdelin et al., 1990; Drachman et al., 1994). One explanation for these failures is that administering treatment at such an advanced disease stage could be too little, too late. An alternative explanation is that the immune system has both a neuroprotective and a neurodegenerative role. Eliminating the entire immune system could result in neurodegeneration because the neuroprotective aspects of the immune system are lost. This hypothesis is supported by the work done in our laboratory studying immune-mediated neuroprotection after axotomy.

2.8. Immune dysregulation in the mSOD1 mouse model of ALS

Multiple studies have measured immune changes throughout the lifespan of the mSOD1^{G93A} mouse model of ALS to identify early alterations that may be causative of the disease. The earliest inflammatory changes in mSOD1 spinal cord tissue have been described at 40-42 doa, at which increased microglia activation, immunoglobulin G (IgG) deposits, and integrin markers have been detected (Alexianu et al., 2001). Additionally, TNFα, IL-1R, and CD86 gene expression are increased at this early timepoint. At 63 doa, further microglial cytokine expression is observed, suggesting early microglia activation occurs in MND (Chen et al., 2004). At symptom onset and disease endstage (approximately 80 – 126 doa), potent increases in microglia and astrocyte activation are

observed, as well as significant increases in inflammatory cytokine protein and apoptotic gene expression (Alexianu et al., 2001; Hensley et al., 2002; Yoshihara et al., 2002; Hensley, 2003; Chen et al., 2004). Overall, these data suggest that immune dysregulation in ALS begins early in the disease and accumulates throughout the disease process.

Depending on the mouse background strain, mSOD1^{G93A} motoneuron disease can progress slowly (C57 background) or rapidly (SJL background). A comparison study was conducted to determine if differential immune responses existed between these two groups. The study focused on changes in the sciatic nerve at approximately similar disease stages of these two strains. In C57 (slow progression) sciatic nerves, higher levels of MHCI, CCL2, and C3 were detected, as well as higher CD8+ T cell infiltration. Conversely, in SJL (fast progression) sciatic nerves, much lower immunoactivation was detected (Nardo et al., 2016). These data suggest that immune activation and inflammatory cytokine production may be neuroprotective and prolong axonal survival, whereas deficient immunoactivation results in accelerated axonal loss. This study supports the hypothesis for this work that dysregulation in the ALS immune system may lead to a loss of neuroprotection, not an augmentation in neurotoxicity.

2.9. T cells in mSOD1 MND

In the early presymptomatic stage of MND in mSOD1 mice, no changes are evident in levels of CD4+ or CD8+ T cells in the peripheral blood (Gravel et al., 2016). However, at end-stage, significant lymphopenia and loss of splenic mass and architecture is evident (Kuzmenok et al., 2006; Banerjee et al., 2008). To test if lymphopenia contributed to mSOD1 disease, adoptive transfer of WT WS to mSOD1 mice was

performed, and no therapeutic benefits were observed (Banerjee et al., 2008). In contrast, regular treatment of mSOD1 mice with WT CD4+ T cells prior to and throughout disease, either enriched for regulatory T cells (CD4+CD25+; Tregs) or effector T cells (CD4+CD25-; Teffs) revealed that Tregs delayed symptom onset and Teffs increased disease latency (Banerjee et al., 2008).

Despite the overall lymphopenia, CD4+ and CD8+ T cells accumulate in the mSOD1 spinal cord with disease progression. To further examine if T cells were neuroprotective or neurotoxic, a T cell receptor (TCR) knockout was crossed with the mSOD1 mouse model, and accelerated disease progression and death was observed in these mice (Chiu et al., 2008). This finding is further confirmed with a similar phenotype observed in both mSOD1/RAG-$1^{-/-}$ mice and mSOD1/$CD4^{-/-}$ transgenic mice (Beers et al., 2008). Altogether, these findings support the hypothesis that CD4+ T cells promote MN survival and delay disease progression in mSOD1 MND.

To test if increasing CD4+ T cell numbers could confer neuroprotection, castration was performed on male mSOD1 mice. Castration results in an increased thymus size and increase in circulating CD4+ T cells; however, this increase in T cells only increased survival by an average of 9 days. Decreased microglia activation was observed in the spinal cord, suggesting that T cell modulation of microglia responses may be neuroprotective (Sheean et al., 2015).

2.10. FNA and mSOD1 MND

One drawback of studying disease progression in the mSOD1 mouse model is that there is no exact timing for disease onset. Even in animals with identical genotypes,

significant differences in disease progression can be observed (Gurney et al., 1994; Haulcomb et al., 2014) MN are also heterogeneously affected by this disease, with some MN dying very early, and some living for the remainder of the animal's lifespan (Fischer et al., 2004). In addition, some MN maintain connection target musculature to endstage (Gurney et al., 1994). To circumvent this problem, FNA can be superimposed onto the mSOD1 mouse model to induce target disconnection of all FMN at the exact same time. Because axotomy simulates the target-disconnection pathology in ALS, essentially all FMN are experiencing the disease pathology simultaneously. To minimize confounding injury with mSOD1 disease processes, the axotomy is induced at 56 doa, a timepoint much earlier than when mSOD1 MND affects FMN survival (136 doa). This timepoint for axotomy was also selected to ensure that the immune system has completely matured in these animals.

When FNA is performed on mSOD1 mice at 56 doa, significantly greater FMN loss is observed in mSOD1 mice at 28 dpo (84 doa). To confirm that the mSOD1 MND was not confounding the axotomy-induced death, FMN were quantified on the uninjured side and the numbers were equivalent to uninjured WT FMN counts (Mesnard et al., 2011). In addition to greater MN death, functional recovery from facial nerve crush is also delayed in mSOD1 mice relative to WT. It should be emphasized here that recovery still occurs in mSOD1 mice, suggesting that the regenerative program within injured MN is still functional (Mesnard et al., 2013). Gene expression profile analysis after facial nerve transection further confirms that the MN regenerative phenotype after axotomy remains comparable to WT, using markers such as Gap-43 and β_{II}-tubulin. In addition, there is deficient activation of the glial response after axotomy. In the uninjured FMN,

mRNA levels of astrocyte and microglia activation genes are increased relative to WT, indicating some baseline glial activation occurring due to the mSOD1 MND. In addition, baseline expression of inflammatory cytokines *Tnfα* and *Ifnγ* (interferon γ) is increased and continues to rise with axotomy (Mesnard et al., 2011; Haulcomb et al., 2014).

A closer examination of cell death pathways in the axotomized mSOD1 FMNuc reveals a high prevalence of both Fas and neuronal nitric oxide synthase (nNos) expression after FNA (Haulcomb et al., 2014). Conversely, no differences were detected in TNFR1 mediated cell death, which is surprising given the significant increase in TNFα detected in mSOD1 CNS tissue. Other mSOD1 studies of Fas/nNos death have determined than MN with multiple different mSOD1 mutations are hypersensitive to Fas/nNos mediated cell death as compared with trophic deprivation or excitotoxic stimulation (Raoul et al., 2002). This difference is specific for mSOD1 MN and is not observed in WT MN. A closer examination reveals that nitric oxide (NO) triggers MN to express Fas ligand (FasL), which may be responsible for potentiating MN death via Fas/nNos pathways.

Because both RAG-2$^{-/-}$ mice and mSOD1 mice suffer similar MN death after FNA, and because immune dysregulation is observed in mSOD1 mice, a study from our laboratory was conducted to assess if mSOD1 splenocytes could confer neuroprotection. Adoptive transfer of mSOD1 WS does not rescue FMN survival after FNA in RAG-2$^{-/-}$ mice. With this finding, the next hypothesis was that mSOD1 CD4+ T cells were ineffective in promoting FMN survival. This hypothesis was disproven when adoptive transfer of isolated mSOD1 CD4+ T cells into RAG-2$^{-/-}$ mice resulted in FMN survival after FNA comparable to WT. To identify if immunotherapy could improve FMN

survival after FNA, mSOD1 mice were injected with either WT WS, WT CD4+ T cells, WT CD4+ depleted splenocytes, or axotomy-activated WT CD4+ T cells. The mSOD1 mice that received WT WS had a significant increase in FMN survival, but the other cell transfers were incapable of rescuing FMN survival, suggesting that the additive benefit of both WT splenocytes and CD4+ T cells could overcome the inhibition of the neuroprotection within the mSOD1 mouse milieu (Mesnard-Hoaglin et al., 2014). These findings suggest that a factor within the mSOD1 WS suppresses CD4+ T cell mediated neuroprotection and form the basis for the work described in this dissertation.

2.11. Aim 1: Determine the source of neuroprotective IL-10 in the axotomized facial motor nucleus

Based on the Xin et al. 2011 study, IL-10 is necessary for CD4+ T cell mediated neuroprotection, although it does not derive from CD4+ T cells. IL-$10^{-/-}$ CD4+ T cells still rescue FMN survival in RAG-$2^{-/-}$ mice, indicating that the neuroprotective IL-10 does not derive from the adaptive arm of the immune system. Finally, IL-10 cannot cross the BBB, therefore leading us to conclude that neuroprotective IL-10 derives from the CNS parenchyma (Kastin et al., 2003). To fully understand the mechanisms of CD4+ T cell-mediated neuroprotection, it is necessary to learn the source and kinetics of IL-10 production after FNA.

The hypothesis for this aim is that CD4+ T cells, after initial activation in the peripheral immune system, migrate to the CNS and interact with MHCII+ microglia. This results in a secondary activation of T cells and expression of IL-4, which shifts the phenotype of microglia towards M2 microglia that produce neuroprotective IL-10.

2.12. Aim 2: Characterize gene expression profile changes after facial nerve axotomy in immunodeficient and WT CD4+ T cell-reconstituted mice

There is a gap in the literature regarding how the adaptive arm of the immune system exerts neuroprotective effects in the facial motor nucleus after axotomy. To address this, the gene expression profile in immunodeficient RAG-2$^{-/-}$ mice will be compared to WT at multiple post-axotomy timepoints. In addition, the gene expression profile of RAG-2$^{-/-}$ mice with adoptive transfer of WT CD4+ T cells will be performed to characterize the neuroprotective effects of CD4+ T cells. Four aspects of the injury response will be assessed: MN regeneration, glial activation, inflammation, and cell death receptor pathways. The hypothesis for this aim is that immunodeficiency will impair the glial microenvironment response to FNA, leading to increased FMN death, and CD4+ T cells will regulate these cellular responses to normal levels.

2.13. Aim 3: Analyze gene expression profile changes after facial nerve axotomy in mice immunoreconstituted with mSOD1 whole splenocytes or mSOD1 CD4+ T cells

To our surprise, mSOD1 CD4+ T cells are capable of neuroprotection, whereas mSOD1 WS are not. This finding suggests that an inhibitory factor within the mSOD1 WS environment impairs CD4+ T cell mediated neuroprotection. To better understand the mechanism behind this, gene expression analysis will be performed to examine the same genes as in Aim 2. As an additional control, a RAG-2$^{-/-}$ + WT WS group will be added for comparison with the mSOD1 WS recipient animals. The hypothesis for Aim 3 is that the RAG-2$^{-/-}$ + mSOD1 WS group gene expression profile will be comparable to

the RAG-2$^{-/-}$ profile with impaired glial microenvironment responses, and the mSOD1 CD4+ T cell treatment group will be comparable to the WT CD4+ T cell group. This hypothesis is based on the assumption that the mSOD1 WS will block the glial microenvironment regulation by CD4+ T cells within the whole splenocyte milieu. However, when the mSOD1 CD4+ T cells are removed from the suppressive environment, they will function comparably to WT CD4+ T cells.

CHAPTER 3: MATERIALS AND METHODS

3.1. Animals used in this study

For this study, the following mouse strains were purchased from The Jackson Laboratory (Bar Harbor, ME): C57BL/6J (WT, 000664), B6(Cg)-*Rag2*$^{tm1.1Cgn}$/J (RAG-2$^{-/-}$, 008449), B6.Cg-Tg(SOD1^{G93A})1Gur/J (mSOD1, 004435), and B6(Cg)-*Il10*$^{tm1.1Karp}$/J (IL-10/GFP, 014530). All purchased mice were obtained at 6 or 7 weeks of age and allowed acclimate for 1 week prior to any manipulation. Female mice were exclusively used for experiments because male mice cannot be co-housed after surgery due to their aggressive nature. The male fighting behavior causes damage to the surgical site, leading to infections that can confound experimental results.

For the IL-10 conditional knockout mice, IL-10 floxed mice were generously provided from Dr. Gang Huang's laboratory at Cincinnati Children's Hospital (Roers et al., 2004). GFAP-cre mice and CX3CR1-cre (CX3C receptor 1) mice were purchased from the Jackson Laboratory (Strains: B6.Cg-Tg(GFAP-cre/ERT2)505Fmv/J, 012849; B.6.129P2(Cg)-*Cx3cr1*$^{tm2.1(cre/ERT)Litt}$/WganJ, 021160). Both cre strains used were tamoxifen-inducible. The breeding scheme between the cre and floxed mouse strains generated GFAP-cre+/IL-10$^{fl/fl}$ and CX3CR1-cre+/IL-10$^{fl/fl}$ mouse strains. For negative controls, cre+/IL-10$^{fl/-}$ and cre-/IL-10$^{fl/fl}$ littermates were used.

All animal procedures complied with National Institutes of Health guidelines on the care and use of laboratory animals and were approved by the Indiana University School of Medicine's Institutional Animal Care and Use Committee. Mice were housed in sterilized microisolater cages with a 12 hr light/dark cycle and fed autoclaved food

pellets and drinking water ad libitum. The animal facility uses a laminar flow system to maintain a pathogen-free environment.

3.2. Genotyping

Tail snips were collected from mice in the cre/lox breeding scheme, and DNA was extracted from them using the Gentra Puregene Mouse Tail Kit (Qiagen, Germantown, MD; 158267). PCR was conducted using genomic DNA, forward and reverse primers (Table 1), and GE Healthcare illustra™ PuReTaq Ready-To-Go™ PCR Beads (Thermo Fisher Scientific, Waltham, MA; 46-001-012). The IL-10 PCR program consisted of the following steps: 95°C for 2 min, 40 cycles of 95°C for 30 sec, 60°C for 45 sec, and 72° C for 45 sec, then 72°C for 5 min. The GFAP-cre and CX3CR1-cre PCR programs consisted of the following steps: 94°C for 2 min, then 10 cycles of 94°C for 20 sec, 65°C for 15 sec (-0.5°C per cycle), and 68°C for 10 sec, then 28 cycles of 94°C for 15 sec, 60°C for 15 sec, and 72°C for 10 sec, then finished at 72°C for 1 min. Both PCR protocols were run on an Eppendorf Model 5333 Mastercycler. The PCR product was run on a 2% agarose gel made in TAE buffer at 150 V for 30-40 min, and the gel was imaged on the Cell Bioscience FluorChem E imager.

3.3. Induction of cre recombinase

Tamoxifen (Sigma-Aldrich, St. Louis, MO; T5648) was dissolved in corn oil at a concentration of 20 mg/ml by shaking overnight at 37°C in a light-blocking vessel. 75 mg/kg of tamoxifen was injected intraperitoneally for 5 consecutive days to induce cre. Cre induction was maintained by tamoxifen injections twice per week until euthanasia.

3.4. Facial nerve axotomy

Aseptic procedures were followed during the surgery following National Institute of Health guidelines. FNA was performed on 8 week old female mice following previously established methods (Olmstead et al., 2015). Briefly, mice were anesthetized with 2.5% isoflurane in 0.9 L/min oxygen, and sedation was monitored by confirming absence of the toe pinch reflex. The area behind the ear was shaved, and the skin was sterilized with alternating wipes of betadine and 70% ethanol, repeated three times. Using spring scissors, an incision approximately 4 mm in length was made behind the ear protuberance. The underlying subcutaneous tissue was bluntly dissected until the facial nerve trunk could be observed exiting the stylomastoid foramen. The nerve was transected, and the remaining nerve stumps were separated to prevent reconnection. The incision was closed with a sterile wound clip, and confirmation of the FNA was performed by assessing whisker movement and eye blink reflexes after completion of the surgery. Animals were monitored post-operatively for complications for five dpo, and the wound clip was removed at 7-10 dpo.

3.5. Isolation and adoptive transfer of whole splenocytes and CD4+ T cells

Donor mice (1:1 donor:recipient ratio) were euthanized with CO_2 inhalation followed by cervical dislocation. The spleen was dissected out and placed in a gentleMACS C Tube (Miltenyi Biotec, San Diego, CA; 130-093-237) with buffer (1× PBS, 0.5% bovine serum albumin, and 2 mM EDTA) and dissociated into a single-cell suspension using a gentleMACS Dissociator following the Miltenyi Biotec gentleMACS

protocol. The suspension was passed through a 70 µm cell filter into a sterile 50 ml conical tube, and centrifuged at 300 x *g* for 10 min at 4°C.

For whole splenocyte collection, red blood cell lysis was performed using ACK Lysing Buffer (Thermo Fisher Scientific; A1049201) for 4 min at RT. The reaction was diluted with 45 ml buffer, then centrifuged at 300 x *g* for 10 min at 4°C. The pellet was resuspended in 1 ml buffer/spleen, filtered, and a cell count was performed. PBS was added to the cell suspension to increase the volume to 45 ml, then the mixture was centrifuged at 300 x *g* for 10 min at 4°C. The pellet was resuspended in PBS to make a 5 x 10^8 cells/ml concentration of whole splenocytes. Immediately prior to injection, cells were passed through a 70 µm cell filter, and 50 x 10^6 WS in 100 µl of PBS were injected into the recipient mouse tail vein.

CD4+ T cell isolation began with generation of a single-cell suspension of whole splenocytes. Red blood cell lysis was not performed to maximize CD4+ T cell yield. The whole splenocyte cell pellet was incubated with CD4 (L3T4) MicroBeads (Miltenyi Biotec, 130-049-201) per manufacturer protocol, and magnetic separation was performed with the Possel_d2 program on an autoMACS™ Pro Separator. A cell count was performed, then cells were washed with PBS and centrifuged at 300 x *g* for 10 min at 4°C. The pellet was resuspended in PBS to make a 5 x 10^7 cells/ml concentration of CD4+ T cells. Immediately prior to injection, cells were passed through a 70 µm cell filter, and 5 x 10^6 CD4+ T cells in 100 µl of PBS were injected into the recipient mouse tail vein.

CD4+ cell fraction purity was measured using flow cytometry with FITC rat anti-mouse CD4 antibody (BD Pharmingen, San Jose, CA; 557307). In the WT CD4+ T cell

treatment group, 97% of the magnetic-sorted splenocytes were CD4+ (data not shown), in accordance with our previously published work (Serpe et al., 2003; Xin et al., 2011). In the mSOD1 CD4+ T cell group, cells were manually sorted due to a malfunction of the AutoMACS, and 75% of cells in the positive fraction were CD4+ (data not shown).

3.6. Laser-capture microdissection

Experimental animals were euthanized via CO_2 inhalation followed by cervical dislocation at 7, 14, 28, and 56 dpo. An unoperated group was also included as a 0 dpo control. Brains were rapidly removed and immediately flash frozen in an *n*-butyl bromide (62.5%) and 2-methyl butane (26.5%) biphasic solution chilled on dry ice to -30ºC, then stored at -80ºC. The brains were embedded in Optimal Cutting Temperature compound, and 25 µm cryostat sections of the entire rostral-caudal extent of the facial nucleus within the brainstem were collected on Leica glass polyethylene foil membrane slides (Nuhsbaum, McHenry, IL, 11505158) and stored at -80ºC. Tissue staining and laser capture microdissection were performed using methods previously described (Mesnard et al., 2010). The right (axotomized, Ax) and left (control, C) facial motor nuclei were laser-captured using a Leica ASLMD, and FMN and surrounding neuropil were collected together.

3.7. RNA extraction and reverse transcription

RNA extraction was performed per the Arcturus PicoPure® RNA Isolation Kit protocol (Thermo Fisher Scientific; KIT0204). RNA yield was quantified with a NanoDrop 2000 Spectrophotometer. 60 ng of RNA was reverse transcribed into cDNA

using the SuperScript® VILO cDNA Synthesis Kit and Master Mix following manufacturer instructions (Thermo Fisher Scientific; 11754050).

3.8. qPCR

qPCR was performed using an Eppendorf Realplex Mastercycler system. The 20 µl reaction volume contained 1 µl of cDNA, 1 µl of 20× TaqMan® FAM gene expression assay (Table 2), 8 µl of 0.002% diethyl pyrocarbonate-treated water, and 10 µl of TaqMan Gene Expression Master Mix (Thermo Fisher Scientific; 4369016). The qPCR program was as follows: UDG optimization at 50°C for 2 min, AmpliTaq Gold Activation at 95°C for 10 min, and then 40 cycles of denaturation at 95°C for 15 sec followed by annealing/extension at 60°C for 1 min.

We have previously established percent-changes in mRNA expression after axotomy using custom-made primers and SYBR® green reagents (Mesnard et al., 2010; Mesnard et al., 2011; Haulcomb et al., 2014). We opted to use the TaqMan assays in these experiments because of their enhanced sensitivity and specificity for gene targets (Alvarez & Done, 2014). To validate use of the TaqMan assays, side-by-side comparisons of results were obtained using the SYBR and TaqMan systems. This comparison revealed that both SYBR and TaqMan yielded similar results for all genes of interest except *Cd68* and *Tnfr1*. To maintain consistency with previously established results, custom primers and TaqMan probes were used for *Cd68* (F 5'-CCCAAATTCAAATCCGAATCC-3', R 5'-GGTACCGTCACAACCTCC-3', probe 5'-AAAGTGAGTGCGTCCCTTGCAGCC-3') and *Tnfr1* (F 5'-

TGCCATGCAGGGTTCTTTCTG-3', R 5'-TTTGCAAGCGGAGGAGGTAGG-3', probe 5'-ACCCAATTCAGGGTGGAAGAAAGGT-3').

3.9. Statistical analysis of qPCR data

The percent change in mRNA expression between axotomized and control facial motor nuclei was calculated using the Pfaffl method, with glyceraldehyde 3-phosphate dehydrogenase (*Gapdh*) as the reference gene (Pfaffl, 2001). Relative gene expression of *Tnfα* compared to *Gapdh* was used to quantify mRNA expression in the axotomized facial motor nucleus because there is no detectable expression of *Tnfα* in the control facial motor nucleus. The Grubbs' test was performed on the calculated values to detect and remove outliers (GraphPad QuickCalcs). Statistical significance was calculated in SigmaPlot 13.0 using two-way ANOVA (factors: group × postoperative time, for each individual gene) followed by Student-Neuman-Keuls post hoc multiple comparisons analysis with a significance level of $p < 0.05$.

To validate that axotomy does not induce mRNA expression changes in the control FMNuc, one-way ANOVA of the relative expression of each gene of interest compared to GAPDH within the control FMNuc was performed at each postoperative timepoint with $p < 0.05$. For all genes examined, no statistically significant changes were detected (data not shown).

3.10. Fluorescent immunohistochemistry

At the appropriate timepoint post-FNA, IL-10/GFP reporter animals were euthanized and brain tissue was extracted following the protocol in section 3.6. Brains

were frozen instead of perfusion-fixed to preserve the GFP signal. After embedding brains in Optimal Cutting Temperature compound, 8 µm cryostat sections of the FMNuc were collected on Fisherbrand Superfrost Plus Microscope Slides (Thermo Fisher Scientific; 12-550-15) and stored in light-tight boxes at -20ºC.

Prior to staining, sections were circled with an Elite PAP Pen (Diagnostic BioSystems, Pleasanton, CA; K039). On-slide fixation was performed with PFA solution (filtered 4% paraformaldehyde in PBS, pH 7.4) for 15 min at RT, then washed with PBS 3 × 5 min in a humidified chamber. Blocking buffer comprised of 10% normal donkey serum (EMD Millipore, Billerica, MA; S30), 1% bovine serum albumin (Jackson Immunoresearch, West Grove, PA; 001-000-162), and 0.01% Triton X-100 in PBS was applied for 1 hr at RT. After the blocking step, primary antibodies diluted in blocking buffer were applied to the slide overnight at 4°C (Table 3). On the following day, slides were washed with PBS 3 × 5 min in a Coplin jar, then returned to the humidified chamber for incubation with secondary antibody diluted in blocking buffer for 1 hr at RT. Afterwards, slides were washed with PBS 3 × 5 min in a Coplin jar. Excess fluid was wiped from the slide, and 100 µl of DAPI Fluoromount-G (SouthernBioTech, Birmingham, AL; 0100-20) was applied before coverslipping. Imaging was performed using an Olympus BX-43 equipped with cellSens Entry version 1.9 software. Image processing, including subtraction of background and adjustments to histograms, were performed in ImageJ version 1.8.0_111.

3.11. Perfusion-fixation of animals

Mice received a lethal overdose of a mixture of 200 mg/kg ketamine and 5 mg/kg xylazine administered intraperitoneally. When the animal was deeply anesthetized, a catheter was inserted into the right ventricle of the heart, and the left ventricle was lanced. 50 ml of PBS then 50 ml of PFA was passed through the animal using a mechanical pump on its slowest setting. The brain was dissected out and placed in a Falcon tube with PFA for 4 hours on ice. The brain was then moved to a new tube with a solution of 30% sucrose in PBS to cryoprotect the tissue. After the tissue had sunk in the sucrose solution, it was stored at -80°C until cryosectioning.

3.12. Thionin stain and facial motoneuron counts

Flash frozen brains were sectioned at 25 µm on a cryostat, and sections containing the FMNuc were collected on Superfrost Plus slides. The sections were post-fixed in 4% PFA for 15 min, then washed in water for 2 × 5 min. Sections were stained with 1X thionin acetate for 10 min, rinsed with water for 30 sec, then dehydrated with a series of 30 sec washes with 50%, 70%, 95%, and 100% EtOH. Slides were incubated in Hemo-De clearing agent (Thermo Fisher Scientific; NC0174259) for a minimum of 3 days before coverslipping with Permount.

An uninvolved investigator coded all slide sets to blind investigators to treatment groups. The FMNuc was located using a Leica DMRB microscope fitted with a digital camera (Microfire Optronics S97808) operated with Neurolucida version 10.31 software. The nucleus ambiguus and facial nerve were used to precisely locate the caudal and rostral edges of the FMNuc. FMN profiles displaying a clear nucleus and nucleolus were

quantified for the entire axotomized and control FMNuc. The Abercrombie correction factor [$N = (n \times T)/(T + D)$] was applied, where N is the actual number of cells, n is the number of nuclear profiles, T is the thickness of the section (25 µm), and D is the average diameter of nuclei (18.8 µm for control, 18.5 µm for axotomized) (Mesnard et al., 2011). Mean percentage FMN survival was quantified by dividing the number of axotomized FMN by control FMN and multiplying by 100%. A student's t-test was performed in Excel 2013 to compare control and experimental groups with $p < 0.05$.

Target	**Primer Sequence (5' → 3')**
IL-10$^{fl/fl}$ F	CCA GCA TAG AGA GCT TGC ATT ACA
IL-10$^{fl/fl}$ R	GAG TCG GTT AGC AGT ATG TTG TCC AG
GFAP-cre F	GCC AGT CTA GCC CAC TCC TT
GFAP-cre R	TCC CTG AAC ATG TCC ATC AG
GFAP-cre internal positive control F	CTA GGC CAC AGA ATT GAA AGA TCT
GFAP-cre internal positive control R	GTA GGT GGA AAT TCT AGC ATC ATC C
CX3CR1-cre common F	AAG ACT CAC GTG GAC CTG CT
CX3CR1-cre mutant R	CGG TTA TTC AAC TTG CAC CA
CX3CR1-cre wild type R	AGG ATG TTG ACT TCC GAG TTG

Table 1: Forward and reverse primer sequences for PCR.

Gene	**TaqMan ID**	**RefSeq Accession Number**
Gfap	Mm01253033_m1	NM_001131020.1, NM_010277.3
Fas	Mm01204974_m1	NM_007987.2
Gap-43	Mm01144975_m1	NM_008083.2
β_{II}-tubulin (Tubb2a)	Mm00809562_s1	NM_009450.2
nNos (Nos1)	Mm00435175_m1	D14552.1 (GenBank)
Tnfα	Mm00443260_g1	NM_013693.3
Gapdh	Mm99999915_g1	NM_001289726.1, NM_008084.3
Arginase 1	Mm00475988_m1	NM_007482.3
Interferon-γ	Mm01168134_m1	NM_008337.3
Interleukin-10	Mm00439614_m1	NM_010548.2
Tradd	Mm01251031_g1	NM_001033161.2
Traf2	Mm00801978_m1	NM_001290413.1, NM_009422.3
Fadd	Mm00438861_m1	NM_010175.5

Table 2: Catalog information for qPCR TaqMan assays ordered from Thermo Fisher Scientific.

Target	Conjugate	Class	Host species	Target species	Conc.	Dilution factor	Company	Catalog Number
GFAP	Alexa Fluor 594	Monoclonal	Mouse	Mouse, Human	1 mg/ml	1:500	Thermo Fisher Scientific	A-21295
GFP	Alexa Fluor 488	Polyclonal	Rabbit	Mouse, Rat, Human	2 mg/ml	1:100	Thermo Fisher Scientific	A-21311
Iba1	None	Polyclonal	Rabbit	Mouse, Rat, Human	0.5 mg/ml	1:500	Thermo Fisher Scientific	019-19741
NeuN	Alexa Fluor 555	Monoclonal	Mouse	Mouse, Rat	0.5 mg/ml	1:200	Millipore	MAB377A5
Secondary	Alexa Fluor 555	Polyclonal	Donkey	Rabbit	2 mg/ml	1:1000	Thermo Fisher Scientific	A-31572

Table 3: Antibody Information

CHAPTER 4: RESULTS

4.1. Aim 1: Determine the source of neuroprotective IL-10 in the axotomized facial motor nucleus

4.1.1. Validation of the IL-10/GFP reporter mouse

An IL-10/GFP reporter mouse was employed to determine what cell type in the CNS parenchyma was responsible for producing neuroprotective IL-10 after FNA. The IL-10/GFP mouse was created by Dr. Christopher Karp's laboratory at Cincinnati Children's Hospital by knocking in an internal ribosome entry site conjugated to the GFP gene between the IL-10 stop and poly-A tail sequences. The final mRNA transcript of the IL-10 gene allows for translation of both the IL-10 and GFP proteins separately (Madan et al., 2009; Sun et al., 2009).

To confirm the insertion of the GFP protein did not affect the axotomy model, FNA was performed on C57Bl/6 (WT) mice and IL-10/GFP reporter mice, and FMN survival was quantified at 28 dpo. IL-10/GFP FMN survival levels were not significantly different from WT (Figure 1, 84 ± 5% and 84 ± 3%, respectively, $p = 0.57$). WT FMN survival levels were comparable to previously published results (Serpe et al., 1999; Mesnard-Hoaglin et al., 2014).

4.1.2. Fluorescent immunohistochemistry of the IL-10/GFP reporter mouse

With confirmation that the IL-10/GFP FMN survival was comparable to WT, fluorescent immunohistochemistry (IHC) was performed to identify which cell types in the CNS produce IL-10. The hypothesis for this experiment was that microglia, not astrocytes or neurons, are the primary producers of IL-10 after FNA. This hypothesis was

based on previous studies in which microglia are described as sources of IL-10, especially in contexts where the microglia have adopted the neuroprotective M2 phenotype (Zhang et al., 2014; Ma et al., 2015; Chu et al., 2016).

4.1.2.1. GFP

First, a characterization of GFP expression in the uninjured FMNuc was performed. Previous results indicate that there exists a baseline expression of IL-10 in the FMNuc, and the immunofluorescence in the reporter mouse line confirms this (Xin et al., 2011). Because the endogenous GFP signal was weak, an anti-GFP antibody was employed to amplify the fluorescent signal. GFP was visibly detected in the uninjured FMNuc, as well as in the vasculature (data not shown). There were no visible differences in GFP expression between the control and axotomized FMNuc. Both punctate and neuronal-like forms of GFP were visible in both C and Ax FMNuc (Figures 2 and 3).

4.1.2.2. Microglia

The Iba1 antibody was used to assess microglia expression of IL-10. Iba1 is a microglia marker that was first described in 1996, and has been used in numerous neuroscience studies, including FNA studies (Imai et al., 1996; Graeber et al., 1998; Ito et al., 1998; Bohatschek et al., 2004a; Almolda et al., 2015). Unfortunately, the Iba1 antibody was ineffective in labeling microglia on flash-frozen brain tissue. When this experiment was conducted on tissue from animals perfusion-fixed with 4% PFA, as described in other GFP reporter mouse experiments, the GFP signal in this specific animal model was ablated (Zamanian et al., 2012; Frakes et al., 2014; Greenhalgh et al.,

2016). When tissue was flash-frozen then fixed on the slide for 15 min in cold 4% PFA, GFP signal was retained and both NeuN and GFAP antibodies worked effectively, however Iba1 failed to label microglia. Alternative antibodies were assessed for their ability to label microglia in flash-frozen tissue, however no success was achieved. Future directions for this experiment include examining alternative fixation strategies, such as 2% PFA or paraformaldehyde/lysine/periodate fixation, for their effectiveness in preserving GFP signal and retaining microglia antigenicity.

4.1.2.3. Astrocytes

Next, GFP expression was assessed in astrocytes of the FMNuc. The astrocyte-specific cell marker used was GFAP, a cytoskeletal protein within astrocytes. Astrocytes exist in a protoplasmic state in the uninjured FMNuc that is GFAP-, and after nerve injury, their phenotype shifts to a fibrillary phenotype that is strongly GFAP+ (Graeber et al., 1988; Hermanson et al., 1995; Laskawi & Wolff, 1996; Klein et al., 1997). In this study, the fibrillary phenotype was first detected at 3 dpo, and increased steadily throughout the timecourse, with the greatest number of GFAP+ astrocytes detected at 28 dpo (Figure 2). At 3 and 7 dpo, GFAP+ astrocytes did not colocalize with GFP. At 10 dpo, both GFAP+/GFP+ and GFAP+/GFP- astrocytes were detected. At 14 and 28 dpo, almost all GFAP+ astrocytes were GFP+. The inset from 28 dpo demonstrates that GFP labels the cytoplasm and processes of astrocytes. The MN-like morphology stain of GFP was still visible throughout the timecourse. Other small cells, likely microglia, were detectable as a DAPI nucleus surrounded by GFP that did not colocalize with NeuN or GFAP. To summarize, axotomy-activated astrocytes are negative for IL-10 in the early

post-axotomy phase, but at the late post-axotomy phase, astrocytes are induced to express IL-10.

4.1.2.4. Neurons

To verify the presence of GFP in the MN, *neu*ronal *n*uclei (NeuN) immunostaining was used to label FMN. NeuN was first described as an exclusive neuronal marker in 1992 (Mullen et al., 1992). It was later discovered that NeuN is the protein product of the Fox-3 gene, and it is a splicing regulator protein that binds RNA that is also a component of the neuronal nuclear matrix (Kim et al., 2009; Dent et al., 2010). After axotomy, NeuN phosphorylation diminishes antibody binding to the target, however this antibody affinity is not completely lost after axotomy (McPhail et al., 2004; Duffy et al., 2011; Tyzack et al., 2014; Yeh et al., 2017).

NeuN staining of uninjured FMN colocalized strongly with the GFP signal, demonstrating that FMN are a source of IL-10 in the homeostatic FMNuc (Figure 3). After facial nerve injury, NeuN intensity decreased significantly relative to the uninjured side from 3-14 dpo, with some recovery of signal at 28 dpo. Although NeuN signal was diminished, there was sufficient signal to allow for GFP colocalization to be examined. From 3-28 dpo, GFP colocalized with NeuN labeling. The inset image from 7 dpo demonstrates this labeling pattern, with GFP visible in the cytoplasm of the FMN, and a central clearing for the center of the nucleus. Overall, based on the GFP morphology and its colocalization with NeuN and DAPI, MN expression of GFP appears to be constant over the postoperative timecourse, with no significant gain or loss of GFP expression

detected. These data suggest that FMN are a significant source of IL-10 both before and after axotomy, with no significant changes induced by axotomy.

4.1.3. Selective knockdown of IL-10 and effects on FMN survival

To identify if a cell-specific source of IL-10 is crucial for FMN survival after injury, cre/lox mice were generated in which the IL-10 gene was floxed in either GFAP-cre or CX3CR1-cre mouse strains. Cre activity was induced with tamoxifen, FNA was performed, and FMN survival was quantified at 28 dpo. The control animals for this experiment were cre-negative or IL-$10^{fl/-}$ littermates that were also treated with tamoxifen and received FNA.

The hypothesis for this experiment was that microglia-derived IL-10 is crucial for FMN survival, therefore, CXCR1-cre+/IL-$10^{fl/fl}$ mice were predicted to have significantly greater loss of FMN after axotomy compared to littermate controls. Based on this hypothesis, we predicted that GFAP-cre+/IL-$10^{fl/fl}$ mice would exhibit FMN survival comparable to WT because microglia-derived IL-10 would be unaffected.

No significant loss of FMN was observed in CXCR1-cre+/IL-$10^{fl/fl}$ mice relative to littermate controls (Figure 4A, n = 8, 88 ± 3%, 83 ± 4%, $p = 0.30$, respectively). Similarly, GFAP-cre+/IL-$10^{fl/fl}$ mice FMN survival was not different from littermate controls (Figure 4B, n = 3, 81 ± 7%, 85 ± 7%, $p = 0.71$, respectively)

Overall, these data suggest that neither microglia- nor astrocyte-specific IL-10 production is critical for FMN survival after FNA. It is possible that mechanisms exist between microglia and astrocytes where one can compensate for the other's lack of IL-10

production to promote FMN survival. Alternatively, the FMN itself may be the source of neuroprotective IL-10.

4.2. Aim 2: Characterize gene expression profile changes after facial nerve axotomy in immunodeficient and WT CD4+ T cell immunoreconstituted mice

4.2.1. Motoneuron regeneration response

4.2.1.1. Gap-43

Gap-43 is a growth cone protein that is necessary for regenerating the daughter axon and reconnecting to target musculature (Bomze et al., 2001; Benowitz & Popovich, 2011). Measurement of *Gap-43* expression after axotomy can be used to assess the MN regeneration response (Tetzlaff et al., 1991; Bisby & Tetzlaff, 1992; Mesnard et al., 2010; Mesnard et al., 2011; Haulcomb et al., 2014).

Analysis of *Gap-43* expression after FNA comparing WT and RAG-$2^{-/-}$ mice revealed a significant effect of group (Figure 5, $F_{1,48} = 6.287$, $p = 0.016$) and postoperative time ($F_{4,48} = 101.069$, $p < 0.001$). In the WT group, expression of *Gap-43* was significantly increased relative to control at 7, 14, and 28 dpo, and levels returned to baseline at 56 dpo (1083 ± 41%, 1239 ± 128%, 351 ± 38%, respectively; $p < 0.05$). In the RAG-$2^{-/-}$ group, *Gap-43* expression was similarly increased relative to control at 7 and 14 dpo, however, levels were not different from baseline at 28 and 56 dpo (873 ± 77%, 1057 ± 79%, respectively; $p < 0.05$). There were no statistically significant differences between the WT and RAG-$2^{-/-}$ groups at any timepoint. This finding suggests that immunodeficiency does not impair the MN regeneration response after axotomy.

With adoptive transfer of WT CD4+ T cells, *Gap-43* expression differed significantly from uninjured control at 7, 14, and 28 dpo, and returned to baseline at 56 dpo (1342 ± 81%, 1286 ± 92%, 485 ± 79%, respectively; $p < 0.05$). *Gap-43* expression was significantly higher in the RAG-$2^{-/-}$ + WT CD4+ group relative to WT at 7 dpo ($p = 0.038$). Comparing RAG-$2^{-/-}$ + WT CD4+ group to RAG-$2^{-/-}$ revealed significant differences in *Gap-43* expression at 7, 14 and 28 dpo ($p < 0.001$, 0.020, and 0.004, respectively). These data indicate that CD4+ T cells modestly enhance the MN regeneration response after axotomy.

4.2.1.2. β_{II}-tubulin

After axotomy, neurons upregulate expression of actin and tubulin cytoskeletal protein expression as part of the axonal regeneration program (Tetzlaff et al., 1988a; Tetzlaff et al., 1991; Bisby & Tetzlaff, 1992). *β_{II}-tubulin* has been previously used a measurement of the MN regeneration response after axotomy (Mesnard et al., 2010; Mesnard et al., 2011).

Analysis of *β_{II}-tubulin* expression after FNA comparing WT and RAG-$2^{-/-}$ mice revealed a significant effect of postoperative time (Figure 6, $F_{4,43} = 57.625$, $p < 0.001$). In the WT group, expression of *β_{II}-tubulin* was significantly increased relative to control at 7, 14, and 28 dpo, and levels returned to baseline at 56 dpo (163 ± 12%, 168 ± 19%, 57 ± 15%, respectively; $p < 0.05$). In the RAG-$2^{-/-}$ group, *β_{II}-tubulin* expression was similarly increased relative to control at 7, 14 and 28 dpo, then returned to baseline at 56 dpo (160 ± 21%, 178 ± 19%, 43 ± 26%, respectively; $p < 0.05$). There were no statistically significant differences between the WT and RAG-$2^{-/-}$ groups at any timepoint. This

finding suggests that immunodeficiency does not alter the MN regeneration response after axotomy.

With adoptive transfer of WT CD4+ T cells, *β_{II}-tubulin* expression was significantly different from uninjured control at 7, 14, and 28 dpo, and returned to baseline at 56 dpo (169 ± 13%, 171 ± 14%, 96 ± 14%, respectively; $p < 0.05$). Comparing the RAG-$2^{-/-}$ + WT CD4+ group to WT revealed no significant differences in *β_{II}-tubulin* expression throughout the timecourse. The comparison of the RAG-$2^{-/-}$ + WT CD4+ group to RAG-$2^{-/-}$ revealed significant differences in *β_{II}-tubulin* expression at 28 dpo ($p = 0.026$). These data indicate that CD4+ T cells do not significantly regulate the MN regeneration response after axotomy. The difference between the immunodeficiency and CD4+ T cell recipient groups may be a consequence of the increased FMN survival at 28 dpo in the CD4+ T cell group, given that *β_{II}-tubulin* is a MN-specific gene (Zhang et al., 2014).

4.2.2. Glial activation response

4.2.2.1. Gfap

Astrocytes play a key role after FNA, and their response to facial nerve injury has been well documented (Tetzlaff et al., 1988b; Hermanson et al., 1995; Laskawi & Wolff, 1996; Klein et al., 1997). The role of GFAP in astrocyte function is previously described in section 4.1.2.3.

Analysis of *Gfap* expression after FNA comparing WT and RAG-$2^{-/-}$ mice revealed a significant effect of group (Figure 7, $F_{1,44} = 12.978$, $p < 0.001$) and postoperative time ($F_{4,44} = 24.101$, $p < 0.001$). In the WT group, expression of *Gfap* was

significantly increased relative to control at 7, 14, 28, and 56 dpo (909 ± 97%, 805 ± 71%, 644 ± 121%, 307 ± 45%, respectively; $p < 0.05$). In the RAG-$2^{-/-}$ group, *Gfap* expression was similarly increased relative to control at 7 and 14 dpo, then fell to baseline levels at 28 and 56 dpo (782 ± 249%, 480 ± 79%, respectively; $p < 0.05$). There were statistically significant differences between the WT and RAG-$2^{-/-}$ groups at 14 and 28 dpo ($p = 0.029$ and 0.003, respectively). This finding suggests that immunodeficiency results in a failure to sustain astrocyte activation for the duration of the timecourse.

With adoptive transfer of WT CD4+ T cells, *Gfap* expression differed significantly from uninjured control at 7, 14, 28, and 56 dpo (646 ± 32%, 911 ± 31% 763 ± 97% 236 ± 79%, respectively; $p < 0.05$). Comparing the RAG-$2^{-/-}$ + WT CD4+ group to WT revealed a significant difference in *Gfap* expression at 7 dpo ($p = 0.011$). Comparing RAG-$2^{-/-}$ + WT CD4+ group to RAG-$2^{-/-}$ revealed significant differences in *Gfap* expression at 14 and 28 dpo ($p < 0.001$ for both). These data indicate that CD4+ T cells are responsible for regulating astrocyte activation after axotomy.

4.2.2.2. Cd68

Cluster of differentiation 68 (CD68) is a transmembrane glycoprotein that belongs to the lysosomal-associated membrane protein (LAMP) family and is highly expressed in myeloid cells (Holness et al., 1993; Holness & Simmons, 1993; Gottfried et al., 2008). CD68 rapidly cycles between the cell surface and the endosomal/lysosomal compartments, with a majority of CD68 found in the late endosomal compartment (Kurushima et al., 2000). CD68 can bind to oxidized low density lipoprotein and liposomes, otherwise its function is largely unknown (Ramprasad et al., 1995). In the

CNS, CD68 expression is commonly used as a proxy measurement for microglia activation (Yoshihara et al., 2002; Chen et al., 2004; Beers et al., 2008).

Analysis of *Cd68* expression after FNA comparing WT and RAG-2$^{-/-}$ groups revealed a significant effect of group (Figure 8, $F_{1,55} = 7.342$, $p = 0.009$) and postoperative time ($F_{4,55} = 17.366$, $p < 0.001$). In the WT group, axotomy significantly increased *Cd68* relative to the uninjured control at 7, 14, and 28 dpo, but not at 56 dpo (823 ± 109%, 772 ± 117%, 664 ± 78%, respectively; $p < 0.05$). In the RAG-2$^{-/-}$ group, *Cd68* expression was also significantly elevated relative to baseline after axotomy at 7 and 14 dpo, but not at 28 and 56 dpo (541 ± 73%, 654 ± 28%, respectively; $p < 0.05$). There was a statistically significant difference between the WT and RAG-2$^{-/-}$ groups at 28 dpo ($p = 0.036$). This finding suggests that immunodeficiency results in dysregulation of the microglia activation response in the late phase post-axotomy.

With adoptive transfer of WT CD4+ T cells, *Cd68* expression was significantly different from baseline at 7, 14, 28, and 56 dpo (749 ± 93%, 810 ± 62%, 626 ± 104%, 363 ± 103%, respectively; $p < 0.05$). There were no statistically significant differences between WT and RAG-2$^{-/-}$ + WT CD4+ groups at any timepoint. Comparing RAG-2$^{-/-}$ and RAG-2$^{-/-}$ + WT CD4+ groups revealed significant differences in *Cd68* expression at 28 and 56 dpo ($p = 0.011$, 0.037, respectively). These data suggest that CD4+ T cells regulate microglia activation after axotomy.

4.2.3. Inflammatory gene expression

4.2.3.1. Tnfα

Tnfα is a proinflammatory cytokine that is necessary for microglia expression of αXβ2 integrin, MHCI, and B7.2 costimulatory molecule expression after facial nerve injury (Raivich, 2002; Bohatschek et al., 2004a; Bohatschek et al., 2004b). Additionally, knocking out both TNFR1&2 simultaneously promotes motoneuron survival after facial nerve injury, suggesting that TNFα may have dual roles in immune-mediated neuroprotection (Raivich, 2002).

For all groups and timepoints, there was no detectable *Tnfα* expression in the C FMNuc. Therefore, data shown is relative gene expression from the axotomized side only.

Analysis of *Tnfα* expression after FNA comparing WT and RAG-$2^{-/-}$ groups revealed a significant effect of group (Figure 9, $F_{1,26} = 10.004$, $p = 0.004$) and a significant interaction between group × postoperative time ($F_{3,26} = 5.166$, $p = 0.006$). In the WT group, axotomy significantly increased *Tnfα* relative to the uninjured control at 7 and 14 dpo, then returned to baseline levels at 28 and 56 dpo ($4.43 \times 10^{-4} \pm 9.09 \times 10^{-5}$, $2.71 \times 10^{-4} \pm 1.04 \times 10^{-4}$, respectively; $p < 0.05$). In the RAG-$2^{-/-}$ group, *Tnfα* expression was never significantly elevated relative to baseline at 7, 14, 28, or 56 dpo. There was a statistically significant difference between the WT and RAG-$2^{-/-}$ groups at 7 dpo ($p < 0.001$). This finding suggests that immunodeficiency impairs early expression of *Tnfα*.

With adoptive transfer of WT CD4+ T cells, *Tnfα* expression differed significantly from baseline at 7, 14, and 28 dpo, then levels returned to baseline at 56 dpo ($3.30 \times 10^{-4} \pm 4.95 \times 10^{-5}$, $5.64 \times 10^{-4} \pm 9.63 \times 10^{-5}$, $3.18 \times 10^{-4} \pm 7.39 \times 10^{-5}$, respectively;

$p < 0.05$). There were statistically significant differences between WT and RAG-$2^{-/-}$ + WT CD4+ groups at 14 dpo ($p = 0.01$). Comparing RAG-$2^{-/-}$ and RAG-$2^{-/-}$ + WT CD4+ groups revealed significant differences in *Tnfα* expression at 7, 14, and 28 dpo ($p = 0.005$, <0.001, 0.037, respectively). These data suggest that CD4+ T cells regulate inflammatory cytokine production after axotomy.

4.2.3.2. Ifn-γ

Ifn-γ expression has been described in previous studies done by our lab in the axotomized FMNuc (Mesnard et al., 2010; Mesnard et al., 2011) using SYBR green reagents and custom primers. With TaqMan assays, *Ifn-γ* expression could not be detected in the C or Ax FMNuc in either WT or RAG-$2^{-/-}$ animals at 0, 7, 14, 28, and 56 dpo (n = 6 per group, per timepoint).

4.2.3.3. Il-10

Il-10 expression has been previously measured in our laboratory in 7 dpo WT and RAG-$2^{-/-}$ mice using SABiosciences primers (Xin et al., 2011). The TaqMan *Il-10* assay was tested on WT animals at all the experimental timepoints (n = 1 per timepoint), and *Il-10* was not detectable in either the C or Ax FMNuc at any of the timepoints (data not shown).

4.2.4. Cell death receptor expression

4.2.4.1. Tnfr1

TNFR1 is a receptor that trimerizes after binding to TNFα, and via two cell signaling cascades, can either induce apoptosis via caspase 8 or trigger inflammatory gene expression via AP-1 and NF-κB (Baud & Karin, 2001; Wajant & Scheurich, 2011). Because of its association with cell death pathways, *Tnfr1* expression was analyzed as a possible contributor to the increased MN death observed in RAG-$2^{-/-}$ mice.

Analysis of *Tnfr1* expression after FNA comparing WT and RAG-$2^{-/-}$ groups revealed a significant effect of postoperative time (Figure 10, $F_{4,46} = 5.643$, $p < 0.001$) and a significant interaction between group × postoperative time ($F_{4,46} = 4.806$, $p = 0.003$). In the WT group, axotomy significantly increased *Tnfr1* relative to the uninjured control only at 7 dpo (119 ± 31%; $p < 0.05$). In the RAG-$2^{-/-}$ group, *Tnfr1* expression was significantly elevated relative to baseline after axotomy only at 14 dpo (139 ± 29%; $p < 0.05$). There was a statistically significant difference between the WT and RAG-$2^{-/-}$ groups at both 7 and 14 dpo ($p < 0.001$, 0.029, respectively). These findings indicate a delayed *Tnfr1* expression in immunodeficient animals relative to WT, correlating with the immunodeficient *Tnfα* expression response described previously.

With adoptive transfer of WT CD4+ T cells, *Tnfr1* expression is significantly different from baseline at 7, 14, 28, and 56 dpo (219 ± 13%, 220 ± 15%, 135 ± 12%, 73 ± 6%, respectively; $p < 0.05$). There were statistically significant differences between WT and RAG-$2^{-/-}$ + WT CD4+ groups at 7, 14, and 28 dpo ($p < 0.001$, < 0.001, 0.005, respectively). Comparing RAG-$2^{-/-}$ and RAG-$2^{-/-}$ + WT CD4+ groups also revealed significant differences in *Tnfr1* expression at 7, 14, and 28 dpo ($p < 0.001$, 0.002, 0.001,

respectively). These data indicate that when CD4+ T cells are isolated from the other cells of the adaptive arm of the immune system, they significantly increase *Tnfr1* expression. This result suggests that other lymphocytes, such as CD8+ T cells or B cells, modulate CD4+ T cell induction of *Tnfr1*. Regardless, this *Tnfr1* expression is likely not associated with increased FMN death because FMN rescue is observed in RAG-$2^{-/-}$ + WT CD4+ T cell mice. Altogether, these data suggest that *Tnfr1* expression after FNA is not correlated with apoptosis, instead, it is more likely associated with NF-κB activation.

4.2.4.2. Tnfr1 transducers: Tradd, Fadd, Traf2

TNFR1 activation can result in induction of cell death or NF-κB activation. TRADD (Tumor necrosis factor receptor type 1-associated death domain) is a protein associated with both signaling pathways. FADD (Fas-associated protein with death domain) is associated with transduction of apoptosis signaling, whereas TRAF2 (TNF receptor-associated factor 2) is associated with NF-κB activation (Baud & Karin, 2001). To determine if these two signaling pathways were differentially regulated by WT CD4+ T cells, mRNA levels of *Tradd, Traf2,* and *Fadd* were measured at 7, 14, and 28 dpo. For the genes examined, no significant induction of expression was observed in either WT or RAG-$2^{-/-}$ + WT CD4+ T cell groups after axotomy (data not shown). When tested by two-way ANOVA, there were no statistically significant differences between WT and RAG-$2^{-/-}$ + WT CD4+ T cell group expression profiles. To better understand the differential regulation of *Tnfr1* expression after FNA, it is necessary to perform protein analysis of TNFR1 and its downstream mediators to quantify protein expression and assess protein activation status.

4.2.4.3. Fas

Fas is a cell death receptor with special relevance to MN death observed in mSOD1 MND. Upon FasL binding, cell death can be induced by two downstream signaling cascades: the death-induced signaling complex (DISC) involving caspases 8 and 3, or the Daxx/Ask1 (death-associated protein 6, apoptosis signal-regulating kinase 1, respectively) signaling cascade resulting in activation of neuronal nitric oxide synthase (nNos) (Raoul et al., 2002; Wajant, 2002). All CNS major cell types can produce FasL, with higher production in neurons and astrocytes (Flugel et al., 2000; Becher et al., 2006; Hovden et al., 2013; Zhang et al., 2014). Neuroimmunology studies reveal that this FasL expression by the brain protects the CNS from peripheral immune cells by utilizing Fas-mediated apoptosis (Flugel et al., 2000; Becher et al., 2006). Examination of cell death pathways in mSOD1 mice reveals that MN, especially from mSOD1 mice, are highly sensitive to Fas and NO mediated death (Raoul et al., 2002). Further work describes that exogenous NO triggers FasL expression in MN (Raoul et al., 2006). Additionally, blocking the Fas signaling cascade by knocking out Daxx results in greater MN survival and decreased FasL expression in mSOD1 mice (Raoul et al., 2006). A study of cell death receptor expression after FNA on mSOD1 mice after FNA revealed that Fas/nNos signaling was highly expressed relative to WT, suggesting that the mSOD1 mutation leads to prominent expression of this cell death pathway (Haulcomb et al., 2014). Because Fas/nNos is related to MN death after target disconnection in mSOD1 MND, we wanted to explore if it played a role in the increased FMN death observed in immunodeficient animals.

Analysis of *Fas* expression after FNA comparing WT and RAG-2$^{-/-}$ groups revealed a significant effect of group (Figure 11, $F_{1,52} = 10.566$, $p = 0.002$) and postoperative time ($F_{4,52} = 3.473$, $p = 0.014$). In the WT group, axotomy significantly increased *Fas* expression relative to the uninjured control at 7, 14, 28, and 56 dpo (70 ± 12%, 62 ± 16%, 62 ± 17%, 63 ± 21%, respectively; $p < 0.05$). In the RAG-2$^{-/-}$ group, *Fas* expression was not significantly elevated relative to baseline after axotomy at any of the examined timepoints. There was a statistically significant difference between the WT and RAG-2$^{-/-}$ groups at both 7 and 14 dpo ($p = 0.002$, 0.043, respectively). These findings suggest that *Fas* expression is not correlated with the increased neuronal loss observed in immunodeficient mice.

With adoptive transfer of WT CD4+ T cells, *Fas* expression differed significantly from baseline at 28 and 56 dpo (76 ± 14%, 84 ± 29%, respectively; $p < 0.05$). There were statistically significant differences between WT and RAG-2$^{-/-}$ + WT CD4+ groups at 7 dpo ($p = 0.004$). Comparing RAG-2$^{-/-}$ and RAG-2$^{-/-}$ + WT CD4+ groups also revealed significant differences in *Fas* expression at 56 dpo ($p = 0.006$). These data suggest that CD4+ T cells do not affect the early expression of *Fas*, however late expression of *Fas* does appear to be regulated by the adaptive arm of the immune system.

4.2.4.4. nNos

As described in the Fas section, nNos is a terminal step of the Fas signaling cascade that leads to apoptosis. Additionally, in the CNS, nNos expression is specifically located within MN, allowing it to be utilized as an indicator of MN-specific cell death (Raoul et al., 2002; Raoul et al., 2006; Haulcomb et al., 2014).

Analysis of *nNos* expression after FNA comparing WT and RAG-2$^{-/-}$ groups revealed a significant effect of postoperative time (Figure 12, $F_{4,44} = 4.036$, $p = 0.007$). In the WT group, axotomy significantly increased *nNos* relative to the uninjured control only at 56 dpo (26 ± 16%, respectively; $p < 0.05$). In the RAG-2$^{-/-}$ group, *nNos* expression was not significantly elevated relative to baseline after axotomy at any of the examined timepoints. There was a statistically significant difference between the WT and RAG-2$^{-/-}$ groups at 28 dpo ($p = 0.042$). These findings suggest that *nNos* expression, at most, is minorly associated with the increased neuronal loss observed at 28 dpo in immunodeficient mice.

With adoptive transfer of WT CD4+ T cells, *nNos* expression differs significantly from baseline at 56 dpo (4 ± 10%, 13 ± 8%, 23 ± 4%, 92 ± 23%, respectively; $p < 0.05$). There were statistically significant differences between WT and RAG-2$^{-/-}$ + WT CD4+ groups at 56 dpo ($p < 0.001$). Comparing RAG-2$^{-/-}$ and RAG-2$^{-/-}$ + WT CD4+ groups also revealed significant differences in *nNos* expression at 56 dpo ($p < 0.001$). These data suggest that CD4+ T cells do not significantly modify *nNos* expression except at the latest stage of the timecourse.

4.3. Aim 3: Analyze gene expression profile changes after facial nerve axotomy in mice immunoreconstituted with mSOD1 whole splenocytes or mSOD1 CD4+ T cells

4.3.1. Motoneuron regeneration response

4.3.1.1. Gap-43

Comparing RAG-2$^{-/-}$ + WT WS mice to WT revealed a significant effect of both group (Figure 13A, $F_{1,38} = 24.023$, $p < 0.001$) and postoperative time ($F_{3,38} = 39.362$, $p <$

0.001). In the RAG-$2^{-/-}$ + WT WS group, *Gap-43* expression was significantly increased relative to uninjured control at 7, 14, and 28 dpo, then levels returned to baseline at 56 dpo (1552 ± 129%, 2064 ± 258%, 1075 ± 305%, respectively; $p < 0.05$). *Gap-43* expression was significantly increased in RAG-$2^{-/-}$ + WT WS mice relative to WT at 7, 14, and 28 dpo ($p = 0.044$, <0.001, 0.002, respectively). These results indicate that provision of WS results in a significant increase in the MN regeneration response relative to WT, however this increased gene expression does not seem to translate to increased FMN survival after FNA.

When RAG-$2^{-/-}$ + mSOD1 WS mice were compared to WT, a significant effect of group (Figure 13B, $F_{1,41} = 31.420$, $p < 0.001$) and postoperative time ($F_{3,41} = 17.889$, $p < 0.001$) was observed. Additionally, there was a significant interaction between group × postoperative time ($F_{3,41} = 3.839$, $p = 0.016$). In the RAG-$2^{-/-}$ + mSOD1 WS group, *Gap-43* expression was significantly increased relative to uninjured control at 7, 14, and 28 dpo, then levels returned to baseline at 56 dpo (3412 ± 662%, 2845 ± 470%, 1370 ± 373%, respectively; $p < 0.05$). *Gap-43* expression was significantly increased in RAG-$2^{-/-}$ + mSOD1 WS mice relative to WT at 7, 14, and 28 dpo ($p < 0.001$, <0.001, 0.030, respectively). These results indicate that mSOD1 WS are also capable of augmenting the MN regeneration response.

When the RAG-$2^{-/-}$ + mSOD1 WS and RAG-$2^{-/-}$ + WT WS groups were compared, the mSOD1 WS treatment resulted in a significantly increased *Gap-43* expression response at 7 dpo (Figure 13C, p = 0.002), and the groups had similar responses for the remainder of the time course. This elevated *Gap-43* expression in the

RAG-2$^{-/-}$ + mSOD1 WS group is an intriguing finding given the increased FMN death observed in these animals after FNA.

When RAG-2$^{-/-}$ + mSOD1 CD4+ T cell mice were compared to WT, a significant effect of group (Figure 13D, $F_{1,42} = 36.893$, $p < 0.001$) and postoperative time ($F_{3,42} = 45.542$, $p < 0.001$) was observed. Additionally, there was a significant interaction between group × postoperative time ($F_{3,42} = 8.172$, $p < 0.001$). In the RAG-2$^{-/-}$ + mSOD1 CD4+ group, *Gap-43* expression was significantly increased relative to uninjured control at 7, 14, and 28 dpo, then levels returned to baseline at 56 dpo (2122 ± 293%, 3064 ± 395%, 820 ± 218%, respectively; $p < 0.05$). *Gap-43* expression was significantly increased in RAG-2$^{-/-}$ + mSOD1 CD4+ mice relative to WT at 7 and 14 dpo ($p = 0.001$, <0.001, respectively). These results indicate that mSOD1 CD4+ T cells increase the MN regeneration response relative to normal baseline.

When the RAG-2$^{-/-}$ + mSOD1 CD4+ and RAG-2$^{-/-}$ + WT CD4+ groups were compared, the mSOD1 CD4+ treatment resulted in a significantly increased *Gap-43* expression response at 7 and 14 dpo (Figure 13E, p = 0.003, <0.001). This elevated *Gap-43* expression in the early phase suggests that the SOD1 mutation within the T cell results in a differential induction of the MN regenerative response relative to WT CD4+ T cells.

Comparing the RAG-2$^{-/-}$ + mSOD1 CD4+ and RAG-2$^{-/-}$ + mSOD1 WS groups revealed a significant difference in *Gap-43* expression at 7 dpo (Figure 13F, $p = 0.019$). Despite the greater FMN loss observed in the RAG-2$^{-/-}$ + mSOD1 WS group, there is a significantly greater MN regeneration response observed in this group in the early phase post-injury relative to the mSOD1 CD4+ T cell recipient group.

4.3.1.2. β_{II}-tubulin

Comparing RAG-$2^{-/-}$ + WT WS mice to WT revealed a significant effect of both group (Figure 14A, $F_{1,33} = 15.900$, $p < 0.001$) and postoperative time ($F_{3,33} = 67.591$, $p < 0.001$). In the RAG-$2^{-/-}$ + WT WS group, *β_{II}-tubulin* expression was significantly increased relative to uninjured control at 7, 14, and 28 dpo, then levels returned to baseline at 56 dpo (198 ± 6%, 216 ± 9%, 127 ± 20%, respectively; $p < 0.05$). *β_{II}-tubulin* expression was significantly increased in RAG-$2^{-/-}$ + WT WS mice relative to WT at 14 and 28 dpo ($p = 0.015$, <0.001, respectively). These data indicate that provision of WS results in a significant increase in the MN regeneration response relative to WT.

When RAG-$2^{-/-}$ + mSOD1 WS mice were compared to WT, a significant effect of group (Figure 14B, $F_{1,37} = 4.829$, $p = 0.034$) and postoperative time ($F_{3,37} = 53.941$, $p < 0.001$) were observed. In the RAG-$2^{-/-}$ + mSOD1 WS group, *β_{II}-tubulin* expression was significantly increased relative to uninjured control at 7, 14, and 28 dpo, then levels returned to baseline at 56 dpo (160 ± 12%, 206 ± 21%, 113 ± 13%, respectively; $p < 0.05$). *β_{II}-tubulin* expression was significantly increased in RAG-$2^{-/-}$ + mSOD1 WS mice relative to WT at 28 dpo ($p = 0.006$). These results indicate that mSOD1 WS can modestly augment the MN regeneration response.

When the RAG-$2^{-/-}$ + mSOD1 WS and RAG-$2^{-/-}$ + WT WS groups were compared, there were no significant differences in the *β_{II}-tubulin* expression response (Figure 14C).

When RAG-$2^{-/-}$ + mSOD1 CD4+ T cell mice were compared to WT, a significant effect of group (Figure 14D, $F_{1,38} = 6.392$, $p = 0.016$) and postoperative time ($F_{3,38} = 69.531$, $p < 0.001$) were observed. Additionally, there was a significant interaction

between group × postoperative time ($F_{3,38} = 5.568$, $p = 0.003$). In the RAG-$2^{-/-}$ + mSOD1 CD4+ group, *β_{II}-tubulin* expression was significantly increased relative to uninjured control at 7, 14, and 28 dpo, then levels returned to baseline at 56 dpo (162 ± 7%, 200 ± 19%, 134 ± 9%, respectively; $p < 0.05$). *β_{II}-tubulin* expression was significantly increased in RAG-$2^{-/-}$ + mSOD1 CD4+ mice relative to WT at 28 dpo ($p < 0.001$). These results indicate that mSOD1 CD4+ T cells modestly increase the MN regeneration response relative to normal baseline.

When the RAG-$2^{-/-}$ + mSOD1 CD4+ and RAG-$2^{-/-}$ + WT CD4+ groups were compared, the mSOD1 CD4+ treatment resulted in a significantly increased *β_{II}-tubulin* expression response at 28 dpo (Figure 14E, p = 0.040). This elevated *β_{II}-tubulin* expression suggests that the mSOD1 mutation within the T cell results in a differential induction of the MN regenerative response relative to WT CD4+ T cells.

Comparing the RAG-$2^{-/-}$ + mSOD1 CD4+ and RAG-$2^{-/-}$ + mSOD1 WS groups revealed no significant differences in *β_{II}-tubulin* throughout the timecourse (Figure 14F). Despite the greater FMN loss observed in the RAG-$2^{-/-}$ + mSOD1 WS group, there is a significantly greater MN regeneration response observed in this group in the early phase post-injury relative to the mSOD1 CD4+ T cell recipient group.

4.3.2. Glial activation response

4.3.2.1. Gfap

Comparing RAG-$2^{-/-}$ + WT WS mice to WT revealed a significant effect of both group (Figure 15A, $F_{1,34} = 98.170$, $p < 0.001$) and postoperative time ($F_{3,34} = 4.847$, $p = 0.006$) on *Gfap* expression. In the RAG-$2^{-/-}$ + WT WS group, *Gfap* expression was

significantly increased relative to uninjured control at 7, 14, 28, and 56 dpo (2234 ± 213%, 2313 ± 255%, 2175 ± 435%, 1492 ± 4%, respectively; $p < 0.05$). *Gfap* expression was significantly increased in RAG-2$^{-/-}$ + WT WS mice relative to WT at 7, 14, 28, and 56 dpo ($p < 0.001$ for each). These results indicate that adoptive transfer of WS results in a significant increase in the astrocyte activation response relative to WT.

When RAG-2$^{-/-}$ + mSOD1 WS mice were compared to WT, a significant effect of group (Figure 15B, $F_{1,38} = 45.296$, $p < 0.001$) and postoperative time ($F_{3,38} = 5.103$, $p = 0.005$) was observed. In the RAG-2$^{-/-}$ + mSOD1 WS group, *Gfap* expression was significantly increased relative to uninjured control at 7, 14, 28, and 56 dpo (2205 ± 178%, 2681 ± 572%, 2080 ± 446%, 1116 ± 254%, respectively; $p < 0.05$). *Gfap* expression was significantly increased in RAG-2$^{-/-}$ + mSOD1 WS mice relative to WT at 7, 14, 28, and 56 dpo ($p < 0.001$ for each). These results indicate that mSOD1 WS are also capable of inducing a strong astrocyte activation response.

When the RAG-2$^{-/-}$ + mSOD1 WS and RAG-2$^{-/-}$ + WT WS groups were compared, there were no significant differences in the *Gfap* expression response (Figure 15C).

When RAG-2$^{-/-}$ + mSOD1 CD4+ T cell mice were compared to WT, a significant effect of group (Figure 15D, $F_{1,39} = 87.272$, $p < 0.001$) and postoperative time ($F_{3,39} = 3.704$, $p = 0.019$) was observed. In the RAG-2$^{-/-}$ + mSOD1 CD4+ group, *Gfap* expression was significantly increased relative to uninjured control at 7, 14, 28, and 56 dpo (2203 ± 385%, 3138 ± 270%, 2969 ± 313%, 1859 ± 515%, respectively; $p < 0.05$). *Gfap* expression was significantly increased in RAG-2$^{-/-}$ + mSOD1 CD4+ mice relative to WT at 7, 14, 28, and 56 dpo ($p = 0.002$, <0.001, <0.001, <0.001, respectively) These results

indicate that mSOD1 CD4+ T cells also significantly increase the astrocyte activation response relative to normal baseline.

When the RAG-$2^{-/-}$ + mSOD1 CD4+ and RAG-$2^{-/-}$ + WT CD4+ groups were compared, the mSOD1 CD4+ treatment resulted in a significantly increased *Gfap* expression response at all post-axotomy timepoints (Figure 15E, $p < 0.001$ for each). This elevated *Gfap* expression suggests that mSOD1 CD4+ T cell differentially affect the astrocyte activation response relative to WT CD4+ T cells.

Comparing the RAG-$2^{-/-}$ + mSOD1 CD4+ and RAG-$2^{-/-}$ + mSOD1 WS groups revealed no significant differences in *Gfap* levels throughout the timecourse (Figure 15F). Despite the greater FMN loss observed in the RAG-$2^{-/-}$ + mSOD1 WS group, there is comparable astrocyte activation observed between the two mSOD1 immunoreconstituted groups.

4.3.2.2. Cd68

Comparing RAG-$2^{-/-}$ + WT WS mice to WT revealed a significant effect of postoperative time (Figure 16A, $F_{1, 46} = 5.795$, $p = 0.002$) on *Cd68* expression. In the RAG-$2^{-/-}$ + WT WS group, *Cd68* expression was significantly increased relative to uninjured control at 7, 14, 28, and 56 dpo (811 ± 55%, 606 ± 49%, 636 ± 92%, 402 ± 106%, respectively; $p < 0.05$). There were no significant differences in *Cd68* expression between RAG-$2^{-/-}$ + WT WS and WT groups. These results indicate that adoptive transfer of WS results in an equivalent microglia activation response relative to WT.

When RAG-$2^{-/-}$ + mSOD1 WS mice were compared to WT, a significant effect of postoperative time (Figure 16B, $F_{3,38} = 6.972$, $p < 0.001$) was observed. In the RAG-$2^{-/-}$ +

mSOD1 WS group, *Cd68* expression was significantly increased relative to uninjured control at 7, 14, 28, and 56 dpo (857 ± 155%, 925 ± 125%, 920 ± 207%, 361 ± 76%, respectively; $p < 0.05$). *Cd68* expression was not significantly different in RAG-$2^{-/-}$ + mSOD1 WS mice relative to WT. These results indicate that mSOD1 WS are also capable of inducing a microglia activation response comparable to WT.

When the RAG-$2^{-/-}$ + mSOD1 WS and RAG-$2^{-/-}$ + WT WS groups were compared, there were no significant differences in the *Cd68* expression response (Figure 16C).

When RAG-$2^{-/-}$ + mSOD1 CD4+ T cell mice were compared to WT, a significant effect of postoperative time (Figure 16D, $F_{1,50} = 9.169$, $p < 0.001$) was observed. In the RAG-$2^{-/-}$ + mSOD1 CD4+ group, *Cd68* expression was significantly increased relative to uninjured control at 7, 14, 28, and 56 dpo (772 ± 127%, 725 ± 37%, 1063 ± 99%, 335 ± 63%, respectively; $p < 0.05$). *Cd68* expression was significantly increased in RAG-$2^{-/-}$ + mSOD1 CD4+ mice relative to WT at 28 dpo ($p = 0.022$) These results indicate that mSOD1 CD4+ T cells can modestly augment the microglia response at the late stage post-axotomy, otherwise the response is largely equivalent to WT.

When the RAG-$2^{-/-}$ + mSOD1 CD4+ and RAG-$2^{-/-}$ + WT CD4+ groups were compared, the mSOD1 CD4+ treatment results in a significantly increased *Cd68* expression response at 28 dpo (Figure 16E, $p = 0.001$). This elevated *Cd68* expression suggests that the there are some differences in the regulatory effects of mSOD1 and WT CD4+ T cells.

Comparing the RAG-$2^{-/-}$ + mSOD1 CD4+ and RAG-$2^{-/-}$ + mSOD1 WS groups revealed no significant differences in *Cd68* levels throughout the timecourse (Figure

16F). Despite the decreased FMN survival in the RAG-2$^{-/-}$ + mSOD1 WS group, there is comparable microglia activation observed between the two mSOD1 immunoreconstitution groups.

4.3.3. Inflammatory gene expression

4.3.3.1. Tnfα

Comparing RAG-2$^{-/-}$ + WT WS mice to WT revealed a significant effect of postoperative time (Figure 17A, $F_{3, 28} = 9.060$, $p < 0.001$) on *Tnfα* expression. There was also a significant interaction between group × postoperative time ($F_{3, 28} = 3.507$, $p = 0.028$). In the RAG-2$^{-/-}$ + WT WS group, *Tnfα* expression was significantly increased relative to uninjured control at 7 and 28 dpo ($2.71 \times 10^{-4} \pm 6.65 \times 10^{-5}$, $3.45 \times 10^{-4} \pm 1.20 \times 10^{-4}$, respectively; $p < 0.05$). There were no significant differences in *Tnfα* expression between RAG-2$^{-/-}$ + WT WS and WT groups. These results indicate that adoptive transfer of WS results in an equivalent inflammatory cytokine expression response relative to WT.

When RAG-2$^{-/-}$ + mSOD1 WS mice were compared to WT, a significant effect of postoperative time (Figure 17B, $F_{3,29} = 7.698$, $p < 0.001$) was observed. There was also a significant interaction between group × postoperative time ($F_{3, 29} = 4.187$, $p = 0.014$). In the RAG-2$^{-/-}$ + mSOD1 WS group, *Tnfα* expression was significantly increased relative to uninjured control at 7, 14, and 28 dpo ($2.16 \times 10^{-4} \pm 5.83 \times 10^{-5}$, $2.70 \times 10^{-4} \pm 1.33 \times 10^{-5}$, $3.67 \times 10^{-4} \pm 4.19 \times 10^{-5}$, respectively; $p < 0.05$). *Tnfα* expression was significantly different in RAG-2$^{-/-}$ + mSOD1 WS mice relative to WT at 7 and 28 dpo ($p = 0.011$,

0.040, respectively). These results indicate that mSOD1 WS elicit a differential *Tnfα* expression response at both early and late post-axotomy phases.

When the RAG-2$^{-/-}$ + mSOD1 WS and RAG-2$^{-/-}$ + WT WS groups were compared, there were no significant differences in the *Tnfα* expression response (Figure 17C).

When RAG-2$^{-/-}$ + mSOD1 CD4+ T cell mice were compared to WT, a significant effect of postoperative time (Figure 17D, $F_{1,29} = 8.417$, $p < 0.001$) was observed. There was also a significant interaction between group × postoperative time ($F_{3, 29} = 3.387$, $p = 0.031$). In the RAG-2$^{-/-}$ + mSOD1 CD4+ group, *Tnfα* expression was significantly increased relative to uninjured control at 28 dpo ($3.10 \times 10^{-4} \pm 8.41 \times 10^{-5}$; $p < 0.05$). There was a significant difference between WT and RAG-2$^{-/-}$ + mSOD1 CD4+ expression of *Tnfα* at 7 dpo ($p = 0.027$).

When the RAG-2$^{-/-}$ + mSOD1 CD4+ and RAG-2$^{-/-}$ + WT CD4+ groups were compared, the mSOD1 CD4+ treatment results in a significantly decreased *Tnfα* expression response at 14 dpo (Figure 17E, $p = 0.003$). This elevated *Tnfα* expression suggests that the mSOD1 CD4+ T cells differentially induce *Tnfα* expression relative to WT CD4+ T cells.

Comparing the RAG-2$^{-/-}$ + mSOD1 CD4+ and RAG-2$^{-/-}$ + mSOD1 WS groups revealed no significant differences in *Tnfα* levels throughout the timecourse (Figure 17F). Although greater FMN loss occurs in the RAG-2$^{-/-}$ + mSOD1 WS group after FNA, the *Tnfα* expression profiles between the two mSOD1 immunoreconstituted groups are similar.

4.3.4. Cell death receptor expression

4.3.4.1. Tnfr1

Comparing RAG-$2^{-/-}$ + WT WS mice to WT revealed a significant effect of postoperative time (Figure 18A, $F_{3, 34} = 5.112$, $p = 0.005$) on *Tnfr1* expression. In the RAG-$2^{-/-}$ + WT WS group, *Tnfr1* expression was significantly increased relative to uninjured control at 7, 14, and 28 dpo (84 ± 2%, 96 ± 4%, 86 ± 17%, respectively; $p < 0.05$). There were no significant differences in *Tnfr1* expression between RAG-$2^{-/-}$ + WT WS and WT groups. These results indicate that adoptive transfer of WS results in an equivalent *Tnfr1* expression response relative to WT.

When RAG-$2^{-/-}$ + mSOD1 WS mice were compared to WT, a significant effect of postoperative time (Figure 18B, $F_{3,38} = 6.638$, $p = 0.001$) was observed. In the RAG-$2^{-/-}$ + mSOD1 WS group, *Tnfr1* expression was significantly increased relative to uninjured control at 7, 14, 28, and 56 dpo (108 ± 5%, 102 ± 13%, 95 ± 13%, 44 ± 9%, respectively; $p < 0.05$). *Tnfr1* expression was not significantly different in RAG-$2^{-/-}$ + mSOD1 WS mice relative to WT. These results indicate that mSOD1 WS are also capable of inducing a *Tnfr1* expression response comparable to WT.

When the RAG-$2^{-/-}$ + mSOD1 WS and RAG-$2^{-/-}$ + WT WS groups were compared, there were no significant differences in the *Tnfr1* expression response (Figure 18C).

When RAG-$2^{-/-}$ + mSOD1 CD4+ T cell mice were compared to WT, a significant effect of postoperative time (Figure 18D, $F_{3,39} = 4.718$, $p = 0.007$) was observed. In the RAG-$2^{-/-}$ + mSOD1 CD4+ group, *Tnfr1* expression was significantly increased relative to uninjured control at 7, 14, 28, and 56 dpo (88 ± 7%, 102 ± 11%, 91 ± 16%, 52 ± 9%,

respectively; $p < 0.05$). There were no significant differences in *Tnfr1* expression between RAG-$2^{-/-}$ + mSOD1 CD4+ mice and WT mice. These results indicate that mSOD1 CD4+ T cells elicit a *Tnfr1* expression response equivalent to WT.

When the RAG-$2^{-/-}$ + mSOD1 CD4+ and RAG-$2^{-/-}$ + WT CD4+ groups were compared, the WT CD4+ treatment results in a significantly increased *Tnfr1* expression response at 7, 14, and 28 dpo (Figure 18E, $p < 0.001$, <0.001, and 0.015, respectively). These differential *Tnfr1* expression responses suggest that mSOD1 mutation affects the activity of isolated CD4+ T cells.

Comparing the RAG-$2^{-/-}$ + mSOD1 CD4+ and RAG-$2^{-/-}$ + mSOD1 WS groups revealed no significant differences in *Tnfr1* levels throughout the timecourse (Figure 18F).

4.3.4.2. Fas

Comparing RAG-$2^{-/-}$ + WT WS mice to WT revealed a significant effect of postoperative time (Figure 19A, $F_{4, 47} = 3.420$, $p = 0.016$) on *Fas* expression. In the RAG-$2^{-/-}$ + WT WS group, *Fas* expression was significantly increased relative to uninjured control at 28 and 56 dpo (65 ± 7%, 65 ± 31%, respectively; $p < 0.05$). There was a significant difference in *Fas* expression between RAG-$2^{-/-}$ + WT WS and WT groups at 7 dpo ($p = 0.024$). These results indicate that adoptive transfer of WS does not increase *Fas* expression to WT levels in the early post-axotomy phase.

When RAG-$2^{-/-}$ + mSOD1 WS mice were compared to WT, a significant effect of postoperative time (Figure 19B, $F_{4,50} = 6.602$, $p < 0.001$) was observed. In the RAG-$2^{-/-}$ + mSOD1 WS group, *Fas* expression was significantly increased relative to uninjured

control at 7, 14, 28, and 56 dpo (72 ± 23%, 55 ± 9%, 133 ± 23%, 82 ± 9%, respectively; $p < 0.05$). *Fas* expression was significantly different in RAG-$2^{-/-}$ + mSOD1 WS mice relative to WT at 28 dpo ($p = 0.006$). These results indicate that mSOD1 WS restore *Fas* expression at the early post-axotomy phase relative to WT levels, and also increase *Fas* expression in the late post-axotomy phase.

When the RAG-$2^{-/-}$ + mSOD1 WS and RAG-$2^{-/-}$ + WT WS groups were compared, there were significant differences in the *Fas* expression response at 7 and 28 dpo (Figure 19C, $p = 0.025$, 0.013, respectively). These findings demonstrate that WT WS do not affect early *Fas* expression, but mSOD1 WS do. At 28 dpo, mSOD1 WS significantly increase *Fas* expression.

When RAG-$2^{-/-}$ + mSOD1 CD4+ T cell mice were compared to WT, a significant effect of postoperative time (Figure 19D, $F_{3,44} = 7.115$, $p < 0.001$) was observed. Also, there was a significant interaction between group × postoperative time ($F_{3,44} = 7.919$, $p < 0.001$). In the RAG-$2^{-/-}$ + mSOD1 CD4+ group, *Fas* expression was significantly increased relative to uninjured control at 28 and 56 dpo (191 ± 32%, 81 ± 15%, respectively; $p < 0.05$). There was a significant difference in *Fas* expression between RAG-$2^{-/-}$ + mSOD1 CD4+ mice and WT mice at 28 dpo ($p < 0.001$). These results indicate that mSOD1 CD4+ T cells also increase *Fas* expression in the late post-axotomy phase.

When the RAG-$2^{-/-}$ + mSOD1 CD4+ and RAG-$2^{-/-}$ + WT CD4+ groups were compared, the mSOD1 CD4+ treatment resulted in a significantly increased *Fas* expression response at 28 dpo (Figure 19E, $p < 0.001$). These findings suggest that mSOD1 mutation affects T cell induction of *Fas* expression.

Comparing the RAG-2$^{-/-}$ + mSOD1 CD4+ and RAG-2$^{-/-}$ + mSOD1 WS groups revealed that the mSOD1 CD4+ T cells elicit a significantly greater *Fas* expression at 28 dpo (Figure 19F, $p = 0.038$). These data show that both mSOD1 lymphocyte groups results in augmented *Fas* expression at both early and late post-axotomy stages, with mSOD1 CD4+ T cells eliciting increased *Fas* expression at the late post-axotomy stage.

4.3.4.3. nNos

Comparing RAG-2$^{-/-}$ + WT WS mice to WT revealed a significant effect of postoperative time (Figure 20A, $F_{3, 34} = 3.333$, $p = 0.031$) on *nNos* expression. In the RAG-2$^{-/-}$ + WT WS group, *nNos* expression was not significantly different from uninjured control at any of the examined timepoints. There were no significant differences in *nNos* expression between RAG-2$^{-/-}$ + WT WS and WT groups. These results indicate that adoptive transfer of WS does not result in a differential *nNos* expression response relative to WT.

When RAG-2$^{-/-}$ + mSOD1 WS mice were compared to WT, a significant effect of group (Figure 20B, $F_{1,39} = 9.997$, $p = 0.003$) was observed. In the RAG-2$^{-/-}$ + mSOD1 WS group, *nNos* expression was significantly increased relative to uninjured control at 28 and 56 dpo (50 ± 25%, 62 ± 20%, respectively; $p < 0.05$). *nNos* expression was significantly different in RAG-2$^{-/-}$ + mSOD1 WS mice relative to WT at 28 dpo ($p = 0.032$). These results indicate that mSOD1 WS significantly increase *nNos* expression at the late post-axotomy phase relative to WT.

When the RAG-2$^{-/-}$ + mSOD1 WS and RAG-2$^{-/-}$ + WT WS groups were compared, there were no significant differences in the *nNos* expression response profiles

(Figure 20C). These findings demonstrate that WT WS and mSOD1 WS elicit comparable *nNos* expression responses.

When RAG-$2^{-/-}$ + mSOD1 CD4+ T cell mice were compared to WT, a significant effect of postoperative time (Figure 20D, $F_{3,38} = 5.804$, $p = 0.002$) was observed. Also, there was a significant interaction between group × postoperative time ($F_{3,38} = 4.647$, $p = 0.007$). In the RAG-$2^{-/-}$ + mSOD1 CD4+ group, *nNos* expression remained at baseline levels for the duration of the timecourse. There was a significant difference in *nNos* expression between RAG-$2^{-/-}$ + mSOD1 CD4+ mice and WT mice at 14 dpo ($p = 0.009$). These results indicate that mSOD1 CD4+ T cells increase *nNos* expression in the early post-axotomy phase.

When the RAG-$2^{-/-}$ + mSOD1 CD4+ and RAG-$2^{-/-}$ + WT CD4+ groups were compared, the WT CD4+ treatment resulted in a significantly increased *nNos* expression response at 56 dpo (Figure 20E, $p < 0.001$). These findings suggest that there is a modest differential effect of the mSOD1 mutation on isolated T cell regulation of *nNos* expression at the late post-axotomy phase.

Comparing the RAG-$2^{-/-}$ + mSOD1 CD4+ and RAG-$2^{-/-}$ + mSOD1 WS groups revealed that the mSOD1 WS treatments elicits a significantly greater *nNos* expression at 7 and 56 dpo (Figure 20F, $p = 0.030$, 0.020, respectively). These data show that adoptive transfer of mSOD1 WS results in a significantly greater expression of a MN-specific death mechanism relative to mSOD1 CD4+ T cells alone.

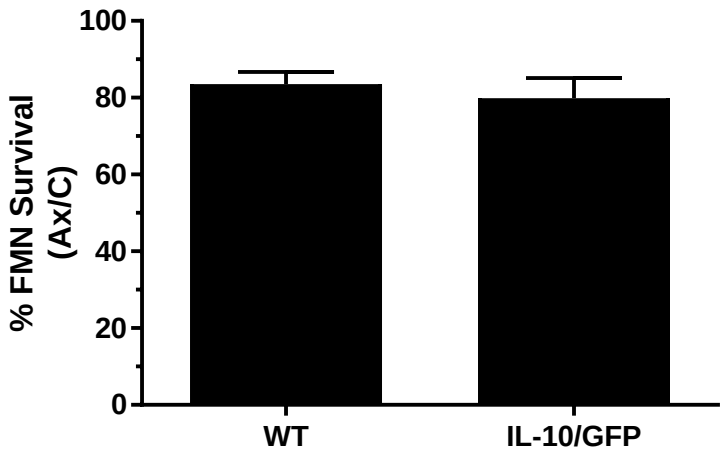

Figure 1: FMN survival in IL-10/GFP mice.

Average percent FMN survival ± SEM after FNA at 28 dpo.

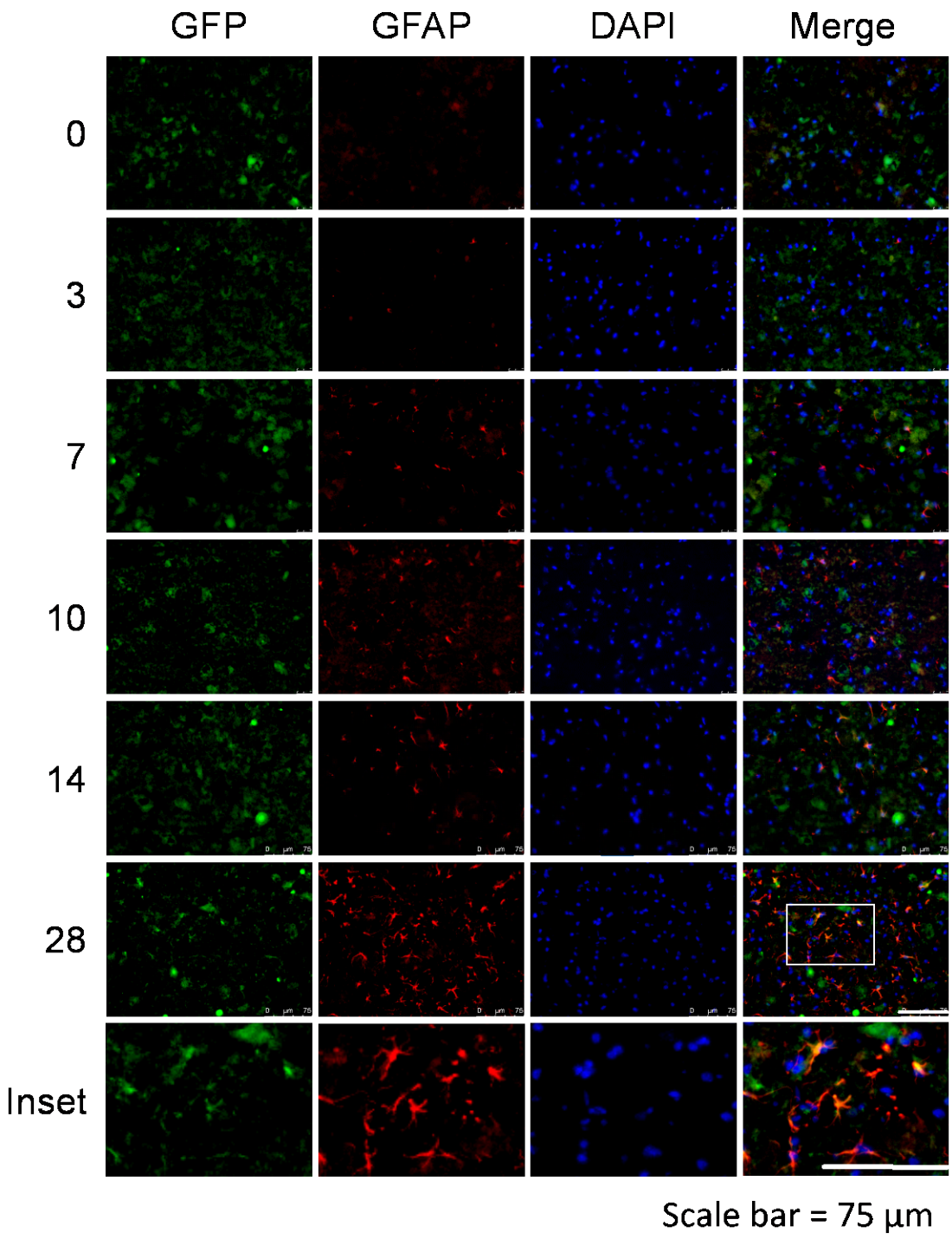

Figure 2: GFAP colocalization with IL-10/GFP.

GFAP fluorescent immunohistochemistry images at 40× magnification for the Ax FMNuc throughout the time course with IL-10/GFP reporter (green), GFAP (red), and nucleus (DAPI, blue) labeling. Numbers in the left correspond to days post-operation (dpo).

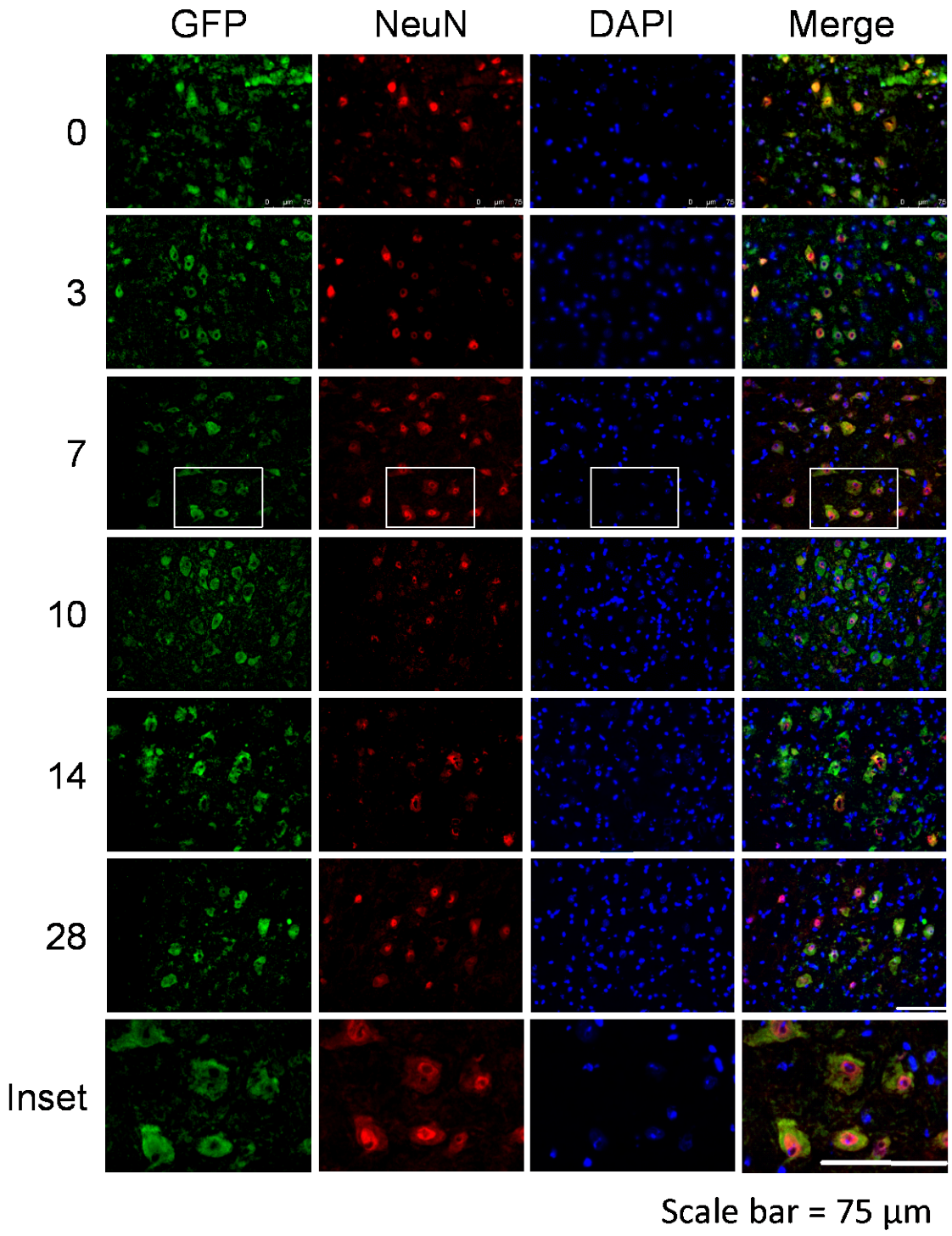

Figure 3: NeuN colocalization with IL-10/GFP.

Fluorescent immunohistochemistry images at 40× magnification of the Ax FMNuc throughout the time course with IL-10/GFP reporter (green), NeuN (red), and nucleus (DAPI, blue) labeling. Left column numbers are days post-operation (dpo).

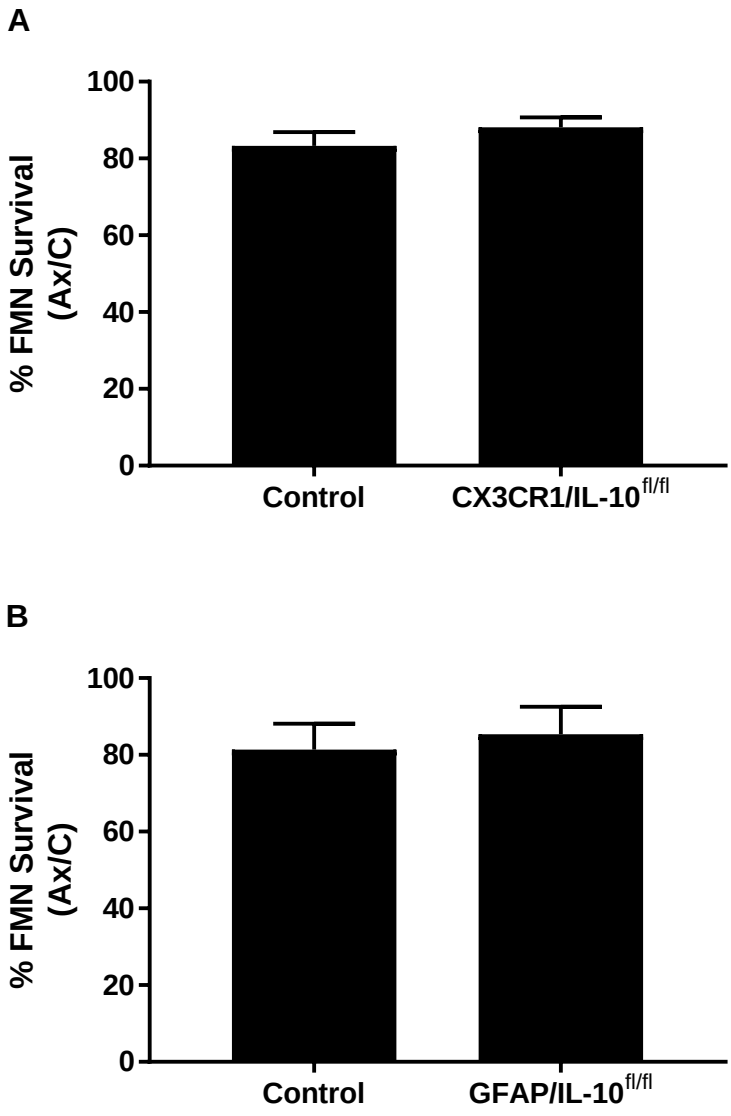

Figure 4: FMN survival in CX3CR1-cre/IL-$10^{fl/fl}$ and GFAP-cre/IL-$10^{fl/fl}$ mice.

Average percent FMN survival ± SEM after FNA at 28 dpo.

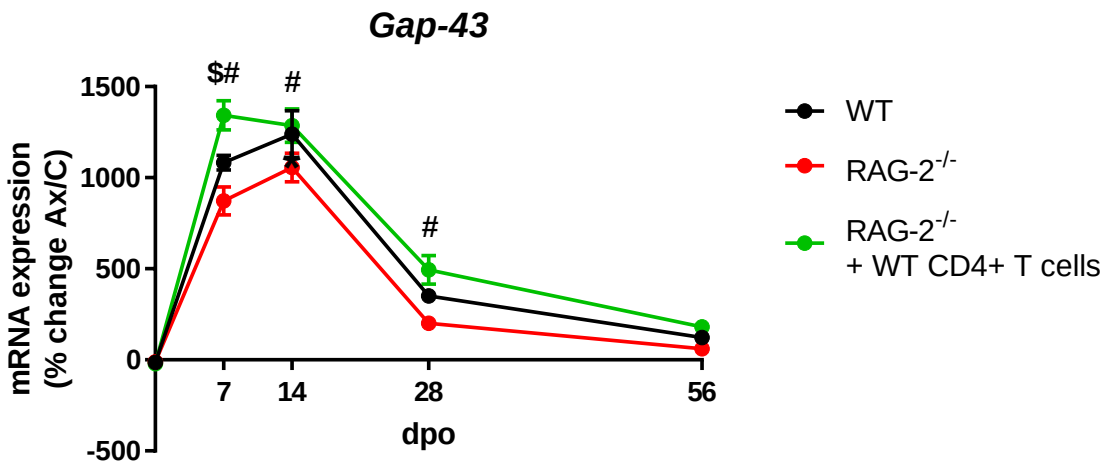

Figure 5: *Gap-43* gene expression profile after FNA in WT, RAG-$2^{-/-}$, and RAG-$2^{-/-}$ + WT CD4+ T cell groups.

mRNA expression of *Gap-43* in the facial motor nucleus following facial nerve axotomy (Ax), relative to the control (C) facial motor nucleus. Mean percent change ± SEM was plotted across uninjured (0) and 7, 14, 28, and 56 days post-operation (dpo) timepoints. Symbols used: *: $p < 0.05$ comparing WT to RAG-$2^{-/-}$; $: $p < 0.05$ comparing WT to RAG-$2^{-/-}$ + CD4+ T cells; and #: $p < 0.05$ comparing RAG-$2^{-/-}$ to RAG-$2^{-/-}$ + CD4+ T cells.

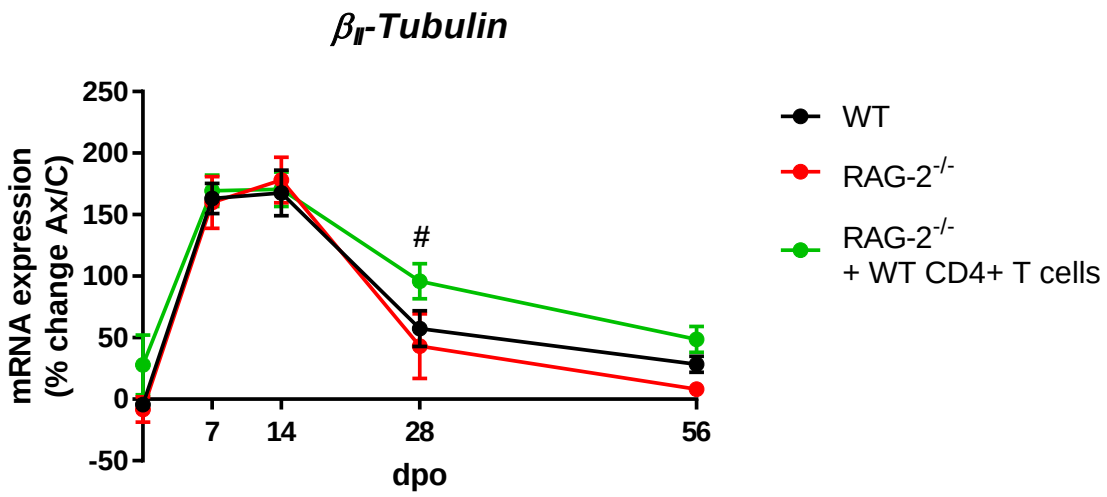

Figure 6: *β_{II}-tubulin* gene expression profile after FNA in WT, RAG-$2^{-/-}$, and RAG-$2^{-/-}$ + WT CD4+ T cell groups.

mRNA expression of *β_{II}-tubulin* in the facial motor nucleus following facial nerve axotomy (Ax), relative to the control (C) facial motor nucleus. Mean percent change ± SEM was plotted across uninjured (0) and 7, 14, 28, and 56 days post-operation (dpo) timepoints. Symbols used: *: $p < 0.05$ comparing WT to RAG-$2^{-/-}$; $: $p < 0.05$ comparing WT to RAG-$2^{-/-}$ + CD4+ T cells; and #: $p < 0.05$ comparing RAG-$2^{-/-}$ to RAG-$2^{-/-}$ + CD4+ T cells.

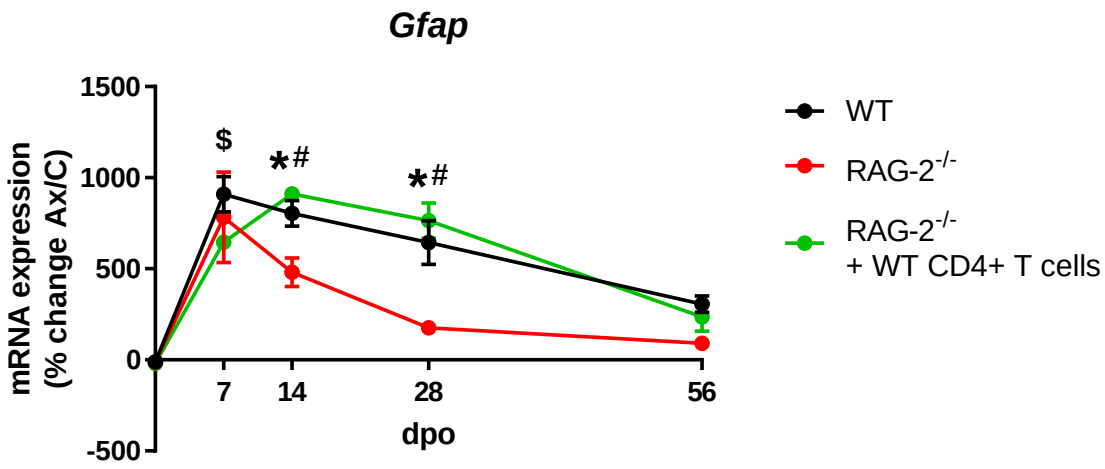

Figure 7: *Gfap* gene expression profile after FNA in WT, RAG-$2^{-/-}$, and RAG-$2^{-/-}$ + WT CD4+ T cell groups.

mRNA expression of *Gfap* in the facial motor nucleus following facial nerve axotomy (Ax), relative to the control (C) facial motor nucleus. Mean percent change ± SEM was plotted across uninjured (0) and 7, 14, 28, and 56 days post-operation (dpo) timepoints. Symbols used: *: $p < 0.05$ comparing WT to RAG-$2^{-/-}$; $: $p < 0.05$ comparing WT to RAG-$2^{-/-}$ + CD4+ T cells; and #: $p < 0.05$ comparing RAG-$2^{-/-}$ to RAG-$2^{-/-}$ + CD4+ T cells.

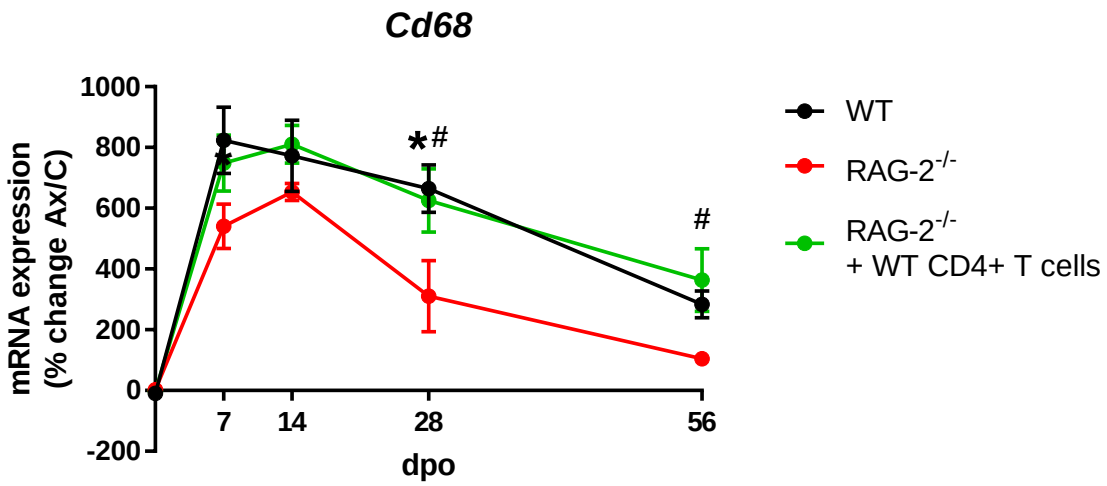

Figure 8: *Cd68* gene expression profile after FNA in WT, RAG-$2^{-/-}$, and RAG-$2^{-/-}$ + WT CD4+ T cell groups.

mRNA expression of *Cd68* in the facial motor nucleus following facial nerve axotomy (Ax), relative to the control (C) facial motor nucleus. Mean percent change ± SEM was plotted across uninjured (0) and 7, 14, 28, and 56 days post-operation (dpo) timepoints. Symbols used: *: $p < 0.05$ comparing WT to RAG-$2^{-/-}$; $: $p < 0.05$ comparing WT to RAG-$2^{-/-}$ + CD4+ T cells; and #: $p < 0.05$ comparing RAG-$2^{-/-}$ to RAG-$2^{-/-}$ + CD4+ T cells.

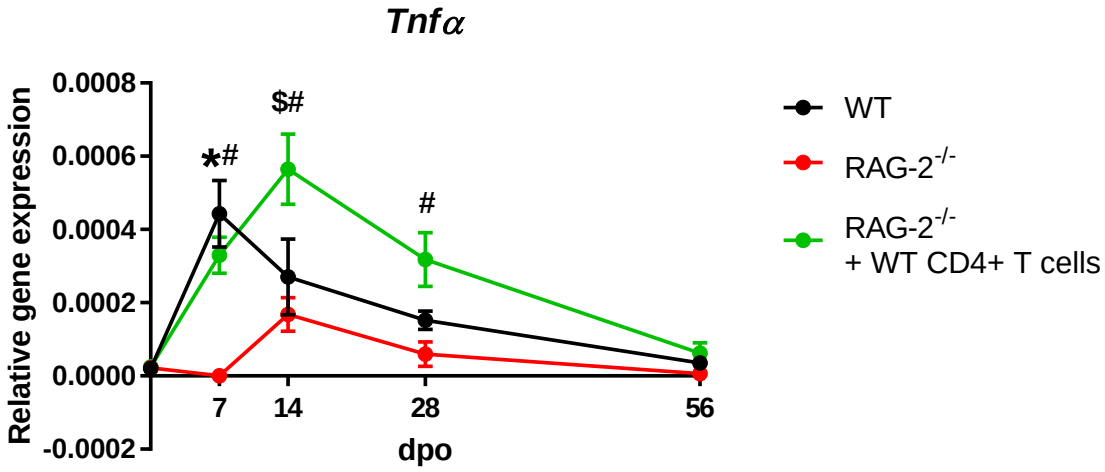

Figure 9: *Tnfα* gene expression profile after FNA in WT, RAG-$2^{-/-}$, and RAG-$2^{-/-}$ + WT CD4+ T cell groups.

mRNA expression of *Tnfα* in the facial motor nucleus following facial nerve axotomy (Ax), relative to the control (C) facial motor nucleus. Mean percent change ± SEM was plotted across uninjured (0) and 7, 14, 28, and 56 days post-operation (dpo) timepoints. Symbols used: *: $p < 0.05$ comparing WT to RAG-$2^{-/-}$; $: $p < 0.05$ comparing WT to RAG-$2^{-/-}$ + CD4+ T cells; and #: $p < 0.05$ comparing RAG-$2^{-/-}$ to RAG-$2^{-/-}$ + CD4+ T cells.

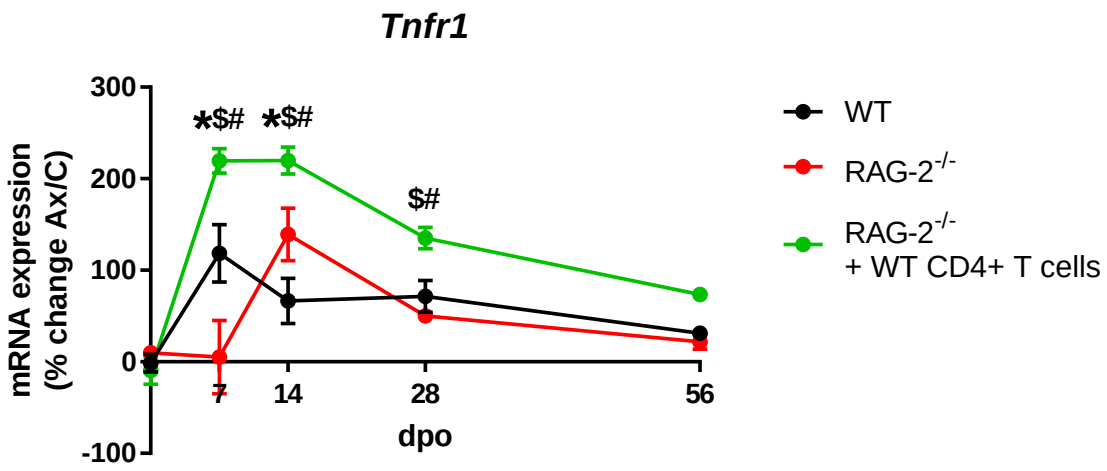

Figure 10: *Tnfr1* gene expression profile after FNA in WT, RAG-$2^{-/-}$, and RAG-$2^{-/-}$ + WT CD4+ T cell groups.

mRNA expression of *Tnfr1* in the facial motor nucleus following facial nerve axotomy (Ax), relative to the control (C) facial motor nucleus. Mean percent change ± SEM was plotted across uninjured (0) and 7, 14, 28, and 56 days post-operation (dpo) timepoints. Symbols used: *: $p < 0.05$ comparing WT to RAG-$2^{-/-}$; $: $p < 0.05$ comparing WT to RAG-$2^{-/-}$ + CD4+ T cells; and #: $p < 0.05$ comparing RAG-$2^{-/-}$ to RAG-$2^{-/-}$ + CD4+ T cells.

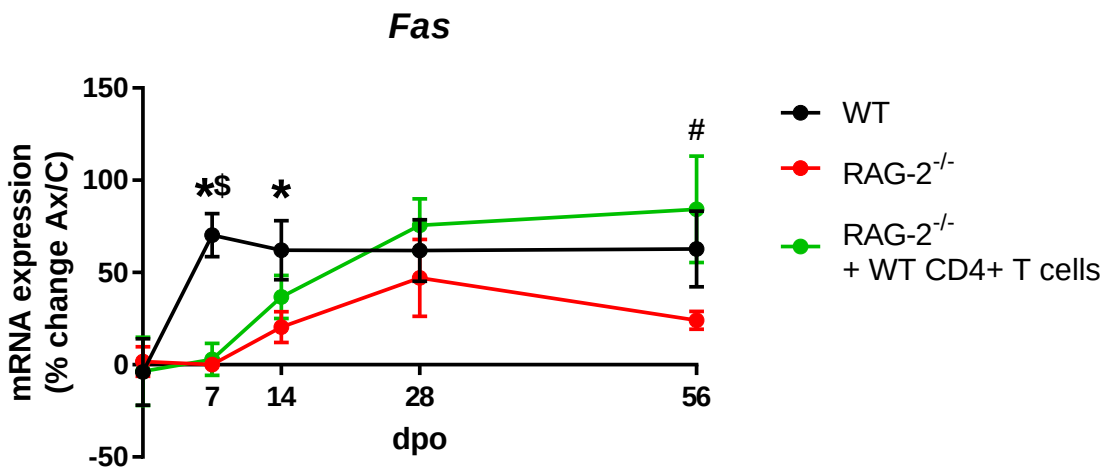

Figure 11: *Fas* gene expression profile after FNA in WT, RAG-$2^{-/-}$, and RAG-$2^{-/-}$ + WT CD4+ T cell groups.

mRNA expression of *Fas* in the facial motor nucleus following facial nerve axotomy (Ax), relative to the control (C) facial motor nucleus. Mean percent change ± SEM was plotted across uninjured (0) and 7, 14, 28, and 56 days post-operation (dpo) timepoints. Symbols used: *: $p < 0.05$ comparing WT to RAG-$2^{-/-}$; $: $p < 0.05$ comparing WT to RAG-$2^{-/-}$ + CD4+ T cells; and #: $p < 0.05$ comparing RAG-$2^{-/-}$ to RAG-$2^{-/-}$ + CD4+ T cells.

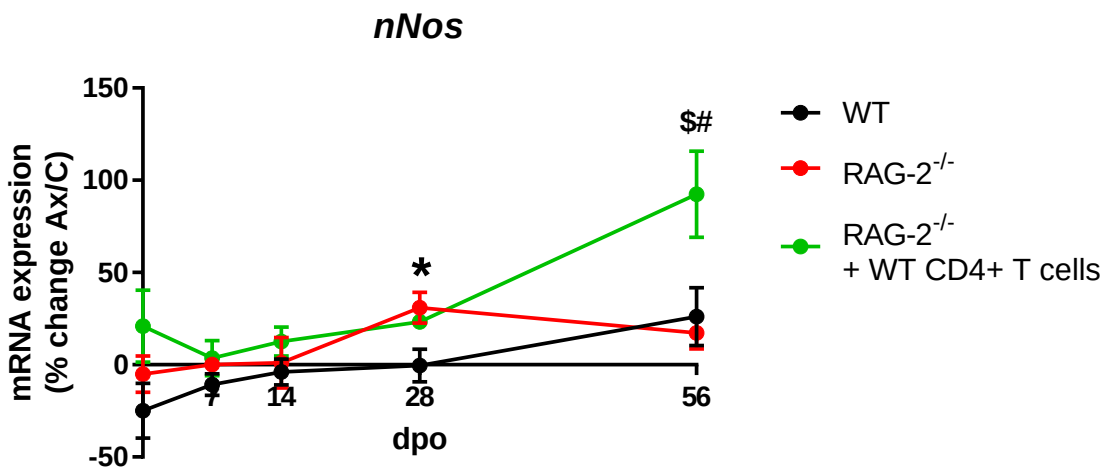

Figure 12: *nNos* gene expression profile after FNA in WT, RAG-$2^{-/-}$, and RAG-$2^{-/-}$ + WT CD4+ T cell groups.

mRNA expression of *nNos* in the facial motor nucleus following facial nerve axotomy (Ax), relative to the control (C) facial motor nucleus. Mean percent change ± SEM was plotted across uninjured (0) and 7, 14, 28, and 56 days post-operation (dpo) timepoints. Symbols used: *: $p < 0.05$ comparing WT to RAG-$2^{-/-}$; $: $p < 0.05$ comparing WT to RAG-$2^{-/-}$ + CD4+ T cells; and #: $p < 0.05$ comparing RAG-$2^{-/-}$ to RAG-$2^{-/-}$ + CD4+ T cells.

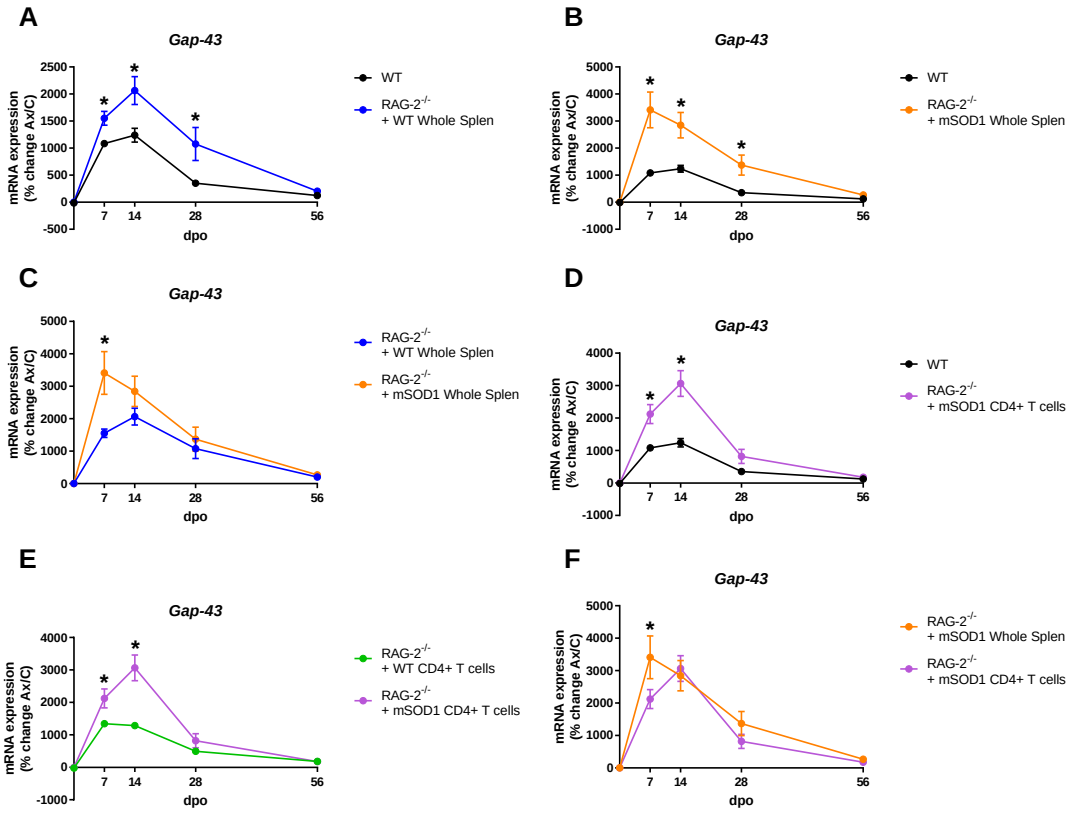

Figure 13: *Gap-43* gene expression profile after FNA in RAG-2$^{-/-}$ + WT WS, RAG-2$^{-/-}$ + mSOD1 WS and RAG-2$^{-/-}$ + mSOD1 CD4+ T cell groups.

mRNA expression of *Gap-43* in the facial motor nucleus following facial nerve axotomy (Ax), relative to the control (C) facial motor nucleus. Mean percent change ± SEM was plotted across uninjured (0) and 7, 14, 28, and 56 days post-operation (dpo) timepoints. Symbols used: *: $p < 0.05$.

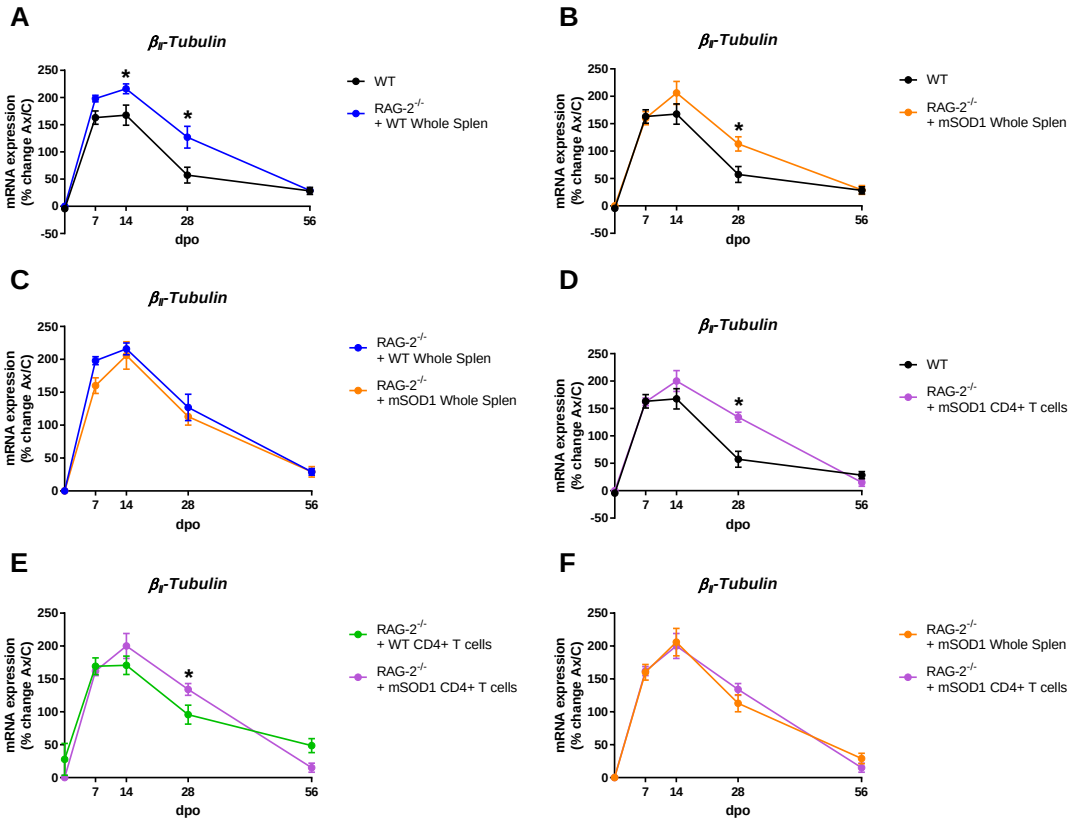

Figure 14: *β_{II}-tubulin* gene expression profile after FNA in RAG-2$^{-/-}$ + WT WS, RAG-2$^{-/-}$ + mSOD1 WS and RAG-2$^{-/-}$ + mSOD1 CD4+ T cell groups.
mRNA expression of *β_{II}-tubulin* in the facial motor nucleus following facial nerve axotomy (Ax), relative to the control (C) facial motor nucleus. Mean percent change ± SEM was plotted across uninjured (0) and 7, 14, 28, and 56 days post-operation (dpo) timepoints. Symbols used: *: $p < 0.05$.

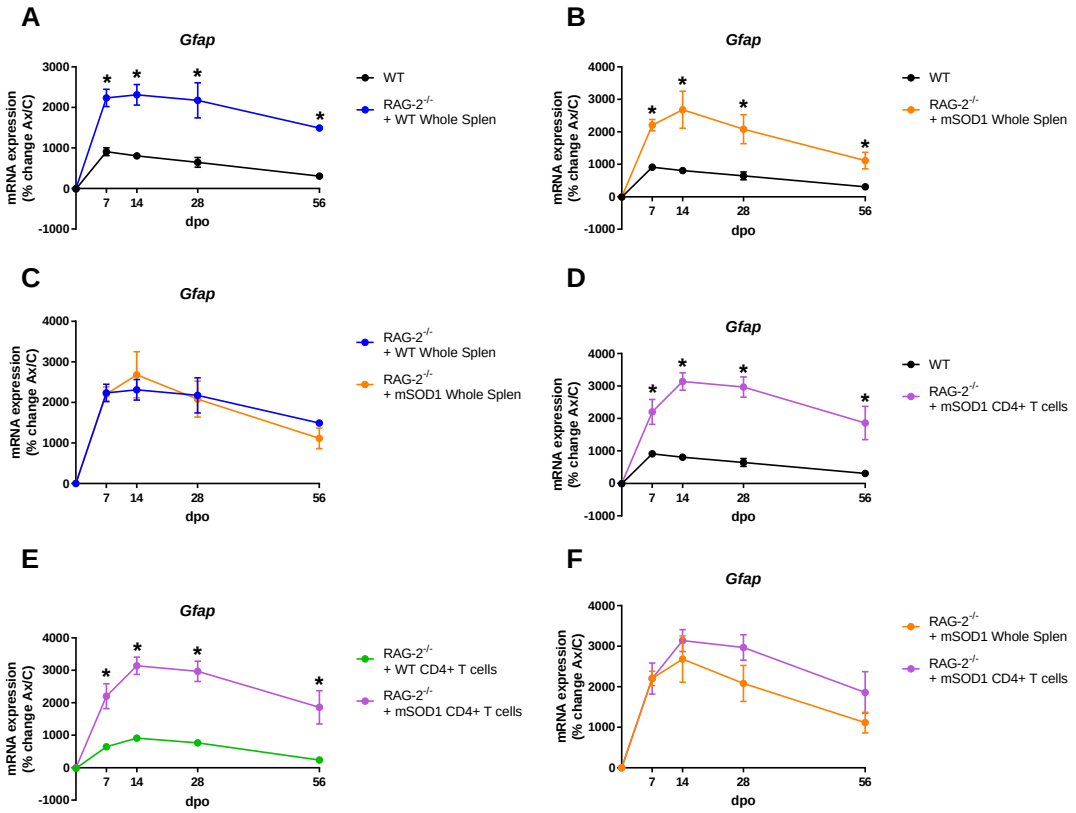

Figure 15: *Gfap* gene expression profile after FNA in RAG-2$^{-/-}$ + WT WS, RAG-2$^{-/-}$ + mSOD1 WS and RAG-2$^{-/-}$ + mSOD1 CD4+ T cell groups.

mRNA expression of *Gfap* in the facial motor nucleus following facial nerve axotomy (Ax), relative to the control (C) facial motor nucleus. Mean percent change ± SEM was plotted across uninjured (0) and 7, 14, 28, and 56 days post-operation (dpo) timepoints. Symbols used: *: $p < 0.05$.

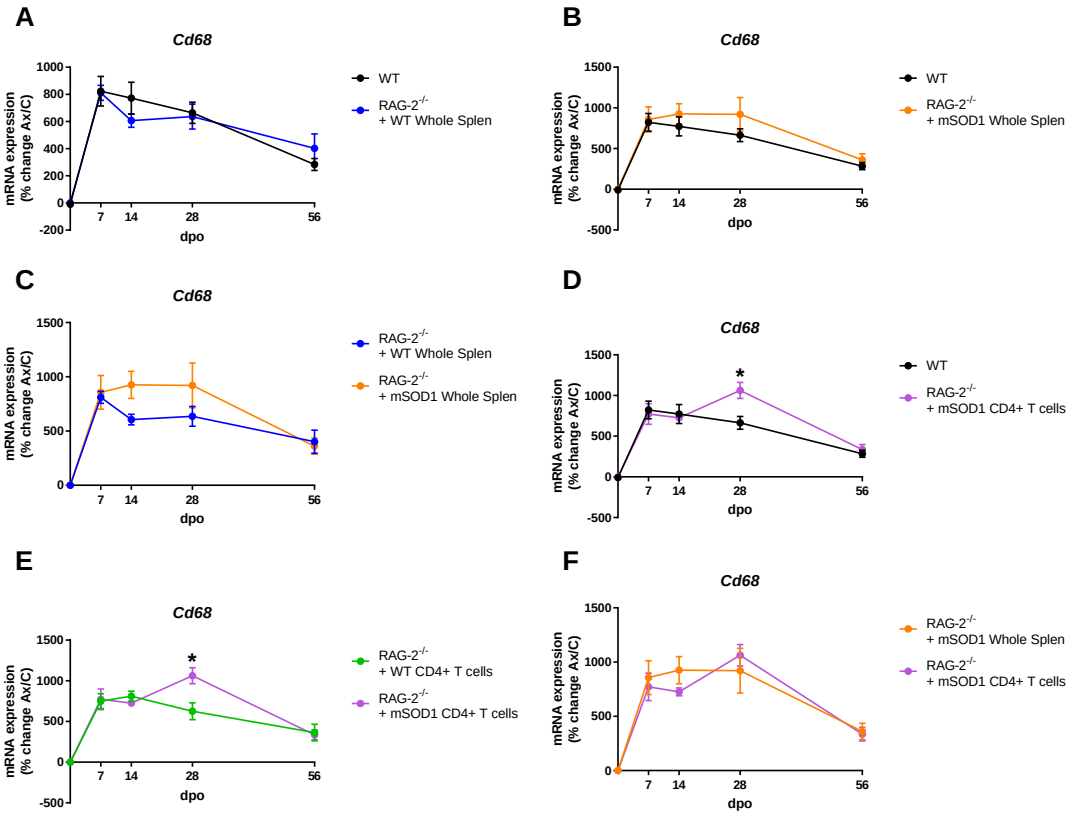

Figure 16: *Cd68* gene expression profile after FNA in RAG-2$^{-/-}$ + WT WS, RAG-2$^{-/-}$ + mSOD1 WS and RAG-2$^{-/-}$ + mSOD1 CD4+ T cell groups.

mRNA expression of *Cd68* in the facial motor nucleus following facial nerve axotomy (Ax), relative to the control (C) facial motor nucleus. Mean percent change ± SEM was plotted across uninjured (0) and 7, 14, 28, and 56 days post-operation (dpo) timepoints. Symbols used: *: $p < 0.05$.

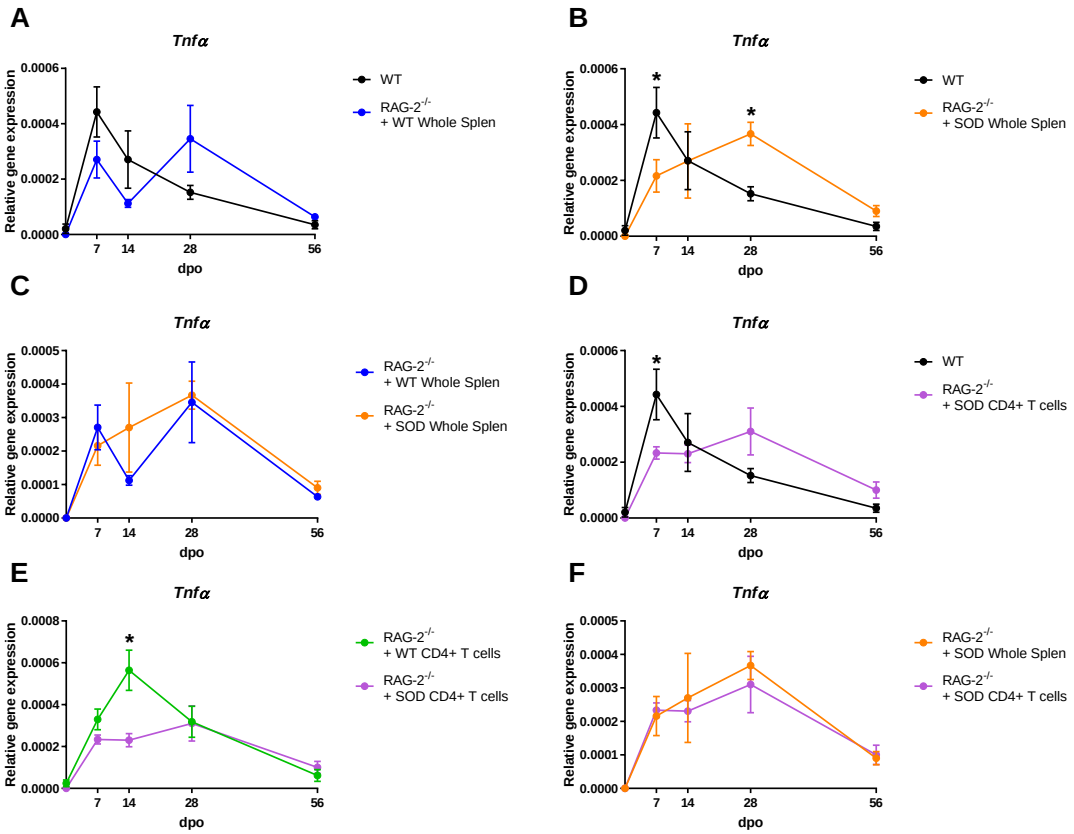

Figure 17: *Tnfα* gene expression profile after FNA in RAG-2$^{-/-}$ + WT WS, RAG-2$^{-/-}$ + mSOD1 WS and RAG-2$^{-/-}$ + mSOD1 CD4+ T cell groups.

mRNA expression of *Tnfα* in the facial motor nucleus following facial nerve axotomy (Ax), relative to the control (C) facial motor nucleus. Mean percent change ± SEM was plotted across uninjured (0) and 7, 14, 28, and 56 days post-operation (dpo) timepoints. Symbols used: *: $p < 0.05$.

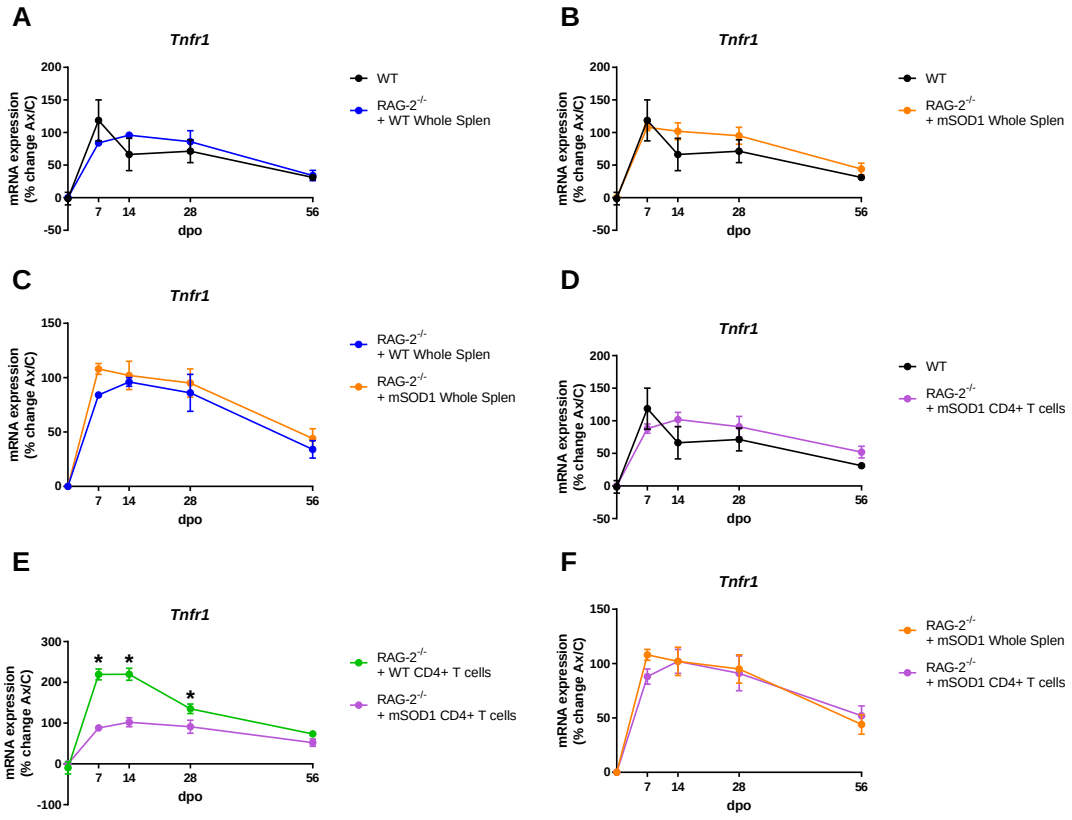

Figure 18: *Tnfr1* gene expression profile after FNA in RAG-2$^{-/-}$ + WT WS, RAG-2$^{-/-}$ + mSOD1 WS and RAG-2$^{-/-}$ + mSOD1 CD4+ T cell groups.

mRNA expression of *Tnfr1* in the facial motor nucleus following facial nerve axotomy (Ax), relative to the control (C) facial motor nucleus. Mean percent change ± SEM was plotted across uninjured (0) and 7, 14, 28, and 56 days post-operation (dpo) timepoints. Symbols used: *: $p < 0.05$.

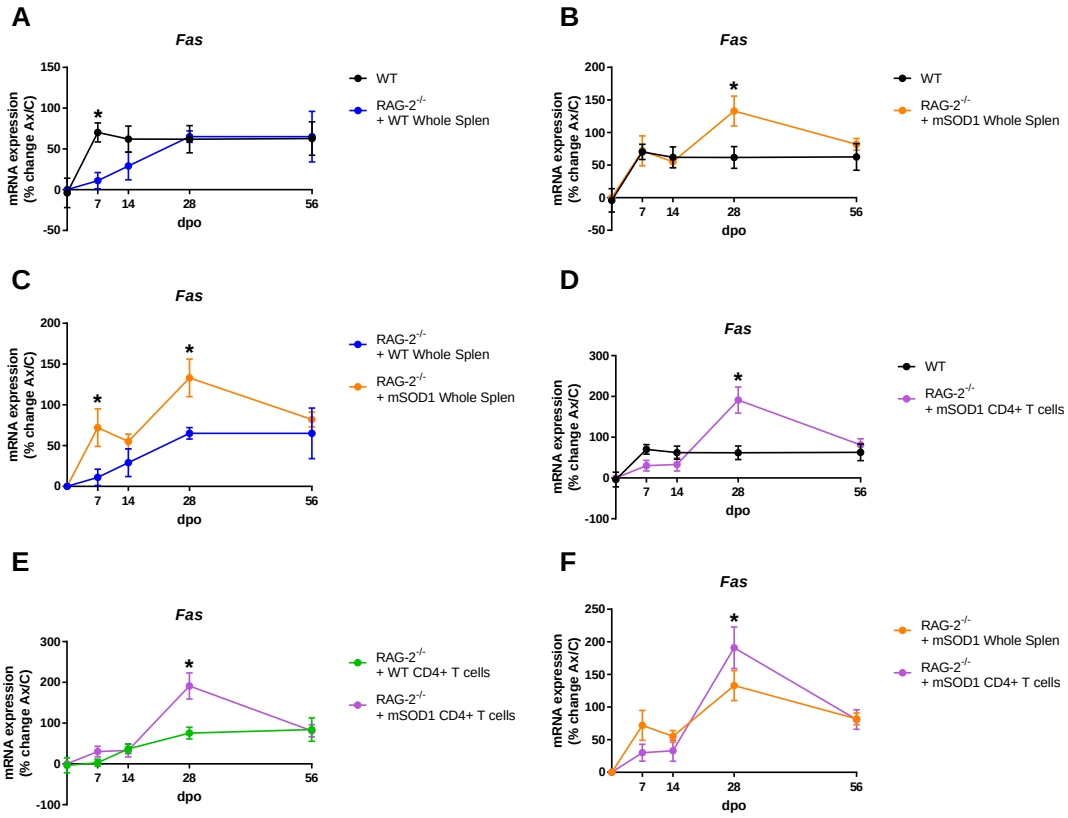

Figure 19: *Fas* gene expression profile after FNA in RAG-2$^{-/-}$ + WT WS, RAG-2$^{-/-}$ + mSOD1 WS and RAG-2$^{-/-}$ + mSOD1 CD4+ T cell groups.

mRNA expression of *Fas* in the facial motor nucleus following facial nerve axotomy (Ax), relative to the control (C) facial motor nucleus. Mean percent change ± SEM was plotted across uninjured (0) and 7, 14, 28, and 56 days post-operation (dpo) timepoints. Symbols used: *: $p < 0.05$.

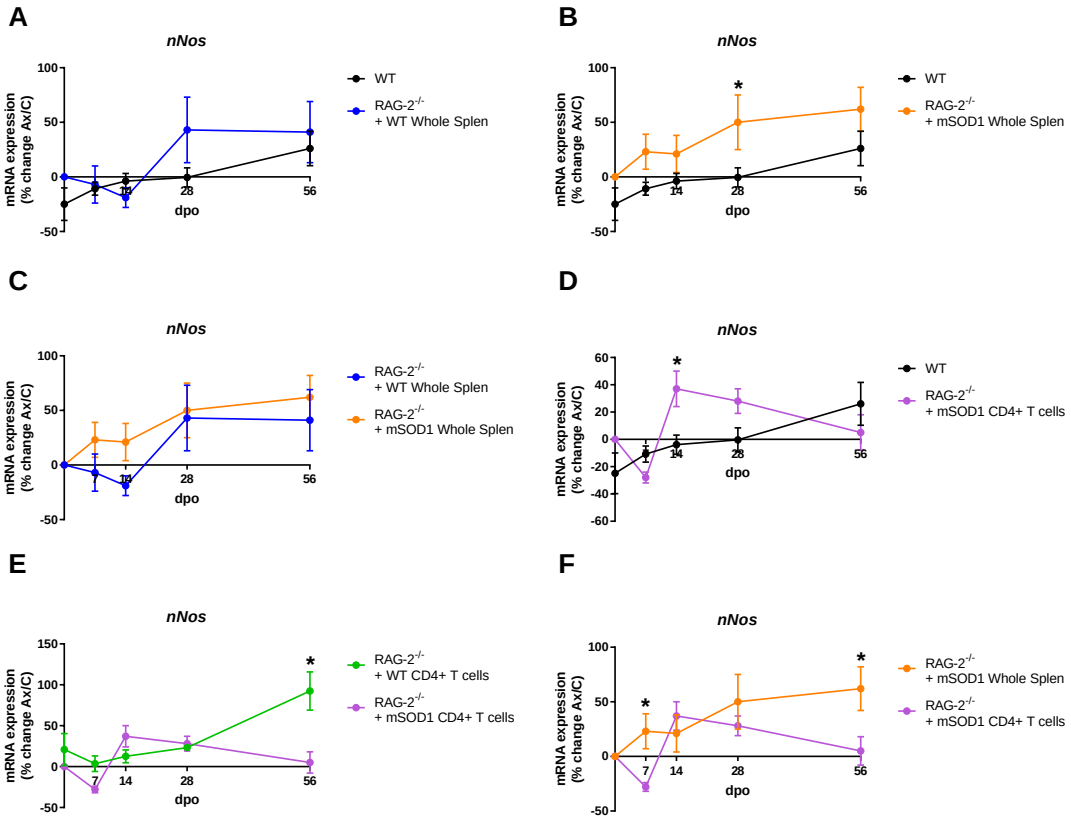

Figure 20: *nNos* gene expression profile after FNA in RAG-2$^{-/-}$ + WT WS, RAG-2$^{-/-}$ + mSOD1 WS and RAG-2$^{-/-}$ + mSOD1 CD4+ T cell groups.

mRNA expression of *nNos* in the facial motor nucleus following facial nerve axotomy (Ax), relative to the control (C) facial motor nucleus. Mean percent change ± SEM was plotted across uninjured (0) and 7, 14, 28, and 56 days post-operation (dpo) timepoints. Symbols used: *: $p < 0.05$.

CHAPTER 5: DISCUSSION

5.1. Aim 1 Discussion

Facial nerve axotomy in immunodeficient mice causes significantly more motoneuron loss relative to WT mice, indicating that the immune system is neuroprotective. This immune-mediated neuroprotection has been subsequently shown to involve both CD4+ T cells and IL-10. IL-10 is an important immunoregulatory factor that reduces inflammatory cytokine production, promotes tissue repair, and exerts therapeutic benefits in many neurodegenerative diseases, including ALS (Kiyota et al., 2012; Joniec-Maciejak et al., 2014; Gravel et al., 2016; Zhou et al., 2016). While IL-10 is necessary for CD4+ T cell-mediated neuroprotection after target disconnection, it appears that CD4+ T cells are not the source of IL-10 (Xin et al., 2011). Rather, evidence in the literature suggests that neuroprotective IL-10 must derive from a CNS source, in part, because it cannot cross the BBB (Kastin et al., 2003; Xin et al., 2011). To fully understand the mechanism of CD4+ T cell-mediated neuroprotection, it is necessary to identify the cell source of IL-10 and its functional significance relative to motoneuron survival after injury.

There is evidence that microglia are the IL-10 source based on the M1/M2 microglia paradigm characterizing neuroprotective M2 microglia as robust manufacturers of IL-10 (Tam & Ma, 2014). Axotomy-activated T cells require antigen presentation in the CNS for neuroprotective secondary re-activation to occur, and microglia are the primary APC in the CNS (Aloisi, 1999; Byram et al., 2004; Byram et al., 2006). Furthermore, T cell-derived IL-4 is required for immune-mediated neuroprotection, and IL-4 promotes the M2 microglia phenotype (Deboy et al., 2006b; Chhor et al., 2013; Tam

& Ma, 2014). Also, IL-10 receptors are expressed by astrocytes and neurons in the facial motor nucleus (Xin et al., 2011). Altogether, this evidence leads to the hypothesis that antigen presentation by microglia activates IL-4 production by CD4+ T cells, which, in turn, induces the M2 microglia phenotype. These M2 microglia produce IL-10 that binds to IL-10 receptors on astrocytes and neurons to regulate their post-axotomy response to promote neuronal survival.

5.1.1. Microglia are an IL-10 source in the axotomized facial motor nucleus

Microglia production of IL-10 before and after facial nerve axotomy was assessed using multiple approaches. IL-10 protein quantification from isolated microglia in the cre/lox mouse validation process proves that microglia are a source of IL-10. However, the kinetics of IL-10 production by microglia within the facial motor nucleus after facial nerve axotomy remain unknown. Technical difficulties arose when immunofluorescent colocalization analysis was performed on IL-10/GFP reporter mice with microglia-specific markers. Specifically, the tissue fixation required to preserve microglia-specific antigens ablates the GFP signal. At this time, the conclusion can be made that microglia produce IL-10, but their production of IL-10 after facial nerve axotomy has yet to be determined.

To address the issue of microglial IL-10 production after FNA, three approaches can be explored. First, alternative tissue fixation strategies could be tested to see if they can preserve both GFP signal and microglia antigenicity. 1% PFA or paraformaldehyde-lysine-periodate (PLP) fixatives are used in other studies to preserve GFP fluorescence (Komis, 2012; Bond, 2013). If this protocol modification succeeds, the amount of

colocalization between the different cell markers and GFP can be quantified using ImageJ, adding a more objective measure of cell-specific IL-10 production. Second, use of a direct IL-10 antibody could be assessed (Park et al., 2007; Wada et al., 2013). This approach was initially avoided because an IL-10 antibody could label both IL-10 within producing cells and effector IL-10 bound to cell receptors, which would confuse which cell is the source of IL-10. A colocalization assessment of the IL-10 antibody against the GFP fluorescence from the IL-10/GFP reporter mouse would support or refute this concern. If the IL-10 antibody staining recapitulated the GFP distribution in the IL-10/GFP reporter, it could be used in immunohistochemistry colocalization with microglia markers on perfused WT brain tissue. Third, flow cytometry could be performed on the FMNuc to characterize IL-10 expression in a cell-specific manner (Cardona et al., 2006; Sun et al., 2009). A potential pitfall of this approach is that the small cell population of the FMNuc (about 2,000 FMN and 4,000-20,000 glia) may lead to detection issues. To resolve this problem, FMNuc from multiple animals could be pooled to reach sufficient cell numbers for flow cytometry. An advantage of this method is that intracellular IL-10 could be directly immunolabeled in WT animals, avoiding the expense associated with IL-10/GFP reporter mice (Xin et al., 2008). Also, mean fluorescence intensity could be measured, allowing for quantification of IL-10 expression by each cell type (Xin et al., 2008). Measuring microglia production of IL-10 after FNA will help in determining the sequence of events involved in immune-mediated neuroprotection.

Numerous studies describe IL-10 production by microglia. Transcriptomic analysis of IL-10 expression in the brain indicates that microglia express more IL-10 transcript than any other CNS cell type (Zhang et al., 2014). Multiple *in vitro*

experiments describe microglial IL-10 mRNA and protein production in both homeostatic conditions and after LPS challenge (Ledeboer et al., 2002; Tam & Ma, 2014; Ooi et al., 2015; Chu et al., 2016; Gravel et al., 2016). *In vivo* LPS challenge also induces IL-10 production by microglia (Gravel et al., 2016). An analysis of cell-specific IL-10 production after LPS injection into rat cerebral cortex using immunofluorescent colocalization determined that microglia are the predominant producers of IL-10 (Park et al., 2007). In normal human brain tissue, microglia are not shown to express IL-10, however in multiple sclerosis lesions and areas of cerebral infarction, microglial expression of IL-10 is observed (Hulshof et al., 2002). Altogether, our work supports the evidence in the literature that microglia produce IL-10, and future experiments will determine the kinetics of IL-10 expression by microglia after facial nerve injury.

5.1.2. Astrocyte expression of IL-10 is induced by axotomy

Astrocyte expression of IL-10 was examined using colocalization immunohistochemistry on IL-10/GFP reporter mice. Unexpectedly, an induction of IL-10 expression in astrocytes following axotomy was observed. The increase in IL-10 expression coincides with the developing astrocyte activation response after axotomy, with maximal astrocytic expression of IL-10 at the late post-axotomy phase. This finding was surprising given that most literature focuses on microglia as the primary IL-10 source. Part of this microglia-centric focus derives from the Ledeboer et al. 2002 study which compared astrocyte and microglia IL-10 mRNA and protein production *in vitro*. This study concluded that microglia express significantly greater quantities of IL-10 at homeostasis and after LPS stimulation than astrocytes. A study of LPS injection into rat

cerebral cortex identified a few astrocytes as immunopositive for IL-10 at 1 dpo using IHC, however microglia colocalized much more strongly with IL-10 at this timepoint (Park et al., 2007). In human brain tissue, astrocytes are the predominant producer of IL-10. Astrocytes constitutively express IL-10 in normal human brain tissue, and in multiple sclerosis lesions and infarcted areas, greater IL-10 expression was observed in astrocytes relative to microglia. Primary human astrocyte *in vitro* examination confirms these findings (Hulshof et al., 2002). Further evidence for IL-10 expression by astrocytes comes from identification of microRNA 181 (miR-181) as a key regulator of astrocyte cytokine expression. Knockdown of miR-181 leads to proinflammatory cytokine production, whereas overexpression of miR-181 significantly increases IL-10 production by astrocytes *in vitro* (Hutchison et al., 2013). Altogether, these findings support the literature describing astrocyte production of IL-10.

One shortcoming of this experiment is that GFAP does not label astrocytes in the uninjured facial motor nucleus (Graeber et al., 1988; Hermanson et al., 1995; Laskawi & Wolff, 1996; Klein et al., 1997; Horvat et al., 2001). Because our results suggest that astrocytes may be a significant source of IL-10 after FNA, it is imperative to assess astrocyte production both pre- and post-injury. To resolve this problem, an ALDH1L1 antibody could be employed, which labels a broader population of astrocytes (Zamanian et al., 2012; Tyzack et al., 2014). ALDH1L1, also known as FDH (10-formyltetrahydrofolate dehydrogenase), is a protein that participates in the production of tetrahydrofolate for nucleotide synthesis and methionine recycling (Krupenko, 2009; Yang et al., 2011). Recent studies advocate the use of ALDH1L1 antibody as a superior pan-astrocyte marker in comparison to GFAP (Cahoy et al., 2008; Yang et al., 2011;

Tong et al., 2014). In addition, combining astrocyte labeling with quantitative measurement of colocalization with GFP will provide an objective characterization of the effect of axotomy on astrocytic IL-10 production. In summary, our findings define a role for astrocytes in anti-inflammatory cytokine production after FNA.

5.1.3. Constitutive neuronal expression of IL-10 is not impacted by axotomy

Neuronal expression of IL-10 was also assessed in this study. The colocalization analysis utilizing IL-10/GFP mice reveals that facial motoneurons constitutively express IL-10, and axotomy does not alter this expression. This finding was unexpected given that most other studies do not report neuronal expression of IL-10. Both transcriptomic and proteomic analysis of neurons do not indicate that neurons are significant producers of IL-10, however homeostatic IL-16 and IL-18 production is described (Yu et al., 2004; Yang et al., 2005; Liao et al., 2008; Dammer et al., 2013; Zhang et al., 2014; Sharma et al., 2015). An extensive human proteome characterization project used immunohistochemistry to determine that neurons highly express IL-10, and glial cells express comparatively low levels of IL-10 (Uhlen 2015). Neuronal expression of other cytokines, such as TNFα, CCL2, IL-6, and TGF-β have been reported both constitutively and after injury (Liu et al., 1994; Acarin et al., 2000; Banisadr et al., 2005; White et al., 2005). A previous study from our laboratory determined that CCL11 expression shifts from neurons to astrocytes in the axotomized facial motor nucleus. As the post-axotomy response resolves, neurons regain CCL11 expression (Wainwright et al., 2009c). Given that IL-10 protein levels do not change in the facial motor nucleus after axotomy, a similar neuron-to-glia shift in IL-10 production could be predicted, however is not

evident in the histology in this study (Xin et al., 2011). A quantitative analysis of cell-specific IL-10 production in the facial motor nucleus is necessary to objectively describe the immunofluorescent findings.

Overall, further characterization of cytokine expression by neurons will help understand their importance in CNS health and disease. Our novel finding of IL-10 production by neurons represents an understudied area of neuroscience and could be a significant contributor to neuroprotective mechanisms.

5.1.4. Neither microglial nor astrocytic IL-10 are required for neuronal survival after axotomy

The functional significance of cell-specific IL-10 production after nerve injury was assessed using conditional knockdown mice. Our hypothesis was that microglia-specific IL-10 was imperative for immune-mediated neuroprotection. When IL-10 was knocked down in microglia, no negative effects on facial motoneuron survival after axotomy were observed, refuting this hypothesis. This finding makes sense in the context of the histology data indicating that microglia, astrocytes, and neurons all produce IL-10. With the discovery that IL-10 expression is induced in astrocytes after axotomy, the effect of IL-10 knockdown in astrocytes was examined, and no effect on motoneuron survival after axotomy was observed.

Together, these data present two possibilities: either a compensatory mechanism exists between astrocytes and microglia for IL-10 production, or neuronal IL-10 is necessary for neuroprotection. Of these two scenarios, neuronal IL-10 is less likely to be the key for neuroprotection because its expression remains unchanged after axotomy.

Instead, compensatory mechanisms between astrocytes and microglia to supplement IL-10 production should be explored. Co-culture studies demonstrate multiple bidirectional communication pathways between astrocytes and microglia. For example, when astrocytes are mechanically stimulated in co-culture, they release ATP that binds to the P2X7 purinergic receptors on microglia, inducing a calcium wave in microglia (Verderio & Matteoli, 2001). Conversely, LPS induces microglia to release ATP, which binds to the purinergic receptor P2Y1R on astrocytes to increase excitatory postsynaptic currents (Pascual et al., 2012). *In vitro*, astrocyte conditioned media regulates microglia production of reactive oxygen species (Min et al., 2006). Microglia conditioned media also regulates astrocyte production of tenascin, an extracellular matrix protein (Smith & Hale, 1997). Microglia express significantly greater quantities of cytokines after LPS challenge when co-cultured with astrocytes than in isolation (Barbierato et al., 2013). Transgenic astrocytes that overexpress either IL-6 or IL-10 *in vivo* induce significant morphological and phenotypic changes in microglia (Almolda et al., 2014; Almolda et al., 2015; Villacampa et al., 2015). This astrocyte-microglia cooperative effort has important implications for neuronal survival after insult. For example, LPS-mediated neurotoxicity is alleviated when both astrocytes and microglia are present because microglial TNFα induces astrocyte production of BDNF and GDNF, promoting neuronal survival (Chen et al., 2015b). Altogether, abundant evidence describes an interdependent relationship between astrocytes and microglia, suggesting that a glial compensatory mechanism likely supplements IL-10 production in the cre/lox knockdown mouse model. To test this hypothesis, a double knockout mouse model could be developed using gene editing technology, such as CRISPR/Cas9, to knock out IL-10 in both cell populations

simultaneously. This experiment would allow us to determine if neuroprotective IL-10 derives specifically from glia.

If glial IL-10 is not responsible for neuroprotection, then neuronal IL-10 production should be examined. To test if neurons are the IL-10 source, the IL-10 flox gene could be crossed with a Thy1-cre or a neurofilament light chain-cre mouse (Pramatarova et al., 2001; Lino et al., 2002; Jaarsma et al., 2008). Given that the immunofluorescence experiment identified neurons as a constitutive source of IL-10, neuronal IL-10 may be neuroprotective after axotomy, or it could serve an important homeostatic function in the facial motor nucleus. Development of this mouse model may reveal a novel interaction between neurons and the microenvironment mediated by IL-10 signaling. Identifying which cells are responsible for IL-10 production after axotomy is important to provide a detailed mechanistic understanding of the function of IL-10 within the CD4+ T cell-mediated neuroprotection paradigm.

5.1.5. IL-10 in other neurological diseases

The study of the cell source of IL-10 and its expression after injury has broad implications for a range of neurological diseases. In many CNS injury and disease models, IL-10 has a neuroprotective function (Kwilasz et al., 2015). IL-10 promotes dopaminergic neuron survival in rodent models of Parkinson's disease (Schwenkgrub et al., 2013; Joniec-Maciejak et al., 2014). In experimental autoimmune encephalitis (EAE), a model of multiple sclerosis, IL-10 deficiency worsens disease progression. In contrast, IL-10 overexpression in T cells confers resistance to EAE, likely due to inhibition of autoimmune Th1 cell development by IL-10 (Bettelli et al., 1998). IL-10 is important for

neuroprotection after spinal cord injury, and administration of IL-10 after spinal cord injury improves motor function and decreases pain-related grooming behaviors (Plunkett et al., 2001; Zhou et al., 2009). IL-10 deficiency also leads to resistance to thermal allodynia in a hot plate test, suggesting IL-10 may play dual roles in pain modulation (Tu et al., 2003). In sciatic nerve crush, IL-10 reduces inflammation at the injury site and promotes functional recovery (Siqueira Mietto et al., 2015). Retinal damage via injection of a neurotoxin is ameliorated via PACAP/IL-10 mediated neuroprotection (Wada et al., 2013). In excitotoxic models of neuronal injury, IL-10 is necessary for preventing neuronal death, likely through reduction of reactive oxygen species production (Grilli et al., 2000; Mesples et al., 2003; Koriauli et al., 2015). IL-10 is also an important modulator of the inflammatory status of the hypothalamus, and alterations in IL-10 level affects feeding behavior and weight gain in animals (Gotoh et al., 2012). In addition, IL-10 is critical for preserving the health of neurons in the penumbra after middle cerebral artery occlusion (Grilli et al., 2000). Overall, there is abundant evidence that IL-10 has a neuroprotective function in the CNS.

In contrast to other neurodegenerative diseases, IL-10 is not explicitly neuroprotective in Alzheimer's disease. IL-10 deficiency in the APP/PS1 (amyloid precursor protein/presenilin 1) model of AD improves plaque clearance and synaptic retention, and modest cognitive benefits are also observed (Guillot-Sestier et al., 2015). This phenomenon is also evident in infectious disease studies, where knockout of IL-10 results in superior resolution of infection because myeloid cell activation and phagocytosis is not suppressed (Jost et al., 2014; Buxbaum, 2015).

5.1.6. Aim 1 summary of findings

The results from Aim 1 indicate that microglia, astrocytes, and neurons are all sources of IL-10; however, neuroprotective IL-10 does not derive exclusively from microglia or astrocytes. Future studies will continue to evaluate cell-specific IL-10 production and its functional significance for neuronal survival after target disconnection. This work has broad implications because of the relevance of IL-10 mediated neuroprotection to multiple neurodegenerative diseases.

5.1.7. Aim 1 revised hypothesis and future directions

The goal of this aim was to understand how IL-10 fit into the sequence of events in CD4+ T cell-mediated neuroprotection. The original hypothesis for this aim was that after axotomy, microglial antigen presentation reactivates CD4+ T cells, resulting in IL-4 production by T cells that, in turn, induces an IL-10-producing M2 microglia phenotype. This hypothesis was based on well-established immunology studies that describe this sequence of events in macrophage activation (Kigerl et al., 2009; Laskin, 2009). The rejection of this hypothesis based on our results implies that this linear sequence of events may not translate to immune-mediated neuroprotection. A closer examination of this hypothesis is warranted so it can be revised appropriately for future studies.

The first potential flaw in this hypothesis is that it assumes that CD4+ T cells interact with microglia in the injured facial motor nucleus. Previous work from our laboratory identified that MHCII within the CNS is required for immune-mediated neuroprotection, which led us to focus on microglia because of their well-defined role in antigen presentation (Aloisi et al., 1998; Byram et al., 2004). However, multiple CNS

cells can express MHCII, including astrocytes, perivascular macrophages, dendritic cells, oligodendrocytes, and endothelial cells in the BBB (Male et al., 1987; Etienne et al., 1999; Hurley, 2003; Liu et al., 2005; Becher et al., 2006; Ernst & Christie, 2006; Gottfried-Blackmore et al., 2009; Zhang et al., 2014). Additionally, quantitative analysis of T cell infiltration and MHCII+ cells reveals that they are a relatively rare presence in the injured facial motor nucleus. Data suggest that approximately 30 – 50 MHCII+ cells and 120 - 150 CD4+ T cells are present in the injured facial motor nucleus, which has a resident population of 4,000 – 20,000 cells (Raivich et al., 1998; Ha et al., 2006; Ha et al., 2007a; Ha et al., 2007b; Dauer et al., 2011; Kandel, 2013; Haulcomb et al., 2014).

An alternative hypothesis is that T cells interact with antigen-MHCII complexes within the BBB. T cells can infiltrate and reside within the Virchow-Robin space between the endothelial cells and astrocytic endfeet (Ransohoff et al., 2003; Becher et al., 2006; Filipello et al., 2016). In this space, pericytes, perivascular macrophages, and perivascular dendritic cells can engage in antigen presentation with the T cell (Hickey & Kimura, 1988; Becher et al., 2006; McMahon et al., 2006). Evidence indicates that MHCII expression is upregulated in perivascular macrophages after FNA (Liu et al., 2005). Also, astrocyte and T cell interactions at the BBB have been demonstrated histologically in experimental autoimmune encephalopathy (Filipello et al., 2016). This antigen presentation can result in bidirectional communication between the T cells and astrocytes (Bertin et al., 2014; Endo et al., 2015; Filipello et al., 2016). Astrocyte cell membranes are connected by gap junctions through which signals can propagate rapidly to the astrocytes in the facial motor nucleus (Almad et al., 2016). Through this interconnected astrocytic web, a small number of interactions between T cells and

astrocytes can translate to extensive regulation of the glial response to injury. This literature supports revising the hypothesis to include astrocytes and other CNS cells as responsible for antigen presentation to T cells.

Advanced imaging modalities can be used to examine the physical location of antigen presentation in the CNS after FNA. Tools such as confocal and two-photon microscopy used on living or explanted tissue have been highly revelatory in EAE. For example, confocal time-lapse imaging of leptomeningeal (pial and subarachnoid meningeal layers) explants demonstrates that T cells migrate through these tissues, interacting and forming immunological synapses with antigen presenting cells along the way (Kivisakk et al., 2009). There is a precedence for rapid explantation of the facial motor nucleus for microglia electrophysiology measurements, providing groundwork for combining live tissue imaging with FNA (Boucsein et al., 2000). In EAE, intravital two-photon imaging shows that T cells crawl along the vascular surface before exiting the vasculature and identifies scanning behavior of T cells in the leptomeninges (Bartholomaus et al., 2009). This imaging method also allowed for quantification of contact frequency and length of interaction time between T cells and APCs within the leptomeninges *in vivo* (Bartholomaus et al., 2009). One advantage of using the EAE model to study T cells in the CNS is that this disease induces a robust T cell response. Translating these methods to our FNA model may be more challenging because comparatively smaller numbers of T cells are activated by this injury. Also, the EAE intravital imaging was performed on the spinal cord, which is considerably easier to access relative to the pons. To circumvent this, alternative peripheral nerve injury models, such as sciatic nerve injury, could be used to gain a better understanding of T cell

interactions within the BBB and meningeal layers in response to axotomy. If these imaging studies demonstrate that CD4+ T cells infiltrate the post-axotomy CNS tissue, an *in vitro* model of the BBB can be employed to determine which factors specifically promote migration (Bertin et al., 2014). This information is important for determining if CD4+ T cell mediated neuroprotection occurs via direct interaction with glia in the CNS, such as in ischemic brain injury, or if CD4+ T cells regulate glial responses indirectly via communication across the BBB (Gill & Veltkamp, 2016).

A second flaw in the original hypothesis is its reliance on the M1/M2 classification of microglia responses. The M1/M2 paradigm evolved from *in vitro* immunological studies of macrophages that described these two major subtypes (Kigerl et al., 2009; Laskin, 2009). Secretion of IFNγ by Th1 cells promotes the M1 phenotype, and M1 cells secrete inflammatory cytokines and reactive oxygen species. Conversely, the M2 phenotype is induced by Th2 production of IL-4, and M2 cells secrete anti-inflammatory and pro-tissue repair cytokines (Kigerl et al., 2009; Laskin, 2009). This paradigm has been adapted to describe microglial responses in the brain, given that microglia and macrophages share a common origin. However, recent in-depth examination of macrophages and microglia has largely disproven this reductionist view of their responses. First, transcriptomic analysis of resident macrophages in multiple tissue types revealed that there is significant diversity in cell phenotype depending on where they reside, thus microglia and macrophages should not be assumed to be similar (Gautier et al., 2012). Second, immunologists have been lobbying for an end to the M1/M2 macrophage labels because there are different interpretations of these phenotypes and this paradigm fails to accurately describe *in vivo* macrophage activation responses

(Martinez & Gordon, 2014; Murray et al., 2014). The publication most responsible for this attitude shift compared 299 human-derived macrophage transcriptomes after *in vitro* activation by 28 different stimuli. When IFNγ and IL-4 stimulation groups were analyzed, a two-dimensional M1/M2 spectrum could be visualized. However, stimulation by other cytokines, pattern recognition receptor ligands, and metabolites resulted in a multi-dimensional range of responses (Xue et al., 2014). In an analysis of microglia responses to traumatic brain injury, expression of prototypical M1 and M2 cytokines are observed simultaneously, further refuting the M1/M2 dichotomy (Morganti et al., 2016). Altogether, this evidence suggests that M1/M2 polarity is an inappropriate paradigm for microglia activation in the CNS. To accurately define the post-axotomy microglia response, transcriptomic analysis of microglia at multiple timepoints after FNA is necessary, with a special focus on cytokine expression. Furthermore, a comparable analysis of astrocytic and neuronal phenotypes after FNA would allow for the most complete understanding of the facial motor nucleus response to peripheral target disconnection. Findings from this transcriptomic analysis should then be validated histologically using *in situ* hybridization and immunohistochemistry. This information will be immensely valuable in gaining a broad, unbiased understanding of neuroinflammatory responses to nerve injury.

The downstream effects of IL-10 were not addressed in this study, however, these effects are the most important information needed to understand immune-mediated neuroprotection. In addressing this question, the lens of immunology may again lead to bias. In the context of traditional immunology, IL-10 is secreted by immune cells to induce the anti-inflammatory response. This response is primarily mediated by IL-10

binding to IL-10R, leading to JAK1 phosphorylation, which then phosphorylates STAT3. Phospho-STAT3 migrates to the nucleus and targets expression of multiple genes, including Socs3 (blocks IL-6), Bcl3 (suppresses TNFα), and Ptpn1 (dephosphorylates phospho-STAT3). IL-10 also suppresses immune cell activation and division, further dampening the immune response (Hutchins et al., 2013). When thinking about the role of IL-10 in the injured facial motor nucleus, it could act on glia to generate an anti-inflammatory microenvironment. However, there is insufficient evidence describing the downstream mechanisms of IL-10-mediated neuroprotection in the CNS (Lobo-Silva et al., 2016). This work is complicated by the fact that STAT3 has 1700 possible genomic targets (Hutchins et al., 2013). In fact, IL-10 neuroprotection in the CNS could occur by a mechanism entirely disparate from its anti-inflammation role. One example of this is Dr. Carla Shatz's work that identified MHCI as a critical molecule for synaptic pruning in neurodevelopment (Boulanger et al., 2001). In the immune system, MHCI is an antigen presenting molecule that interacts with CD8 on T cells. In the CNS, a blind screen of molecules identified MHCI as a necessary component for synaptic formation in visual system development (Corriveau et al., 1998). Further studies demonstrated that MHCI in the CNS does not rely on CD8 for its effects in synaptic elimination. Instead, MHCI is a significant regulator of long-term depression and calcium-permeable AMPA receptors (Lee et al., 2014). These MHCI studies reveal that the nervous system can reappropriate immune system proteins for their own devices. This conclusion is especially thought-provoking given that our data demonstrate that neurons produce IL-10 constitutively. A thorough examination of IL-10's downstream effects on astrocytes, microglia, and neurons is warranted to understand its role in regulating CNS responses to injury. To

accomplish this, cell cultures could be exposed to IL-10 and subsequent effects on cell transcriptomes could be analyzed. These findings would then be verified in mouse models that receive intrathecal IL-10 infusion via an osmotic pump. Dose-dependent curve analysis would further confirm these findings and provide important mechanistic information of IL-10-mediated neuroprotection.

Another potential problem in this experiment design is its foundation on the IL-$10^{-/-}$ mouse data. In the Xin et al. 2011 study, IL-$10^{-/-}$ mice experience significantly more FMN loss after FNA, suggesting that IL-10 is important for neuroprotection. The IL-$10^{-/-}$ mouse is commonly used as a model of inflammatory bowel disease because IL-10 deficiency results in profound gut inflammation and intestinal disease (Kuhn et al., 1993; Kiesler et al., 2015). This significant alteration in gut homeostasis has a significant impact on the animal's microbiome, which, in turn, can lead to a dramatically different immune system profile (Round & Mazmanian, 2009). By this logic, the neuronal death after injury in these IL-$10^{-/-}$ animals could be due to immune system abnormalities resultant from a defective microbiome. Alternatively, IL-10 deficiency could indirectly lead to neuronal death because expression of other cytokines after axotomy could be dysregulated. Roles for IL-4, IL-6, PACAP, TNFα, and other cytokines have all been explored using the FNA model (Zhou et al., 1999; Streit et al., 2000; Terrado et al., 2000; Bohatschek et al., 2004a; Moran & Graeber, 2004; Deboy et al., 2006b; Armstrong et al., 2008). As so many cytokines are important for neuron survival after injury, using global cytokine knockout mice could cause a "butterfly effect," hindering interpretation of these studies. On a broader level, these cytokine knock-out/knock-in experiments are small steps to incrementally understand the mechanisms of immune-mediated neuroprotection.

These major disadvantage of this experimental approach is that it resembles the Indian parable of blind men examining an elephant. Each blind person touches a specific part of the elephant, either its belly, tusk, ear, or trunk, and each person comes to a different incorrect conclusion about what the creature is. This parable exemplifies the risk of bias in narrowly focused scientific approaches. To avoid bias and to make significant progress in this field, it is necessary to use big-data approaches to see the full picture of the neuroimmune response to peripheral nerve injury.

The ultimate goal of this work is to understand the mechanism of immune-mediated neuroprotection in the normal animal. To address this question, I propose this revised hypothesis: CD4+ T cells interact with antigen presenting cells in the CNS, which leads to cytokine expression changes in the facial motor nucleus that promotes motoneuron survival after axotomy. First, confocal microscopy and intravital two-photon microscopy should be used to determine where and when CD4+ T cells interact with CNS antigen presenting cells. After identifying the location of antigen presentation, whether it is the Virchow-Robin space, leptomeninges. or CNS parenchyma, flow cytometry can then be used to identify the antigen presenting cells in this area. Potential APCs could include perivascular macrophages, perivascular dendritic cells, or astrocytes. With that information, the phenotypic changes of resident cells in the facial motor nucleus after T cell reactivation occurs should next be examined. Single-cell RNA sequencing on a collection of facial motoneurons, astrocytes, and microglia would provide a complete profile of what cytokines are being expressed by each cell type after axotomy pre- and post-T cell interaction with CNS APCs. These findings should then be confirmed by *in situ* hybridization, immunofluorescence, flow cytometry, and/or

quantitative protein analysis. Extensive studies of how these CNS cell types respond to cytokines is also warranted to avoid making erroneous assumptions of these cytokine effects based on immunological studies. Altogether, by using a “big data” approach and avoiding biased thinking, the role of T cells and cytokines in immune-mediated neuroprotection can be more effectively determined.

5.2. Aim 2 Discussion

As previously discussed in Aim 1, immunodeficient mice lacking the adaptive arm of the immune system have increased motoneuron death relative to WT mice after facial nerve axotomy, indicating that the immune system is neuroprotective (Serpe et al., 1999). Immunoreconstitution of these mice with whole splenocytes, which contain B and T cells, restores motoneuron survival after injury to normal levels (Serpe et al., 1999; Serpe et al., 2003). Subsequent experiments identified CD4+ T cells as the key cell required for immune-mediated neuroprotection (Serpe et al., 2003).

This discovery of the role of the immune system in central neuroprotection has important implications for neurodegenerative diseases. For example, immunodysregulation is evident in patients with ALS, including decreased circulating CD4+ T cells and increased cytokine levels in the peripheral blood (Hovden et al., 2013; Chen et al., 2014; Lu et al., 2016). The mSOD1 mouse model of ALS also exhibits significant immune changes, including profound lymphopenia, loss of splenic mass, and failure of T cells to respond to immunization (Kuzmenok et al., 2006; Banerjee et al., 2008). Immunologic manifestations associated with mSOD1 motoneuron disease are

evident in CNS tissue as early as 40 days of age, suggesting that the immune system may participate in the development of ALS disease pathology (Alexianu et al., 2001).

When FNA is superimposed on mSOD1 mice at the presymptomatic stage, increased motoneuron death is observed, with survival levels comparable to immunodeficient mice (Mesnard et al., 2011). Examination of the central molecular response to injury reveals that the motoneuron regeneration response remains intact. Instead, there is significant dysregulation of the glial microenvironment response to injury, as well as increased expression of the Fas/nNos cell death mechanism (Mesnard et al., 2011; Haulcomb et al., 2014). This finding was initially surprising because it was predicted that mSOD1 motoneuron disease would have an intrinsic negative effect on motoneuron health and function. These results shifted the focus of our work towards the microenvironment surrounding the motoneuron as the possible causative agent for increased motoneuron death in injury and disease. Altogether, this evidence leads to the theory that the immune system may be responsible for regulating the post-injury glial microenvironment response to promote motoneuron survival.

To test this theory, the effect of immunodeficiency on the central molecular response to facial nerve axotomy was characterized. Also, the neuroprotective effects of CD4+ T cells were examined to describe the mechanism of immune-mediated neuroprotection. This is the first study of its kind to examine the effects of the peripheral immune system on the central molecular response to nerve injury. The prediction for this aim was that the molecular expression pattern after axotomy in RAG-$2^{-/-}$ mice would parallel the mSOD1 pattern of intact motoneuron regeneration, dysregulated glial microenvironment activation, and increased death receptor expression. It was also

expected that CD4+ T cell recipients would exhibit a normal microenvironment and cell death response to injury. In summary, the hypothesis for this aim is that immunodeficiency will impair the glial microenvironment response to FNA, leading to greater motoneuron death, and administration of CD4+ T cells will regulate glial responses to normal levels to promote motoneuron survival.

5.2.1. The motoneuron regeneration response to peripheral nerve injury is unaffected by the adaptive arm of the immune system

The first question addressed was whether peripheral immune status affected the motoneuron regeneration response to axotomy. In agreement with the original hypothesis, there is no observed effect of immunodeficiency on motoneuron regeneration-associated gene expression after injury. In CD4+ T cell reconstituted mice, a small increase in cytoskeletal gene expression was noted and is likely the result of the increased number of surviving motoneurons or permissive effects of the presence of CD4+ T cells on neuroregeneration.

An interesting finding is that there is equivalent motoneuron regeneration gene expression in the RAG-$2^{-/-}$ group relative to WT at 28 dpo, despite a 25% reduction in facial motoneurons in the RAG-$2^{-/-}$ group. These data suggest that motoneurons that survive axotomy may express a higher concentration of regeneration-associated genes. For the first two weeks after axotomy, motoneurons significantly upregulate expression of cytoskeletal genes to regrow the daughter axon (Bisby & Tetzlaff, 1992). If the axon fails to reconnect to target musculature within a period of time, cytoskeletal gene expression is deactivated, and the loss of trophic support from the peripheral muscle can

lead to motoneuron death (Lieberman, 1971; Grafstein, 1975). For unknown reasons, there are differential motoneuron survival responses to axotomy in the facial motor nucleus. Kinetic analysis of FMN loss after FNA reveals that approximately 15% of neurons die, 35% of neurons depend on the immune system for survival, and 50% of neurons survive the injury, even as far as 6 months post-axotomy (Serpe et al., 2000, unpublished data). A subnuclear distribution pattern of FMN death after FNA is evident, with the ventrolateral (VL) subnucleus exhibiting the most FMN death (70% survival) and the ventromedial (VM) subnucleus having the least FMN death (97% survival) (Canh et al., 2006). Molecular expression profiles comparing the axotomized VL and VM subnuclei determined that higher regenerative gene expression was measured in the VL subnucleus (Mesnard et al., 2010). One would predict that with the increased motoneuron death in the VL is due to a reduced regenerative capacity, however this is not the case. Collectively, these data suggest that neuroregenerative gene expression does not equate with increased neuronal survival after axotomy. However, this molecular approach only assesses surviving motoneurons, which may have a robust regenerative program that skews the gene expression analysis. To explain why some motoneurons are predisposed to die, it is important to identify the intrinsic determinants of both motoneuron death and survival after axotomy. To accomplish this, I propose performing single-cell RNA sequencing of 100 axotomized facial motoneurons at 1 dpo, before any motoneuron death occurs. Considering that there are three fates (forever die, forever survive, or survival depends on immune system), I predict that the phenotypes of these 100 FMN will cluster into 3 groups with a similar distribution as the FMN survival pattern (15/35/50%). Analyzing the differences between these phenotypic clusters would allow for

identification of genes associated with survival or death after axotomy. These associations could be verified using an *in vitro* axotomy model, where siRNAs could be used to test if the neuronal genes identified are pro- or anti-survival (Gomis-Ruth et al., 2014). Drugs that regulate these genes could be screened for using this *in vitro* approach, then translated to peripheral nerve injury in rodent models, with the goal of achieving total and permanent motoneuron survival after injury. Ultimately, the goal of these experiments would be to find clinically relevant drugs that regulate pro-survival gene targets as a new therapy for promoting neuronal survival after nerve injury.

Overall, the findings from Aim 2 demonstrate that the motoneuron regeneration response is resilient within the context of immunodeficiency. The same conclusion is drawn from the study of the motoneuron regeneration response to axotomy in the mSOD1 mouse (Mesnard et al., 2011; Haulcomb et al., 2014). Findings that complete functional recovery occurs in RAG-2$^{-/-}$ and mSOD1 mice after facial nerve crush further support this claim that motoneuron regeneration remains intact in models of immunodeficiency or motoneuron disease (Beahrs et al., 2010; Mesnard et al., 2013). Overall, these results signify that immunodeficiency only impacts neuronal survival, not the regeneration response.

5.2.2. Central glial activation after peripheral nerve injury is regulated by CD4+ T cells

The effect of immune status on activation of astrocytes and microglia after facial nerve injury was also assessed. In the immunodeficient group, initial astrocyte and microglia activation is intact, however there is a failure to sustain glial activation in the middle and late post-axotomy phases. This dysregulation is most prominent in astrocytes.

The CD4+ T cell recipient group did not exhibit this decreased glial activation, indicating that CD4+ T cells are responsible for maintaining glial responses. This claim is further supported by evidence that T cells infiltrate the axotomized facial motor nucleus at 14 dpo, the timepoint at which astrocyte activation depends on the presence of CD4+ T cells (Raivich et al., 1998; Hurley, 2003; Ha et al., 2007b; Almolda et al., 2014). Collectively, the data from Aim 2 suggest that early, innate glial responses are retained in immunodeficient mice, and continued glial activation relies on CD4+ T cells.

Additional studies have identified decreased astrocyte and microglia activation in immunodeficient mice. For example, decreased microglia activation is observed in a T cell receptor (TCR) knockout/mSOD1 transgenic mouse (Chiu et al., 2008). CD4-deficient mice have decreased astrocyte activation relative to WT in a spinal nerve injury model of neuropathic pain (Cao & DeLeo, 2008). Decreased astrogliosis is evident in a combined RAG-2$^{-/-}$/APP/PS1 mouse model of Alzheimer's disease (Spani et al., 2015). A possible mechanism for T cell induction of astrocyte activation is during the T cell secondary reactivation process in the CNS. As described in the section 5.1.7, T cells may interact with astrocytes during antigen presentation or by transmitting signals through the BBB (Aloisi, 1999; Almad et al., 2016). This astrocyte activation can have downstream effects on microglia activation responses through IL-6 and MCSF production, possibly explaining the concurrent decrease in microglia activation in immunodeficient mice (Klein et al., 1997; Almolda et al., 2014).

In the mSOD1 molecular response to FNA, decreased astrocyte and microglia activation is also evident. Contrary to the immunodeficient model, astrocyte and microglia activation is decreased at both early and late post-axotomy stages in the

mSOD1 model of motoneuron disease (Haulcomb et al., 2014). This lack of astrocyte activation could be due to an intrinsic dysregulation of the astrocytic phenotype in the mSOD1 group. Evidence suggests that isolated mSOD1 astrocytes are intrinsically neurotoxic, supporting this claim that the mSOD1 transgene significantly alters astrocyte behavior (Di Giorgio et al., 2007; Haidet-Phillips et al., 2011; Chen et al., 2015a). Alternatively, the effect of the mSOD1 mutation on the peripheral immune system's ability to regulate astrocyte activation could contribute to astrocyte dysregulation after peripheral nerve injury. Section 5.3.2. in the Aim 3 discussion addresses this question.

To summarize, these findings demonstrate that the peripheral immune system, specifically CD4+ T cells, is responsible for sustaining central glial activation after peripheral nerve injury. There is differential dysregulation of the glial activation response in RAG-2$^{-/-}$ animals relative to mSOD1 animals. In immunodeficiency, initial glial activation occurs normally, however glial activation is not sustained throughout the time course. In mSOD1 animals, deficient glial activation is evident in both early and late post-axotomy phases, suggesting a factor outside the peripheral immune system could be contributing to microenvironment dysregulation in axotomy-induced target disconnection.

5.2.3. Central inflammatory cytokine expression after peripheral nerve injury is regulated by CD4+ T cells

To measure the effect of immune status on inflammatory cytokine expression, *Tnfα* gene expression was analyzed. Immunodeficiency resulted in a loss of early *Tnfα* expression, followed by a return to normal levels for the remainder of the time course.

The CD4+ T cell recipient group had normal levels of early *Tnfα*, followed by an augmented response relative to WT. These data suggest that *Tnfα* expression, especially in the early phase, is regulated by CD4+ T cells. This early timepoint is concurrent with the timing of T cell reactivation in the injured facial motor nucleus (Byram et al., 2004). Additionally, TNFα is an important regulator of glial activation. For example, TNFα increases astrocyte connectivity and induces nitric oxide production by microglia (Hensley, 2003; Almad et al., 2016). The recovery of late *Tnfα* expression in immunodeficient mice may coincide with microglia phagocytosis of dead facial motoneurons (Raivich et al., 1998).

In mSOD1 mice, both *Tnfα* and *Ifnγ* are expressed constitutively in the uninjured facial motor nucleus, indicating a proinflammatory CNS environment. Axotomy induces greater expression of these inflammatory cytokines (Mesnard et al., 2011; Haulcomb et al., 2014). This basal inflammatory phenotype may be the result of mSOD1 affecting NF-κB regulation in microglia, leading to dysregulated overexpression of inflammatory cytokines (Frakes et al., 2014). On the other hand, the mSOD1 mutation could impact the peripheral immune system's ability to regulate the glial microenvironment, thus resulting in uncontrolled neuroinflammation. Collectively, these findings suggest that there is a "Goldilocks zone" for the central TNFα response after peripheral nerve injury. Sufficient TNFα is needed for activation of immune-mediated neuroprotective mechanisms, but excessive TNFα may result in neurotoxicity.

It is necessary to perform protein analysis to verify these gene expression findings. mRNA analysis of neurons compared to neuropil within the axotomized facial motor nucleus demonstrate that *Tnfα* transcript is only detectable in the neuropil

(Mesnard et al., 2010). Microglia are the most likely source of TNFα in the facial motor nucleus based on transcriptomic data, however there is also evidence for neuronal production of TNFα in other areas of the brain (Liu et al., 1994; Acarin et al., 2000; Zhang et al., 2014). Identifying the cell source of TNFα will provide further mechanistic information of how CD4+ T cells influence the central response to peripheral nerve injury. Discovering that immune status impacts central TNFα production also encourages studying expression of other relevant cytokines to obtain a more complete characterization of the post-axotomy microenvironment response in immunocompetent and immunodeficient groups (Alexianu et al., 2001; Chen et al., 2004).

Altogether, this work suggests that CD4+ T cells are required for early TNFα expression, which may be a key regulatory molecule in initiating signaling cascades that promote glial activation and neuroprotection.

5.2.4. No relationship is evident between increased neuronal death and gene expression of cell death mechanisms in immunodeficient animals after peripheral nerve injury

Examination of the prevalence of either the TNFR1 or Fas/nNos death mechanisms was performed because there is increased neuronal death in the immunodeficient group. Unexpectedly, neither death mechanism was prominently expressed in RAG-2$^{-/-}$ mice. A delayed *Tnfr1* response was evident in RAG-2$^{-/-}$ mice relative to WT, coinciding with the lack of early *Tnfα* expression. There was no significant increase in Fas or nNos expression in immunodeficient mice relative to control. In contrast, mSOD1 mice exhibit a prominent peak in Fas expression in the late post-axotomy phase, coinciding with the timing of motoneuron death in this group

(Haulcomb et al., 2014). A motoneuron-specific downstream mediator of Fas death, nNos, is also upregulated in the mSOD1 group. Fas/nNos mediated motoneuron death has been well-described in ALS disease pathology, and its role in motoneuron death after target disconnection represents a unique finding warranting further study (Raoul et al., 2002; Raoul et al., 2006).

Surprisingly, in RAG-2$^{-/-}$ mice that received adoptive transfer of CD4+ T cells, a heightened *Tnfr1* response was detected throughout the post-axotomy timecourse, mirroring the increased *Tnfα* expression in this group. Because this experimental group does not experience significant motoneuron death after FNA, it is unlikely that this increased *Tnfr1* is inducing apoptosis. TNFR1 could be utilized by CD4+ T cells to upregulate adhesion molecule expression in astrocytes to assist T cell migration into the CNS parenchyma (Archambault et al., 2005). Also, CD4+ T cell induction of *Tnfr1* could be regulating cytokine expression by acting through its secondary signaling pathway that induces NF-κB (Baud & Karin, 2001; McCoy & Tansey, 2008; Wajant & Scheurich, 2011). To determine if the apoptotic or immunoregulatory signaling pathway was being induced, gene expression of *Fadd* (apoptosis), *Traf2* (immunoregulation), and *Tradd* (both), was measured (Hsu et al., 1996; Sohda et al., 2015). No significant differences in gene expression were found in any of these genes when the CD4+ T cell recipient group was compared to WT. Downstream signaling through TNFR1 may not be detectable on the gene expression level, therefore, protein analysis of these mediators would need to be conducted to address this question.

To summarize, neither death mechanism examined in this study is clearly connected to the increased motoneuron death in immunodeficient mice. In CD4+ T cell

recipients, an increased *Tnfr1* expression response is observed, indicating that isolated CD4+ T cells may act in a differential manner than in their *in situ* environment. The implications for this finding is further explored in Aim 3, when gene expression analysis is performed on immunodeficient mice reconstituted with whole splenocytes.

5.2.5. Aim 2 summary of findings

The results from Aim 2 indicate that CD4+ T cell-mediated neuroprotection following facial nerve axotomy occurs via regulation of the glial microenvironment response to injury, rather than a direct action on motoneuron regeneration or suppression of a cell death mechanism. The mechanism of this immune-mediated neuroprotection may rely on TNFα/TNFR1 signaling to permit T cell migration into the CNS or regulate the neuroinflammatory response to peripheral nerve injury. These findings define an important role for the peripheral immune system in affecting central responses to peripheral nerve injury.

5.2.6. Future directions

The primary goal of this aim was to broadly identify the mechanism of immune-mediated neuroprotection in the facial motor nucleus after axotomy. With the recognition that glial regulation significantly depends on CD4+ T cells, an in-depth examination of glial phenotype is warranted. GFAP and CD68 are commonly used markers for astrocyte and microglia reactivity, however they only represent a small aspect of the glial response (Laskawi & Wolff, 1996; Brettschneider et al., 2012; Marshall et al., 2013). Acquisition of single cell RNA-seq information from a collection of astrocytes and microglia at

various post-axotomy timepoints will provide a more complete picture of the injury response. Comparing WT and immunodeficient RNA-seq information will further identify which genes are specifically regulated by the adaptive arm of the immune system. These findings can be compared to other glial transcriptomic analyses to identify similarities to other disease contexts, for example, mSOD1 motoneuron disease, ischemia, or neuroinflammation (Zamanian et al., 2012; Chiu et al., 2013; Liddelow et al., 2017). These transcriptomic analysis results should also be confirmed using protein quantification methods because there are can be differences between gene and protein expression (Hensley et al., 2002; Hensley, 2003). The findings can also be verified histologically using both *in situ* hybridization and immunohistochemistry.

Also, a histological comparison of WT and immunodeficient mouse glial responses would be useful in determining the morphological manifestations of decreased glial activation. *In vitro* comparison of RAG-2$^{-/-}$ and WT microglia responses to LPS reveals no significant differences in cytokine expression or morphological changes (Beers et al., 2008). Examination of microglia histology after facial nerve axotomy in immunodeficient mice would reveal if they are capable of proliferation and synaptic stripping (Graeber et al., 1993; Graeber et al., 1998; Boucsein et al., 2000). Studying astrocyte reactions is important for assessing if their morphological shift from protoplasmic to fibrillary phenotypes is affected by immunodeficiency, or if they fail to replace microglia in synaptic stripping at later post-axotomy timepoints (Tetzlaff et al., 1988b; Moran & Graeber, 2004).

In addition to glial activation, differences in TNFα expression in the early post-axotomy phase were observed in immunodeficient mice. This finding suggests that early

TNFα may be an important signaling component for CD4+ T cell regulation of the glial microenvironment after axotomy. To explore this further, a TNFα blockade could be imposed after FNA in WT mice to observe if it inhibits CD4+ T cell-mediated neuroprotection. For this experiment, either a soluble TNFR or a TNFR-blocking antibody could be used to inhibit TNFα signaling between 3-14 dpo (Terrado et al., 2000). Quantification of FMN survival after FNA at 28 dpo could then be used to measure if TNFα blockade during this time frame resulted in decreased FMN survival. In this experiment, I hypothesize that blocking TNFα at timepoints during which T cells are being reactivated in the CNS environment would impede glial activation and result in increased motoneuron death. Examination of cell-specific sources of TNFα could then be conducted to identify which CNS cells are the key participants in this process.

One criticism for this work is its reliance on the RAG-2$^{-/-}$ mouse, which may be an inappropriate model because the lifelong immunodeficiency causes significant physiological changes. For example, immunodeficient mice are reported to have decreased cognitive function and impaired hippocampal neurogenesis (Kipnis et al., 2004; Brynskikh et al., 2008; Wolf et al., 2009; Spani et al., 2015). Also, immunodeficiency has significant impacts on the host microbiome, which can translate into neurological effects (Round & Mazmanian, 2009; Mulle et al., 2013; Zhang et al., 2015). For example, gut bacteria production of tryptophan metabolites confers neuroprotection in EAE (Rothhammer et al., 2016). A recent publication identified microbiome alterations in mSOD1 mice, and treatment with bacterial products extended mSOD1 mouse survival by an average of 38 days (Zhang et al., 2017). In this study, it is

possible that a secondary abnormality resultant from immunodeficiency may be increasing motoneuron death after axotomy.

To test this theory, anti-CD4 antibodies could be administered to a WT mouse to selectively eliminate CD4+ T cells (Ghobrial et al., 1989; Archambault et al., 2005). This approach allows the animal to grow and develop with an intact immune system, thereby avoiding the secondary effects associated with lifelong immunodeficiency. This alternative mouse model of CD4+ T cell deficiency should exhibit immunodeficient-like FMN death after FNA, if the original hypothesis for this work is correct. One drawback for these antibody-depletion models is that the T cell elimination may result in peripheral immune activation, and multiple treatments are needed to maintain continuous deprivation of CD4+ T cells. Also, CD4+ T cells sequestered in the CNS may escape the antibody depletion. Despite these potential pitfalls, this approach may be necessary to validate the CD4+ T cell-mediated neuroprotection paradigm.

5.3. Aim 3 Discussion

Disconnection from target musculature is the hallmark of early presymptomatic disease pathology in ALS (Fischer et al., 2004; Dadon-Nachum et al., 2011). Axotomy-induced target disconnection results in a similar injury response profile as seen in mSOD1 motoneuron disease pathology (Mesnard et al., 2011). When facial nerve axotomy is superimposed on presymptomatic mSOD1 mice, increased motoneuron death is observed, similar to the immunodeficient response to nerve injury (Serpe et al., 1999; Mariotti et al., 2002; Mesnard et al., 2011). This finding is surprising because, in theory, mSOD1 mice have an intact immune system. To test the neuroprotective capacity of

mSOD1 lymphocytes, facial nerve axotomy was administered to RAG-2$^{-/-}$ mice immunoreconstituted with mSOD1 whole splenocytes, and the mSOD1 immune cells failed to protect motoneurons from death. In contrast, isolated mSOD1 CD4+ T cells are capable of rescuing motoneuron survival to normal levels, suggesting that a factor within the mSOD1 whole splenocyte environment inhibits mSOD1 CD4+ T cell-mediated neuroprotection (Mesnard-Hoaglin et al., 2014).

The conclusion from Aim 2 is that WT CD4+ T cells promote neuronal survival after injury by regulating the glial microenvironment response to injury. This result leads us to hypothesize that the mSOD1 whole splenocyte environment suppresses CD4+ T cell regulation of glial responses to target disconnection. By comparing post-axotomy molecular responses, we predicted a dysregulated glial response would be evident in the RAG-2$^{-/-}$ + mSOD1 WS group, similar to what was observed in the immunodeficient group in Aim 2. We also predicted that the glial response in the mSOD1 CD4+ T cell recipient group would be comparable to the WT counterpart. As an additional control, a WT whole splenocyte reconstitution group was added to confirm that whole splenocyte treatment results in a WT-like molecular response after axotomy.

5.3.1. WT whole splenocyte reconstitution of immunodeficient mice results in a differential gene expression response relative to WT

When the molecular response of WT whole splenocyte recipient mice was compared to WT, many unexpected differences were found. First, whole splenocyte recipients had an increased motoneuron regenerative response to injury relative to WT. This finding could be the result of CD8+ T or B cells generating a permissive

environment that promotes motoneuron regenerative gene expression. Other studies have identified CD8+ T cell infiltration of the injured facial motor nucleus, supporting this hypothesis (Ha et al., 2007a).

Additionally, a significant increase in astrocyte activation is observed in whole splenocyte recipients relative to both WT and isolated WT CD4+ T cell recipients. An interaction between CD8+ T or B cells and astrocytic endfeet at the BBB could result in this hyperactivated astrocyte response. Depending on immune status, there appears to be three levels of astrocyte activation: the reduced response with immunodeficiency, the normal response in WT and CD4+ T cell recipients, and an increased response with whole splenocyte recipients. This pattern suggests that astrocytes are highly sensitive to peripheral immune status. Their presence at the BBB uniquely situates them to be both sensors and transducers of communication signals between the periphery and the CNS. Astrocytes are commonly described as innate immune cells because of their functional role in the BBB, expression of pattern recognition receptors, and participation in antigen presentation (Carpentier et al., 2005; Farina et al., 2007; Ransohoff & Brown, 2012). The results from this study also suggest that astrocytes may also act as an extension of the adaptive arm of the immune system transducing immune-mediated neuroprotective signals from the peripheral blood to the CNS. Further work is needed to support this claim.

Microglia activation and inflammatory cytokine expression response to axotomy in whole splenocyte recipient mice are equivalent to WT. This finding suggests that CD8+ T and B cells do not significantly affect these responses, supporting the conclusion

from Aim 2 that CD4+ T cells are specifically responsible for regulation of these responses.

The Tnfr1 response in whole splenocyte recipients is also equivalent to the WT response. In contrast, isolated WT CD4+ T cell recipients exhibit a heightened Tnfr1 response relative to both of these groups. These data suggest that whole splenocyte components regulate CD4+ T cell effects on the facial motor nucleus. The impact of the increased Tnfr1 with isolated CD4+ T cells is unknown, though hypothesized to be related to regulation of cytokine expression and T cell infiltration into the CNS. Overall, data from this experiment indicate that CD4+ T cell induction of Tnfr1 can be differentially regulated depending on the presence of CD8+ T or B cells.

As expected, whole splenocyte recipients did not have increased Fas or nNos expression relative to WT after axotomy. The only significant difference in expression responses was decreased early Fas expression in all three RAG-$2^{-/-}$ animal groups, with or without immunoreconstitution. The implications for this difference are unknown, however do not seem to correspond with motoneuron survival after injury.

To summarize, whole splenocyte adoptive transfer into immunodeficient mice results in a differential molecular response to injury relative to both WT and isolated WT CD4+ T cell recipient animals. Also, it was discovered that astrocytes are highly sensitive to peripheral immune status.

These significant differences between WT and WT whole splenocyte reconstituted mice are unexpected and deserve further investigation. WT whole splenocyte transfer into immunodeficient mice restores both circulating lymphocytes and nodular architecture in the spleen (Serpe et al., 1999). One possible explanation for the

differences between these two groups is that the grafted immune cells may have different phenotypic behaviors relative to their host. These effects may be perpetuated by microbiome differences in RAG-2$^{-/-}$ mice relative to WT (Zhang et al., 2015). Furthermore, the post-mortem whole splenocyte collection protocol may cause significant, permanent changes to lymphocyte behavior. An extensive evaluation of whole splenocyte engraftment into RAG-2$^{-/-}$ mice may also explain the different observed molecular responses. The effectiveness of tail vein injection of whole splenocytes used in this study could be compared to bone marrow transplant immunoreconstitution, which would include more progenitor cells and may more closely approximation the WT immune status (Beers et al., 2008; Bottcher et al., 2013). A parabiosis procedure connecting a WT and RAG-2$^{-/-}$ mouse could also be an alternative immunoreconstitution strategy to provide *in vivo* WT lymphocytes to an immunodeficient animal with minimal cellular processing (Bottcher et al., 2013). These experimental approaches would help in identifying why WT whole splenocyte transfer into RAG-2$^{-/-}$ mice does not result in a similar molecular response to injury compared to WT.

5.3.2. MN death in mSOD1 whole splenocyte recipients is not due to immunodeficient-like microenvironment dysregulation

Next, the molecular response to peripheral target disconnection of immunodeficient mice reconstituted with mSOD1 whole splenocytes was evaluated. These responses were compared to WT whole splenocyte recipients instead of WT because of the significant differences found in comparing the molecular response of these two groups.

First, motoneuron regeneration is not impaired in mSOD1 whole splenocyte recipients, in agreement with prior studies and the Aim 2 findings (Mesnard et al., 2011; Haulcomb et al., 2014). Surprisingly, there is no impairment in astrocyte or microglia activation in mSOD1 versus WT whole splenocyte recipients. This finding refutes the original hypothesis that mSOD1 whole splenocytes block CD4+ T cell regulation of the microenvironment to injury. In addition, the astrocyte hyperactivation in WT whole splenocyte recipients is also observed in mSOD1 whole splenocyte recipients, further supporting the claim that astrocytes are acutely sensitive to peripheral immune status.

An area for future study is an in-depth examination of the astrocytic response to injury. It is possible that mSOD1 whole splenocytes induce an alternative activation status of astrocytes that is neurotoxic, whereas WT whole splenocytes promote a neuroprotective astrocytic phenotype. A study from Dr. Ben Barres' laboratory characterizes two polar astrocytic phenotypes induced by neuroinflammatory or ischemic CNS injuries (Zamanian et al., 2012; Liddelow et al., 2017). A major discovery from their work is that C3, a complement protein, is prominently and exclusively expressed in neurotoxic astrocyte phenotypes, and astrocytic C3 is identified in multiple neurodegenerative diseases (Liddelow et al., 2017). Gene expression analysis of C3 could be employed to identify, on a broad level, if different astrocyte phenotypes are evident when comparing mSOD1 and WT whole splenocyte recipient groups. In addition, use of single cell RNA-seq on a collection of post-axotomy astrocytes is warranted to compare the astrocytic response of WT or mSOD1 whole splenocyte recipient groups. Overall, the current data suggest that glial activation is unimpaired in mSOD1 whole splenocyte

recipients, however, further characterization of astrocyte phenotype is necessary to rule out neurotoxic astrocytic phenotype activation.

Another interesting finding is that *Tnfα* expression in mSOD1 versus WT whole splenocyte recipient groups are comparable. In contrast, significant dysregulation of *Tnfα* expression is observed in mSOD1 mice both at homeostasis and after injury (Mesnard et al., 2011; Haulcomb et al., 2014). In mSOD1 whole splenocyte recipients, there is no induction of *Tnfα* in the homeostatic facial motor nucleus, and axotomy-induced *Tnfα* expression is regulated to normal levels. The findings suggest that the peripheral immune system is likely not the cause of increased *Tnfα* in mSOD1 mice, and instead, the mSOD1 transgene is inducing effects in the facial motor nucleus. To confirm this, the immune system could be depleted in mSOD1 animals using irradiation or chemotherapeutic drugs and TNFα expression in the CNS could be measured. No change in TNFα expression in the CNS would confirm that neuroinflammation with mSOD1 motoneuron disease is the result of intrinsic processes independent from the peripheral immune system. Alternatively, an increase in TNFα expression would suggest that the immune system dampens neuroinflammation, whereas a decrease in expression would indicate that the immune system exacerbates neuroinflammation. Also, the timing of this aberrant cytokine production in the mSOD1 mouse model is unknown. Evidence suggests that neuroinflammation occurs presymptomatically, even as early as 50 days of age, however the exact age of onset is not known (Hensley et al., 2002; Chen et al., 2004). The most thorough examination of temporal gene expression in mSOD1 animals utilized only female littermate controls for the male experimental animals, which may confound the detection of early TNFα changes (Chen et al., 2004). Analyzing the expression of

neuroinflammatory-associated genes at regular intervals from 1 – 90 doa in the CNS, nerve, and muscle tissue will provide important information about the onset and progression of axonal die-back disease pathology in mSOD1 mice (Dadon-Nachum et al., 2011).

When cell death mechanism pathways were compared, no significant differences in Tnfr1 expression after injury were observed in mSOD1 whole splenocyte recipients relative to control. Overall, this evidence suggests that Tnfr1 is not prominently associated with the facial motoneuron death after axotomy observed in mSOD1, RAG-$2^{-/-}$, or RAG-$2^{-/-}$ + mSOD1 whole splenocyte groups (Mesnard-Hoaglin et al., 2014).

In contrast, a prominent induction of Fas expression was observed in mSOD1 versus WT whole splenocyte recipients. This induction profile matches the Fas gene expression profile in mSOD1 mice, suggesting that mSOD1 peripheral immune cells may induce central motoneuron death mechanisms (Haulcomb et al., 2014). This finding was surprising because the original study describing Fas expression in ALS characterizes it as a cell autonomous death mechanism. This study revealed that mSOD1 motoneurons are highly susceptible to Fas and nitric oxide triggered death, however, they have normal responses to trophic deprivation and excitoxicity (Raoul et al., 2002). Furthermore, this increased sensitivity to Fas-mediated death is only detectable in mSOD1 motoneurons, not sensory, cortical, or cerebellar neurons (Raoul et al., 2002). Follow-up work discovered a Fas/FasL feedback loop within mSOD1 neurons that fit with the cell autonomous ALS theory. In this loop, FasL expression by neurons results in Daxx induction of nNos, resulting in neuron-specific nitric oxide production that perpetuates

FasL expression in neurons. Knocking out the Daxx gene significantly increases motoneuron survival in mSOD1 animals and reduces neuronal FasL expression. Altogether, the Fas death pathway in motoneuron disease seemed to result from intrinsic dysregulation within the motoneuron, however this study suggests that the peripheral immune system may significantly contribute to the induction of Fas-mediated cell death.

To summarize, mSOD1 whole splenocyte transfer into immunodeficient mice does not result in an immunodeficient-like central molecular response to peripheral nerve injury. Instead, these data suggest that motoneuron death could occur by two mechanisms. First, induction of a neurotoxic glial phenotype by mSOD1 whole splenocytes may promote neuronal death. Second, mSOD1 whole splenocytes could cause increased motoneuron death by aberrant induction of Fas/nNos expression in the post-axotomy facial motor nucleus.

5.3.3. Pro-survival molecular responses induced by mSOD1 CD4+ T cells significantly differ from WT CD4+ T cells

The central molecular response to axotomy was measured in mSOD1 CD4+ T cell recipients, and unexpected differences in comparison with WT CD4+ T cell recipients were discovered. Motoneuron regeneration responses are significantly elevated in mSOD1 versus WT CD4+ T cell recipients, especially axon growth-cone associated proteins. Additionally, a three-fold increase in astrocyte activation was detected in mSOD1 versus WT CD4+ T cell recipients. This increased astrocyte response may translate into enhanced motoneuron regeneration gene expression because astrocyte and neuronal interactions are tightly linked (Acarin et al., 2000; Tian et al., 2012). One

explanation for the increased astrocyte response is that an instigating factor within the mSOD1 mouse environment induces a CD4+ T cell phenotype that is a potent astrocyte activator. If this phenotype is maintained in the adoptive transfer process, it could be responsible for increased astrocyte induction. This astrocyte response is axotomy-dependent, as no induction of astrocyte activity is observed in the uninjured facial motor nucleus of mSOD1 CD4+ T cell recipients (data not shown).

Another distinction between WT and mSOD1 CD4+ T cells is the differential induction of Tnfr1 expression after axotomy. Increased Tnfr1 expression in WT CD4+ T cell recipients in Aim 2 led to the conclusion that isolated CD4+ T cells behave in a differential manner than in the immunocompetent environment. Unexpectedly, this behavior does not hold true in the mSOD1 CD4+ T cell group because the *Tnfr1* response in mSOD1 CD4+ T cell recipients approximates normal levels. These findings provide support for the claim that there are significant phenotypic differences between WT and mSOD1 CD4+ T cells.

Additionally, an increased Fas induction in the late post-axotomy phase is observed in mSOD1 CD4+ T cell, not WT CD4+ T cell, recipients. This Fas expression is likely linked to the mSOD1 transgene's effects on peripheral immune cells, and these data suggest that CD4+ T cells alone are capable of inducing this Fas expression.

Altogether, mSOD1 and WT CD4+ T cells differentially regulate the molecular response within the injured facial motor nucleus to promote neuronal survival. The distinct motoneuron, astrocyte, and cell death pathway expression patterns suggest that significant phenotypic differences exist between mSOD1 and WT CD4+ T cells, refuting

the original hypothesis that they act in an identical manners to protect injured motoneurons.

5.3.4. Differential induction of motoneuron-specific death mechanisms in mSOD1 whole splenocyte versus mSOD1 CD4+ T cell reconstituted immunodeficient mice

The ultimate goal for Aim 3 was to identify significant differences in regulation of the central molecular response to facial nerve injury in immunodeficient mice reconstituted with either mSOD1 whole splenocytes or isolated mSOD1 CD4+ T cells. Because mSOD1 whole splenocytes fail to rescue neuronal survival after axotomy, it was hypothesized that CD4+ T cell-mediated regulation of the glial microenvironment was inhibited in the whole splenocyte environment. To our surprise, there was equivalent regulation of microenvironment responses by both mSOD1 whole splenocytes and CD4+ T cells. This study only used two markers to assess the glial response to injury, and studying additional markers of glial activation status will allow for characterization of neuroprotective or neurotoxic glial phenotypes. Additionally, mSOD1 whole splenocytes did not negatively impact the motoneuron regeneration response or the TNFα/TNFR1 axis.

In this study, the only observed gene expression change between mSOD1 whole splenocytes and CD4+ T cells that could potentially explain the increased neuronal death is increased nNos expression at both early and late timepoints in mSOD1 whole splenocyte recipients. Fas, an upstream inducer of nNos expression, is increased in the late post-axotomy phase in both mSOD1 whole splenocyte and CD4+ T cell recipients, mimicking the expression response seen in the mSOD1 mouse (Haulcomb et al., 2014).

This finding indicates that the mSOD1 immune system, specifically CD4+ T cells, could be responsible for mediating Fas expression induction. However, only the mSOD1 whole splenocyte recipients exhibit a significant increase in nNos, suggesting that motoneuron death due to Fas/nNos signaling is restricted to mSOD1 whole splenocyte recipients, not isolated mSOD1 CD4+ T cell recipients. These results suggest that either CD8+ T or B cells are responsible for promoting motoneuron death by induction of nNos.

To summarize, these gene expression data suggest that the increased motoneuron death observed in mSOD1 whole splenocytes could be due to peripheral immune induction of a motoneuron-specific death pathway prevalent in ALS. Isolated mSOD1 CD4+ T cells are able to protect motoneuron survival because the cell inducing nNos neurotoxicity is not present. An alternative hypothesis is that mSOD1 whole splenocytes may promote a neurotoxic glial phenotype relative to mSOD1 CD4+ T cells.

5.3.5. Aim 3 summary of findings and revised hypothesis

The results from Aim 3 lead to the conclusion that WT whole splenocytes and CD4+ T cells can both be neuroprotective via differential regulation of the central response to axotomy, with astrocytic activation playing a prominent role. Importantly, target genes thought to be necessary for neuronal survival are upregulated in mSOD1 whole splenocyte recipients. Furthermore, motoneuron regeneration gene expression after axotomy does not correlate with motoneuron survival after injury, as a regenerative phenotype occurred in the facial motor nucleus regardless of immunodeficiency or disease status. However, astrocyte activation was found to be highly dependent on

peripheral immune status, suggesting that astrocytes play a major role in transducing peripheral immune signals into the CNS.

The hypothesis that the mSOD1 whole splenocyte environment inhibits CD4+ T cell-mediated microenvironment regulation, as well as facial motoneuron rescue, after axotomy is not supported by these data. Instead, there are several other possible explanations. For example, generation of a neurotoxic astrocyte phenotype could be induced by mSOD1 whole splenocytes. Additionally, mSOD1 whole splenocytes may promote the Fas/nNos motoneuron-specific death mechanism after axotomy.

5.3.6. Future directions

Glial phenotype characterization, especially the astrocyte response to facial nerve injury, should be performed in mSOD1 whole splenocyte and mSOD1 CD4+ T cell reconstituted animals. As described in section 5.3.2., C3 can be used as a broad marker for neurotoxic astrocytes, and this may be a good starting point for identifying differential astrocyte activation by mSOD1 whole splenocytes or mSOD1 CD4+ T cells. The different astrocyte activation responses can be further examined by performing transcriptomic analysis of their post-axotomy response (Zamanian et al., 2012; Liddelow et al., 2017).

Additionally, the results in Aims 1, 2, and 3 suggest the astrocyte may be an especially important component of immune-mediated neuroprotection. These findings have been largely unexpected because the original hypothesis suggested that microglia were the cells responsible for transducing neuroprotective CD4+ T cell signaling into the CNS. Instead, this work indicates that astrocytes are the CNS mediators of T cell

neuroprotection. Alternatively, neuroprotection could require a cooperative effort of both microglia and astrocytes to promote neuronal survival. A novel way to test these theories is to employ PLX3997, a drug that eliminates >99% of microglia in the brain (Elmore et al., 2014; Elmore et al., 2015). Administration of this drug for two months to continuously eliminate microglia has no significant effects on motor function, cognition, or learning in mice (Elmore et al., 2014). Superimposing FNA on microglia-depleted mice would reveal if astrocytes alone are capable of mediating neuroprotective mechanisms to promote motoneuron survival the facial motor nucleus.

The Fas/nNos induction by mSOD1 whole splenocytes and mSOD1 CD4+ T cells requires further analysis. To test if Fas-mediated motoneuron death is induced by mSOD1 whole splenocytes, the downstream signaling cascade of Fas could be disrupted to see if facial motoneuron survival is rescued after FNA. A RAG-$2^{-/-}$/$Daxx^{-/-}$ mouse could be generated and receive an adoptive transfer of mSOD1 whole splenocytes, and facial motoneuron survival at 28 dpo FNA could be quantified. This experiment would support or refute the claim that increased neuronal death in mSOD1 whole splenocyte recipient mice is due to peripheral immune system induction of Fas-mediated cell death. Confocal microscopy of CD8+ T or B cells could be used to identify if these cells directly infiltrate the CNS parenchyma or communicate across the BBB to induce Fas/nNos expression. Also, mSOD1 whole splenocytes could be depleted of CD8+ T cells or B cells using negative selection magnetic cell sorting before adoptive transfer into RAG-$2^{-/-}$ animals. FMN survival at 28 dpo FNA could then be quantified in these two groups to identify which cell type is responsible for promoting motoneuron death after peripheral nerve injury.

5.4. Significance of findings

The work presented in this dissertation advances our understanding of the mechanisms underlying immune-mediated neuroprotection after neuronal injury or disease. Regarding the role of IL-10 in facial motoneuron survival after axotomy, we have determined that multiple sources of IL-10, both neuronal and glial, could contribute to peripheral immune cell-mediated neuroprotection. These experiments used an *in vivo* approach for assessing cell-specific cytokine production, an important innovation considering the failure of *in vitro* findings to translate meaningfully to whole-organism studies. Future studies characterizing central cytokine expression after peripheral nerve injury will be crucial for developing a broader picture of the immune response within the injured facial motor nucleus. Characterization of the central molecular response to peripheral nerve injury in immunodeficient versus immunocompetent mice also provides novels insights. The discovery that CD4+ T cells are responsible for molecular regulation of the CNS microenvironment after peripheral target disconnection is important in view of the role of CD4+ T cells in many neurodegeneration diseases. Finally, this work provides support for the non-cell autonomous theory of motoneuron death in ALS through use of the axotomy model of target disconnection. Restriction of the mSOD1 mutation to the peripheral immune system compartment results in significant alterations in the central response to peripheral nerve injury, suggesting that the ALS immune system may contribute to disease pathology. These contributions may involve promotion of neurotoxic glial phenotypes or induction of motoneuron-specific death mechanisms, and studying these effects further will elucidate new therapeutic strategies utilizing immunotherapy as a treatment for ALS.

REFERENCES

Acarin, L., Gonzalez, B., & Castellano, B. (2000). Neuronal, astroglial and microglial cytokine expression after an excitotoxic lesion in the immature rat brain. *Eur J Neurosci, 12*(10), 3505-3520.

Alexianu, M. E., Kozovska, M., & Appel, S. H. (2001). Immune reactivity in a mouse model of familial ALS correlates with disease progression. *Neurology, 57*(7), 1282-1289.

Alfahad, T., & Nath, A. (2013). Retroviruses and amyotrophic lateral sclerosis. *Antiviral Res, 99*(2), 180-187.

Almad, A. A., Doreswamy, A., Gross, S. K., Richard, J. P., Huo, Y., Haughey, N., & Maragakis, N. J. (2016). Connexin 43 in astrocytes contributes to motor neuron toxicity in amyotrophic lateral sclerosis. *Glia, 64*(7), 1154-1169.

Almolda, B., de Labra, C., Barrera, I., Gruart, A., Delgado-Garcia, J. M., Villacampa, N., . . . Castellano, B. (2015). Alterations in microglial phenotype and hippocampal neuronal function in transgenic mice with astrocyte-targeted production of interleukin-10. *Brain Behav Immun, 45*, 80-97.

Almolda, B., Villacampa, N., Manders, P., Hidalgo, J., Campbell, I. L., Gonzalez, B., & Castellano, B. (2014). Effects of astrocyte-targeted production of interleukin-6 in the mouse on the host response to nerve injury. *Glia, 62*(7), 1142-1161.

Aloisi, F. (1999). The role of microglia and astrocytes in CNS immune surveillance and immunopathology. *Adv Exp Med Biol, 468*, 123-133.

Aloisi, F., Ria, F., Columba-Cabezas, S., Hess, H., Penna, G., & Adorini, L. (1999). Relative efficiency of microglia, astrocytes, dendritic cells and B cells in naive CD4+ T cell priming and Th1/Th2 cell restimulation. *Eur J Immunol, 29*(9), 2705-2714.

Aloisi, F., Ria, F., Penna, G., & Adorini, L. (1998). Microglia are more efficient than astrocytes in antigen processing and in Th1 but not Th2 cell activation. *J Immunol, 160*(10), 4671-4680.

Alvarez, M. L., & Done, S. C. (2014). SYBR(R) Green and TaqMan(R) quantitative PCR arrays: expression profile of genes relevant to a pathway or a disease state. *Methods Mol Biol, 1182*, 321-359.

Ankeny, D. P., & Popovich, P. G. (2007). Central nervous system and non-central nervous system antigen vaccines exacerbate neuropathology caused by nerve injury. *Eur J Neurosci, 25*(7), 2053-2064.

Archambault, A. S., Sim, J., Gimenez, M. A., & Russell, J. H. (2005). Defining antigen-dependent stages of T cell migration from the blood to the central nervous system parenchyma. *Eur J Immunol, 35*(4), 1076-1085.

Armstrong, B. D., Abad, C., Chhith, S., Cheung-Lau, G., Hajji, O. E., Nobuta, H., & Waschek, J. A. (2008). Impaired nerve regeneration and enhanced neuroinflammatory response in mice lacking pituitary adenylyl cyclase activating peptide. *Neuroscience, 151*(1), 63-73.

Ashwell, K. W. (1982). The adult mouse facial nerve nucleus: morphology and musculotopic organization. *J Anat, 135*(Pt 3), 531-538.

Bahia El Idrissi, N., Bosch, S., Ramaglia, V., Aronica, E., Baas, F., & Troost, D. (2016). Complement activation at the motor end-plates in amyotrophic lateral sclerosis. *J Neuroinflammation, 13*(1), 72.

Banerjee, R., Mosley, R. L., Reynolds, A. D., Dhar, A., Jackson-Lewis, V., Gordon, P. H., . . . Gendelman, H. E. (2008). Adaptive immune neuroprotection in G93A-SOD1 amyotrophic lateral sclerosis mice. *PLoS One, 3*(7), e2740.

Banisadr, G., Gosselin, R. D., Mechighel, P., Kitabgi, P., Rostene, W., & Parsadaniantz, S. M. (2005). Highly regionalized neuronal expression of monocyte chemoattractant protein-1 (MCP-1/CCL2) in rat brain: evidence for its colocalization with neurotransmitters and neuropeptides. *J Comp Neurol, 489*(3), 275-292.

Barbierato, M., Facci, L., Argentini, C., Marinelli, C., Skaper, S. D., & Giusti, P. (2013). Astrocyte-microglia cooperation in the expression of a pro-inflammatory phenotype. *CNS Neurol Disord Drug Targets, 12*(5), 608-618.

Bartholomaus, I., Kawakami, N., Odoardi, F., Schlager, C., Miljkovic, D., Ellwart, J. W., . . . Flugel, A. (2009). Effector T cell interactions with meningeal vascular structures in nascent autoimmune CNS lesions. *Nature, 462*(7269), 94-98.

Baud, V., & Karin, M. (2001). Signal transduction by tumor necrosis factor and its relatives. *Trends Cell Biol, 11*(9), 372-377.

Beahrs, T., Tanzer, L., Sanders, V. M., & Jones, K. J. (2010). Functional recovery and facial motoneuron survival are influenced by immunodeficiency in crush-axotomized mice. *Exp Neurol, 221*(1), 225-230.

Becher, B., Bechmann, I., & Greter, M. (2006). Antigen presentation in autoimmunity and CNS inflammation: how T lymphocytes recognize the brain. *J Mol Med (Berl), 84*(7), 532-543.

Beers, D. R., Henkel, J. S., Zhao, W., Wang, J., & Appel, S. H. (2008). CD4+ T cells support glial neuroprotection, slow disease progression, and modify glial morphology in an animal model of inherited ALS. *Proc Natl Acad Sci U S A, 105*(40), 15558-15563.

Benowitz, L. I., & Popovich, P. G. (2011). Inflammation and axon regeneration. *Curr Opin Neurol, 24*(6), 577-583.

Berdan, R. C., Easaw, J. C., & Wang, R. (1993). Alterations in membrane potential after axotomy at different distances from the soma of an identified neuron and the effect of depolarization on neurite outgrowth and calcium channel expression. *J Neurophysiol, 69*(1), 151-164.

Bertin, J., Jalaguier, P., Barat, C., Roy, M. A., & Tremblay, M. J. (2014). Exposure of human astrocytes to leukotriene C4 promotes a CX3CL1/fractalkine-mediated transmigration of HIV-1-infected CD4(+) T cells across an in vitro blood-brain barrier model. *Virology, 454-455*, 128-138.

Bettelli, E., Das, M. P., Howard, E. D., Weiner, H. L., Sobel, R. A., & Kuchroo, V. K. (1998). IL-10 is critical in the regulation of autoimmune encephalomyelitis as demonstrated by studies of IL-10- and IL-4-deficient and transgenic mice. *J Immunol, 161*(7), 3299-3306.

Bisby, M. A., & Tetzlaff, W. (1992). Changes in cytoskeletal protein synthesis following axon injury and during axon regeneration. *Mol Neurobiol, 6*(2-3), 107-123.

Blinzinger, K., & Kreutzberg, G. (1968). Displacement of synaptic terminals from regenerating motoneurons by microglial cells. *Z Zellforsch Mikrosk Anat, 85*(2), 145-157.

Bohatschek, M., Kloss, C. U., Hristova, M., Pfeffer, K., & Raivich, G. (2004a). Microglial major histocompatibility complex glycoprotein-1 in the axotomized facial motor nucleus: regulation and role of tumor necrosis factor receptors 1 and 2. *J Comp Neurol, 470*(4), 382-399.

Bohatschek, M., Kloss, C. U., Pfeffer, K., Bluethmann, H., & Raivich, G. (2004b). B7.2 on activated and phagocytic microglia in the facial axotomy model: regulation by interleukin-1 receptor type 1, tumor necrosis factor receptors 1 and 2 and endotoxin. *J Neuroimmunol, 156*(1-2), 132-145.

Boillee, S., Yamanaka, K., Lobsiger, C. S., Copeland, N. G., Jenkins, N. A., Kassiotis, G., . . . Cleveland, D. W. (2006). Onset and progression in inherited ALS determined by motor neurons and microglia. *Science, 312*(5778), 1389-1392.

Bomze, H. M., Bulsara, K. R., Iskandar, B. J., Caroni, P., & Skene, J. H. (2001). Spinal axon regeneration evoked by replacing two growth cone proteins in adult neurons. *Nat Neurosci, 4*(1), 38-43.

Bond, M. (2013). What is the best fixation for fluorescence microscopy of GFP tagged proteins? Retrieved from https://www.researchgate.net/post/What_is_the_best_fixation_for_fluorescence_microscopy_of_GFP_tagged_proteins

Bottcher, C., Fernandez-Klett, F., Gladow, N., Rolfes, S., & Priller, J. (2013). Targeting myeloid cells to the brain using non-myeloablative conditioning. *PLoS One, 8*(11), e80260.

Boucsein, C., Kettenmann, H., & Nolte, C. (2000). Electrophysiological properties of microglial cells in normal and pathologic rat brain slices. *Eur J Neurosci, 12*(6), 2049-2058.

Boulanger, L. M., Huh, G. S., & Shatz, C. J. (2001). Neuronal plasticity and cellular immunity: shared molecular mechanisms. *Curr Opin Neurobiol, 11*(5), 568-578.

Brannagan, T. H., 3rd. (2012). Current issues in peripheral neuropathy. *J Peripher Nerv Syst, 17 Suppl 2*, 1-3.

Brettschneider, J., Toledo, J. B., Van Deerlin, V. M., Elman, L., McCluskey, L., Lee, V. M., & Trojanowski, J. Q. (2012). Microglial activation correlates with disease progression and upper motor neuron clinical symptoms in amyotrophic lateral sclerosis. *PLoS One, 7*(6), e39216.

Brites, D., & Vaz, A. R. (2014). Microglia centered pathogenesis in ALS: insights in cell interconnectivity. *Front Cell Neurosci, 8*, 117.

Brown, R. H., Jr., Hauser, S. L., Harrington, H., & Weiner, H. L. (1986). Failure of immunosuppression with a ten- to 14-day course of high-dose intravenous cyclophosphamide to alter the progression of amyotrophic lateral sclerosis. *Arch Neurol, 43*(4), 383-384.

Bryan, L., Kaye, W., Antao, V., Mehta, P., Muravov, O., & Horton, D. K. (2016). Preliminary Results of National Amyotrophic Lateral Sclerosis (ALS) Registry Risk Factor Survey Data. *PLoS One, 11*(4), e0153683.

Brynskikh, A., Warren, T., Zhu, J., & Kipnis, J. (2008). Adaptive immunity affects learning behavior in mice. *Brain Behav Immun, 22*(6), 861-869.

Bunton-Stasyshyn, R. K., Saccon, R. A., Fratta, P., & Fisher, E. M. (2015). SOD1 Function and Its Implications for Amyotrophic Lateral Sclerosis Pathology: New and Renascent Themes. *Neuroscientist, 21*(5), 519-529.

Buxbaum, L. U. (2015). Interleukin-10 from T cells, but not macrophages and granulocytes, is required for chronic disease in Leishmania mexicana infection. *Infect Immun, 83*(4), 1366-1371.

Byram, S. C., Carson, M. J., DeBoy, C. A., Serpe, C. J., Sanders, V. M., & Jones, K. J. (2004). CD4-positive T cell-mediated neuroprotection requires dual compartment antigen presentation. *J Neurosci, 24*(18), 4333-4339.

Byram, S. C., Serpe, C. J., DeBoy, C. A., Sanders, V. M., & Jones, K. J. (2006). Motoneurons and CD4+ effector T cell subsets: Neuroprotection and repair. *Clinical Neuroscience Research, 6*(1–2), 86-96.

Byram, S. C., Serpe, C. J., Pruett, S. B., Sanders, V. M., & Jones, K. J. (2003). Natural killer cells do not mediate facial motoneuron survival after facial nerve transection. *Brain, Behavior, and Immunity, 17*(6), 417-425.

Cahoy, J. D., Emery, B., Kaushal, A., Foo, L. C., Zamanian, J. L., Christopherson, K. S., . . . Barres, B. A. (2008). A transcriptome database for astrocytes, neurons, and oligodendrocytes: a new resource for understanding brain development and function. *J Neurosci, 28*(1), 264-278.

Calvo, A. C., Manzano, R., Mendonca, D. M., Munoz, M. J., Zaragoza, P., & Osta, R. (2014). Amyotrophic lateral sclerosis: a focus on disease progression. *Biomed Res Int, 2014*, 925101.

Cammermeyer, J. (1963). Peripheral Chromatolysis after Transection of Mouse Facial Nerve. *Acta Neuropathol, 3*, 213-230.

Campbell, W. W. (2008). Evaluation and management of peripheral nerve injury. *Clin Neurophysiol, 119*(9), 1951-1965.

Canh, M. Y., Serpe, C. J., Sanders, V., & Jones, K. J. (2006). CD4(+) T cell-mediated facial motoneuron survival after injury: Distribution pattern of cell death and rescue throughout the extent of the facial motor nucleus. *J Neuroimmunol, 181*(1-2), 93-99.

Cao, L., & DeLeo, J. A. (2008). CNS-infiltrating CD4+ T lymphocytes contribute to murine spinal nerve transection-induced neuropathic pain. *Eur J Immunol, 38*(2), 448-458.

Cardona, A. E., Huang, D., Sasse, M. E., & Ransohoff, R. M. (2006). Isolation of murine microglial cells for RNA analysis or flow cytometry. *Nat Protoc, 1*(4), 1947-1951.

Carpentier, P. A., Begolka, W. S., Olson, J. K., Elhofy, A., Karpus, W. J., & Miller, S. D. (2005). Differential activation of astrocytes by innate and adaptive immune stimuli. *Glia, 49*(3), 360-374.

Castellano, B., Bosch-Queralt, M., Almolda, B., Villacampa, N., & Gonzalez, B. (2016). Purine Signaling and Microglial Wrapping. *Adv Exp Med Biol, 949*, 147-165.

Casula, M., Iyer, A. M., Spliet, W. G., Anink, J. J., Steentjes, K., Sta, M., . . . Aronica, E. (2011). Toll-like receptor signaling in amyotrophic lateral sclerosis spinal cord tissue. *Neuroscience, 179*, 233-243.

Chen, H., Qian, K., Chen, W., Hu, B., Blackbourn, L. W. t., Du, Z., . . . Zhang, S. C. (2015a). Human-derived neural progenitors functionally replace astrocytes in adult mice. *J Clin Invest, 125*(3), 1033-1042.

Chen, L. C., Smith, A., Ben, Y., Zukic, B., Ignacio, S., Moore, D., & Lee, N. (2004). Temporal gene expression patterns in G93A/SOD1 mouse. *Amyotroph Lateral Scler Other Motor Neuron Disord, 5*(3), 164-171.

Chen, S. H., Oyarzabal, E. A., Sung, Y. F., Chu, C. H., Wang, Q., Chen, S. L., . . . Hong, J. S. (2015b). Microglial regulation of immunological and neuroprotective functions of astroglia. *Glia, 63*(1), 118-131.

Chen, X., Feng, W., Huang, R., Guo, X., Chen, Y., Zheng, Z., & Shang, H. (2014). Evidence for peripheral immune activation in amyotrophic lateral sclerosis. *J Neurol Sci, 347*(1-2), 90-95.

Chhor, V., Le Charpentier, T., Lebon, S., Ore, M. V., Celador, I. L., Josserand, J., . . . Fleiss, B. (2013). Characterization of phenotype markers and neuronotoxic potential of polarised primary microglia in vitro. *Brain Behav Immun, 32*, 70-85.

Chiu, I. M., Chen, A., Zheng, Y., Kosaras, B., Tsiftsoglou, S. A., Vartanian, T. K., . . . Carroll, M. C. (2008). T lymphocytes potentiate endogenous neuroprotective inflammation in a mouse model of ALS. *Proc Natl Acad Sci U S A, 105*(46), 17913-17918.

Chiu, I. M., Morimoto, E. T., Goodarzi, H., Liao, J. T., O'Keeffe, S., Phatnani, H. P., . . . Maniatis, T. (2013). A neurodegeneration-specific gene-expression signature of acutely isolated microglia from an amyotrophic lateral sclerosis mouse model. *Cell Rep, 4*(2), 385-401.

Chu, C. H., Wang, S., Li, C. L., Chen, S. H., Hu, C. F., Chung, Y. L., . . . Hong, J. S. (2016). Neurons and astroglia govern microglial endotoxin tolerance through macrophage colony-stimulating factor receptor-mediated ERK1/2 signals. *Brain Behav Immun, 55*, 260-272.

Ciaramitaro, P., Mondelli, M., Logullo, F., Grimaldi, S., Battiston, B., Sard, A., . . . Cocito, D. (2010). Traumatic peripheral nerve injuries: epidemiological findings, neuropathic pain and quality of life in 158 patients. *J Peripher Nerv Syst, 15*(2), 120-127.

Cirulli, E. T., Lasseigne, B. N., Petrovski, S., Sapp, P. C., Dion, P. A., Leblond, C. S., . . . Goldstein, D. B. (2015). Exome sequencing in amyotrophic lateral sclerosis identifies risk genes and pathways. *Science, 347*(6229), 1436-1441.

Corriveau, R. A., Huh, G. S., & Shatz, C. J. (1998). Regulation of class I MHC gene expression in the developing and mature CNS by neural activity. *Neuron, 21*(3), 505-520.

Cragg, B. G. (1970). What is the signal for chromatolysis? *Brain Res, 23*(1), 1-21.

Dadon-Nachum, M., Melamed, E., & Offen, D. (2011). The "dying-back" phenomenon of motor neurons in ALS. *J Mol Neurosci, 43*(3), 470-477.

Dammer, E. B., Duong, D. M., Diner, I., Gearing, M., Feng, Y., Lah, J. J., . . . Seyfried, N. T. (2013). Neuron enriched nuclear proteome isolated from human brain. *J Proteome Res, 12*(7), 3193-3206.

Dauer, D. J., Huang, Z., Ha, G. K., Kim, J., Khosrowzadeh, D., & Petitto, J. M. (2011). Age and facial nerve axotomy-induced T cell trafficking: relation to microglial and motor neuron status. *Brain Behav Immun, 25*(1), 77-82.

DeBoy, C. A., Byram, S. C., Serpe, C. J., Wisuri, D., Sanders, V. M., & Jones, K. J. (2006a). CD4+CD25+ regulatory T cells and CD1-restricted NKT cells do not mediate facial motoneuron survival after axotomy. *J Neuroimmunol, 176*(1-2), 34-38.

Deboy, C. A., Xin, J., Byram, S. C., Serpe, C. J., Sanders, V. M., & Jones, K. J. (2006b). Immune-mediated neuroprotection of axotomized mouse facial motoneurons is dependent on the IL-4/STAT6 signaling pathway in CD4(+) T cells. *Exp Neurol, 201*(1), 212-224.

Dent, M. A., Segura-Anaya, E., Alva-Medina, J., & Aranda-Anzaldo, A. (2010). NeuN/Fox-3 is an intrinsic component of the neuronal nuclear matrix. *FEBS Lett, 584*(13), 2767-2771.

Di Giorgio, F. P., Carrasco, M. A., Siao, M. C., Maniatis, T., & Eggan, K. (2007). Non-cell autonomous effect of glia on motor neurons in an embryonic stem cell-based ALS model. *Nat Neurosci, 10*(5), 608-614.

Drachman, D. B., Chaudhry, V., Cornblath, D., Kuncl, R. W., Pestronk, A., Clawson, L., . . . et al. (1994). Trial of immunosuppression in amyotrophic lateral sclerosis using total lymphoid irradiation. *Ann Neurol, 35*(2), 142-150.

Duffy, A. M., Schaner, M. J., Wu, S. H., Staniszewski, A., Kumar, A., Arevalo, J. C., . . . Scharfman, H. E. (2011). A selective role for ARMS/Kidins220 scaffold protein in spatial memory and trophic support of entorhinal and frontal cortical neurons. *Exp Neurol, 229*(2), 409-420.

Ehrhart, J., Smith, A. J., Kuzmin-Nichols, N., Zesiewicz, T. A., Jahan, I., Shytle, R. D., . . . Garbuzova-Davis, S. (2015). Humoral factors in ALS patients during disease progression. *J Neuroinflammation, 12*, 127.

Elmore, M. R., Lee, R. J., West, B. L., & Green, K. N. (2015). Characterizing newly repopulated microglia in the adult mouse: impacts on animal behavior, cell morphology, and neuroinflammation. *PLoS One, 10*(4), e0122912.

Elmore, M. R., Najafi, A. R., Koike, M. A., Dagher, N. N., Spangenberg, E. E., Rice, R. A., . . . Green, K. N. (2014). Colony-stimulating factor 1 receptor signaling is necessary for microglia viability, unmasking a microglia progenitor cell in the adult brain. *Neuron, 82*(2), 380-397.

Endo, F., Komine, O., Fujimori-Tonou, N., Katsuno, M., Jin, S., Watanabe, S., . . . Yamanaka, K. (2015). Astrocyte-derived TGF-beta1 accelerates disease progression in ALS mice by interfering with the neuroprotective functions of microglia and T cells. *Cell Rep, 11*(4), 592-604.

Ernst, C., & Christie, B. R. (2006). Isolectin-IB 4 as a vascular stain for the study of adult neurogenesis. *J Neurosci Methods, 150*(1), 138-142.

Etienne, S., Bourdoulous, S., Strosberg, A. D., & Couraud, P. O. (1999). MHC class II engagement in brain endothelial cells induces protein kinase A-dependent IL-6 secretion and phosphorylation of cAMP response element-binding protein. *J Immunol, 163*(7), 3636-3641.

Farina, C., Aloisi, F., & Meinl, E. (2007). Astrocytes are active players in cerebral innate immunity. *Trends Immunol, 28*(3), 138-145.

Filipello, F., Pozzi, D., Proietti, M., Romagnani, A., Mazzitelli, S., Matteoli, M., . . . Grassi, F. (2016). Ectonucleotidase activity and immunosuppression in astrocyte-CD4 T cell bidirectional signaling. *Oncotarget, 7*(5), 5143-5156.

Fischer, L. R., Culver, D. G., Tennant, P., Davis, A. A., Wang, M., Castellano-Sanchez, A., . . . Glass, J. D. (2004). Amyotrophic lateral sclerosis is a distal axonopathy: evidence in mice and man. *Experimental Neurology, 185*(2), 232-240.

Flugel, A., Schwaiger, F. W., Neumann, H., Medana, I., Willem, M., Wekerle, H., . . . Graeber, M. B. (2000). Neuronal FasL induces cell death of encephalitogenic T lymphocytes. *Brain Pathol, 10*(3), 353-364.

Frakes, A. E., Ferraiuolo, L., Haidet-Phillips, A. M., Schmelzer, L., Braun, L., Miranda, C. J., . . . Kaspar, B. K. (2014). Microglia induce motor neuron death via the classical NF-kappaB pathway in amyotrophic lateral sclerosis. *Neuron, 81*(5), 1009-1023.

Gautier, E. L., Shay, T., Miller, J., Greter, M., Jakubzick, C., Ivanov, S., . . . Immunological Genome, C. (2012). Gene-expression profiles and transcriptional regulatory pathways that underlie the identity and diversity of mouse tissue macrophages. *Nat Immunol, 13*(11), 1118-1128.

Ghobrial, R. R., Boublik, M., Winn, H. J., & Auchincloss, H., Jr. (1989). In vivo use of monoclonal antibodies against murine T cell antigens. *Clin Immunol Immunopathol, 52*(3), 486-506.

Gill, D., & Veltkamp, R. (2016). Dynamics of T cell responses after stroke. *Curr Opin Pharmacol, 26*, 26-32.

Gomis-Ruth, S., Stiess, M., Wierenga, C. J., Meyn, L., & Bradke, F. (2014). Single-cell axotomy of cultured hippocampal neurons integrated in neuronal circuits. *Nat Protoc, 9*(5), 1028-1037.

Gordon, T., & Borschel, G. H. (2016). The use of the rat as a model for studying peripheral nerve regeneration and sprouting after complete and partial nerve injuries. *Exp Neurol*.

Gotoh, K., Inoue, M., Masaki, T., Chiba, S., Shimasaki, T., Ando, H., . . . Yoshimatsu, H. (2012). A novel anti-inflammatory role for spleen-derived interleukin-10 in obesity-induced hypothalamic inflammation. *J Neurochem, 120*(5), 752-764.

Gottfried-Blackmore, A., Kaunzner, U. W., Idoyaga, J., Felger, J. C., McEwen, B. S., & Bulloch, K. (2009). Acute in vivo exposure to interferon-gamma enables resident brain dendritic cells to become effective antigen presenting cells. *Proc Natl Acad Sci U S A, 106*(49), 20918-20923.

Gottfried, E., Kunz-Schughart, L. A., Weber, A., Rehli, M., Peuker, A., Muller, A., . . . Kreutz, M. (2008). Expression of CD68 in non-myeloid cell types. *Scand J Immunol, 67*(5), 453-463.

Graber, D. J., Hickey, W. F., & Harris, B. T. (2010). Progressive changes in microglia and macrophages in spinal cord and peripheral nerve in the transgenic rat model of amyotrophic lateral sclerosis. *J Neuroinflammation, 7*, 8.

Graeber, M. B., Bise, K., & Mehraein, P. (1993). Synaptic stripping in the human facial nucleus. *Acta Neuropathol, 86*(2), 179-181.

Graeber, M. B., Lopez-Redondo, F., Ikoma, E., Ishikawa, M., Imai, Y., Nakajima, K., . . . Kohsaka, S. (1998). The microglia/macrophage response in the neonatal rat facial nucleus following axotomy. *Brain Res, 813*(2), 241-253.

Graeber, M. B., Tetzlaff, W., Streit, W. J., & Kreutzberg, G. W. (1988). Microglial cells but not astrocytes undergo mitosis following rat facial nerve axotomy. *Neurosci Lett, 85*(3), 317-321.

Grafstein, B. (1975). The nerve cell body response to axotomy. *Exp Neurol, 48*(3 pt. 2), 32-51.
Gravel, M., Beland, L. C., Soucy, G., Abdelhamid, E., Rahimian, R., Gravel, C., & Kriz, J. (2016). IL-10 Controls Early Microglial Phenotypes and Disease Onset in ALS Caused by Misfolded Superoxide Dismutase 1. *J Neurosci, 36*(3), 1031-1048.
Greenhalgh, A. D., Passos Dos Santos, R., Zarruk, J. G., Salmon, C. K., Kroner, A., & David, S. (2016). Arginase-1 is expressed exclusively by infiltrating myeloid cells in CNS injury and disease. *Brain Behav Immun, 56*, 61-67.
Grilli, M., Barbieri, I., Basudev, H., Brusa, R., Casati, C., Lozza, G., & Ongini, E. (2000). Interleukin-10 modulates neuronal threshold of vulnerability to ischaemic damage. *Eur J Neurosci, 12*(7), 2265-2272.
Guillot-Sestier, M. V., Doty, K. R., Gate, D., Rodriguez, J., Jr., Leung, B. P., Rezai-Zadeh, K., & Town, T. (2015). Il10 deficiency rebalances innate immunity to mitigate Alzheimer-like pathology. *Neuron, 85*(3), 534-548.
Guntinas-Lichius, O., Schulte, E., Stennert, E., & Neiss, W. F. (1997). The use of texture analysis to study the time course of chromatolysis. *J Neurosci Methods, 78*(1-2), 1-6.
Gurney, M. E., Pu, H., Chiu, A. Y., Dal Canto, M. C., Polchow, C. Y., Alexander, D. D., . . . et al. (1994). Motor neuron degeneration in mice that express a human Cu,Zn superoxide dismutase mutation. *Science, 264*(5166), 1772-1775.
Ha, G. K., Huang, Z., Parikh, R., Pastrana, M., & Petitto, J. M. (2007a). Immunodeficiency impairs re-injury induced reversal of neuronal atrophy: relation to T cell subsets and microglia. *Exp Neurol, 208*(1), 92-99.
Ha, G. K., Huang, Z., & Petitto, J. M. (2007b). Prior facial motor neuron injury elicits endogenous T cell memory: relation to neuroregeneration. *J Neuroimmunol, 183*(1-2), 111-117.
Ha, G. K., Huang, Z., Streit, W. J., & Petitto, J. M. (2006). Endogenous T lymphocytes and microglial reactivity in the axotomized facial motor nucleus of mice: effect of genetic background and the RAG2 gene. *J Neuroimmunol, 172*(1-2), 1-8.
Ha, G. K., Pastrana, M., Huang, Z., & Petitto, J. M. (2008). T cell memory in the injured facial motor nucleus: relation to functional recovery following facial nerve crush. *Neurosci Lett, 443*(3), 150-154.
Haidet-Phillips, A. M., Hester, M. E., Miranda, C. J., Meyer, K., Braun, L., Frakes, A., . . . Kaspar, B. K. (2011). Astrocytes from familial and sporadic ALS patients are toxic to motor neurons. *Nat Biotechnol, 29*(9), 824-828.
Haulcomb, M. M., Mesnard, N. A., Batka, R. J., Alexander, T. D., Sanders, V. M., & Jones, K. J. (2014). Axotomy-induced target disconnection promotes an additional death mechanism involved in motoneuron degeneration in amyotrophic lateral sclerosis transgenic mice. *J Comp Neurol, 522*(10), 2349-2376.
Hensley, K. (2003). Message and protein-level elevation of tumor necrosis factor α (TNFα) and TNFα-modulating cytokines in spinal cords of the G93A-SOD1 mouse model for amyotrophic lateral sclerosis. *Neurobiology of Disease, 14*(1), 74-80.
Hensley, K., Floyd, R. A., Gordon, B., Mou, S., Pye, Q. N., Stewart, C., . . . Williamson, K. (2002). Temporal patterns of cytokine and apoptosis-related gene expression in

spinal cords of the G93A-SOD1 mouse model of amyotrophic lateral sclerosis. *J Neurochem, 82*(2), 365-374.
Hermanson, M., Olsson, T., Westermark, B., & Funa, K. (1995). PDGF and its receptors following facial nerve axotomy in rats: expression in neurons and surrounding glia. *Exp Brain Res, 102*(3), 415-422.
Hickey, W. F., & Kimura, H. (1988). Perivascular microglial cells of the CNS are bone marrow-derived and present antigen in vivo. *Science, 239*(4837), 290-292.
Holmoy, T., Roos, P. M., & Kvale, E. O. (2006). ALS: cytokine profile in cerebrospinal fluid T-cell clones. *Amyotroph Lateral Scler, 7*(3), 183-186.
Holness, C. L., da Silva, R. P., Fawcett, J., Gordon, S., & Simmons, D. L. (1993). Macrosialin, a mouse macrophage-restricted glycoprotein, is a member of the lamp/lgp family. *J Biol Chem, 268*(13), 9661-9666.
Holness, C. L., & Simmons, D. L. (1993). Molecular cloning of CD68, a human macrophage marker related to lysosomal glycoproteins. *Blood, 81*(6), 1607-1613.
Horvat, A., Schwaiger, F., Hager, G., Brocker, F., Streif, R., Knyazev, P., . . . Kreutzberg, G. W. (2001). A novel role for protein tyrosine phosphatase shp1 in controlling glial activation in the normal and injured nervous system. *J Neurosci, 21*(3), 865-874.
Houdek, M. T., & Shin, A. Y. (2015). Management and complications of traumatic peripheral nerve injuries. *Hand Clin, 31*(2), 151-163.
Hovden, H., Frederiksen, J. L., & Pedersen, S. W. (2013). Immune system alterations in amyotrophic lateral sclerosis. *Acta Neurol Scand, 128*(5), 287-296.
Hsu, H., Shu, H. B., Pan, M. G., & Goeddel, D. V. (1996). TRADD-TRAF2 and TRADD-FADD interactions define two distinct TNF receptor 1 signal transduction pathways. *Cell, 84*(2), 299-308.
Huebner, E. A., & Strittmatter, S. M. (2009). Axon regeneration in the peripheral and central nervous systems. *Results Probl Cell Differ, 48*, 339-351.
Huh, G. S., Boulanger, L. M., Du, H., Riquelme, P. A., Brotz, T. M., & Shatz, C. J. (2000). Functional requirement for class I MHC in CNS development and plasticity. *Science, 290*(5499), 2155-2159.
Hulshof, S., Montagne, L., De Groot, C. J., & Van Der Valk, P. (2002). Cellular localization and expression patterns of interleukin-10, interleukin-4, and their receptors in multiple sclerosis lesions. *Glia, 38*(1), 24-35.
Hurley, S. (2003). Facial nerve axotomy in aged and young adult rats: analysis of the glial response. *Neurobiology of Aging, 24*(3), 511-518.
Hutchins, A. P., Diez, D., & Miranda-Saavedra, D. (2013). The IL-10/STAT3-mediated anti-inflammatory response: recent developments and future challenges. *Brief Funct Genomics, 12*(6), 489-498.
Hutchison, E. R., Kawamoto, E. M., Taub, D. D., Lal, A., Abdelmohsen, K., Zhang, Y., . . . Mattson, M. P. (2013). Evidence for miR-181 involvement in neuroinflammatory responses of astrocytes. *Glia, 61*(7), 1018-1028.
Ilieva, H., Polymenidou, M., & Cleveland, D. W. (2009). Non-cell autonomous toxicity in neurodegenerative disorders: ALS and beyond. *J Cell Biol, 187*(6), 761-772.
Imai, Y., Ibata, I., Ito, D., Ohsawa, K., & Kohsaka, S. (1996). A novel gene iba1 in the major histocompatibility complex class III region encoding an EF hand protein

expressed in a monocytic lineage. *Biochem Biophys Res Commun, 224*(3), 855-862.

Isokawa-Akesson, M., & Komisaruk, B. R. (1987). Difference in projections to the lateral and medial facial nucleus: anatomically separate pathways for rhythmical vibrissa movement in rats. *Exp Brain Res, 65*(2), 385-398.

Ito, D., Imai, Y., Ohsawa, K., Nakajima, K., Fukuuchi, Y., & Kohsaka, S. (1998). Microglia-specific localisation of a novel calcium binding protein, Iba1. *Brain Res Mol Brain Res, 57*(1), 1-9.

Jaarsma, D., Teuling, E., Haasdijk, E. D., De Zeeuw, C. I., & Hoogenraad, C. C. (2008). Neuron-specific expression of mutant superoxide dismutase is sufficient to induce amyotrophic lateral sclerosis in transgenic mice. *J Neurosci, 28*(9), 2075-2088.

Jinno, S., & Yamada, J. (2011). Using comparative anatomy in the axotomy model to identify distinct roles for microglia and astrocytes in synaptic stripping. *Neuron Glia Biol, 7*(1), 55-66.

Joniec-Maciejak, I., Ciesielska, A., Wawer, A., Sznejder-Pacholek, A., Schwenkgrub, J., Cudna, A., . . . Czlonkowski, A. (2014). The influence of AAV2-mediated gene transfer of human IL-10 on neurodegeneration and immune response in a murine model of Parkinson's disease. *Pharmacol Rep, 66*(4), 660-669.

Jost, N. H., Abel, S., Hutzler, M., Sparwasser, T., Zimmermann, A., Roers, A., . . . Hansen, W. (2014). Regulatory T cells and T-cell-derived IL-10 interfere with effective anti-cytomegalovirus immune response. *Immunol Cell Biol, 92*(10), 860-871.

Kalla, R., Liu, Z., Xu, S., Koppius, A., Imai, Y., Kloss, C. U., . . . Raivich, G. (2001). Microglia and the early phase of immune surveillance in the axotomized facial motor nucleus: impaired microglial activation and lymphocyte recruitment but no effect on neuronal survival or axonal regeneration in macrophage-colony stimulating factor-deficient mice. *J Comp Neurol, 436*(2), 182-201.

Kandel, E. R. (2013). *Principles of neural science* (5th ed.). New York: McGraw-Hill.

Kastin, A. J., Akerstrom, V., & Pan, W. (2003). Interleukin-10 as a CNS therapeutic: the obstacle of the blood–brain/blood–spinal cord barrier. *Molecular Brain Research, 114*(2), 168-171.

Kelemen, J., Hedlund, W., Orlin, J. B., Berkman, E. M., & Munsat, T. L. (1983). Plasmapheresis with immunosuppression in amyotrophic lateral sclerosis. *Arch Neurol, 40*(12), 752-753.

Kiesler, P., Fuss, I. J., & Strober, W. (2015). Experimental Models of Inflammatory Bowel Diseases. *Cell Mol Gastroenterol Hepatol, 1*(2), 154-170.

Kigerl, K. A., Gensel, J. C., Ankeny, D. P., Alexander, J. K., Donnelly, D. J., & Popovich, P. G. (2009). Identification of two distinct macrophage subsets with divergent effects causing either neurotoxicity or regeneration in the injured mouse spinal cord. *J Neurosci, 29*(43), 13435-13444.

Kim, K. K., Adelstein, R. S., & Kawamoto, S. (2009). Identification of neuronal nuclei (NeuN) as Fox-3, a new member of the Fox-1 gene family of splicing factors. *J Biol Chem, 284*(45), 31052-31061.

Kipnis, J., Cohen, H., Cardon, M., Ziv, Y., & Schwartz, M. (2004). T cell deficiency leads to cognitive dysfunction: implications for therapeutic vaccination for

schizophrenia and other psychiatric conditions. *Proc Natl Acad Sci U S A, 101*(21), 8180-8185.

Kivisakk, P., Imitola, J., Rasmussen, S., Elyaman, W., Zhu, B., Ransohoff, R. M., & Khoury, S. J. (2009). Localizing central nervous system immune surveillance: meningeal antigen-presenting cells activate T cells during experimental autoimmune encephalomyelitis. *Ann Neurol, 65*(4), 457-469.

Kiyota, T., Ingraham, K. L., Swan, R. J., Jacobsen, M. T., Andrews, S. J., & Ikezu, T. (2012). AAV serotype 2/1-mediated gene delivery of anti-inflammatory interleukin-10 enhances neurogenesis and cognitive function in APP+PS1 mice. *Gene Ther, 19*(7), 724-733.

Klein, M. A., Moller, J. C., Jones, L. L., Bluethmann, H., Kreutzberg, G. W., & Raivich, G. (1997). Impaired neuroglial activation in interleukin-6 deficient mice. *Glia, 19*(3), 227-233.

Komis, G. (2012). GFP fluorescence after fixation. Retrieved from https://www.researchgate.net/post/GFP_fluorescence_after_fixation10

Koriauli, S., Natsvlishvili, N., Barbakadze, T., & Mikeladze, D. (2015). Knockdown of interleukin-10 induces the redistribution of sigma1-receptor and increases the glutamate-dependent NADPH-oxidase activity in mouse brain neurons. *Biol Res, 48*, 55.

Krupenko, S. A. (2009). FDH: an aldehyde dehydrogenase fusion enzyme in folate metabolism. *Chem Biol Interact, 178*(1-3), 84-93.

Kuhle, J., Lindberg, R. L., Regeniter, A., Mehling, M., Steck, A. J., Kappos, L., & Czaplinski, A. (2009). Increased levels of inflammatory chemokines in amyotrophic lateral sclerosis. *Eur J Neurol, 16*(6), 771-774.

Kuhn, R., Lohler, J., Rennick, D., Rajewsky, K., & Muller, W. (1993). Interleukin-10-deficient mice develop chronic enterocolitis. *Cell, 75*(2), 263-274.

Kurushima, H., Ramprasad, M., Kondratenko, N., Foster, D. M., Quehenberger, O., & Steinberg, D. (2000). Surface expression and rapid internalization of macrosialin (mouse CD68) on elicited mouse peritoneal macrophages. *J Leukoc Biol, 67*(1), 104-108.

Kuzmenok, O. I., Sanberg, P. R., Desjarlais, T. G., Bennett, S. P., & Garbuzova-Davis, S. N. (2006). Lymphopenia and spontaneous autorosette formation in SOD1 mouse model of ALS. *J Neuroimmunol, 172*(1-2), 132-136.

Kwilasz, A. J., Grace, P. M., Serbedzija, P., Maier, S. F., & Watkins, L. R. (2015). The therapeutic potential of interleukin-10 in neuroimmune diseases. *Neuropharmacology, 96*(Pt A), 55-69.

Kwon, M. S., Noh, M. Y., Oh, K. W., Cho, K. A., Kang, B. Y., Kim, K. S., . . . Kim, S. H. (2014). The immunomodulatory effects of human mesenchymal stem cells on peripheral blood mononuclear cells in ALS patients. *J Neurochem, 131*(2), 206-218.

Laskawi, R., & Wolff, J. R. (1996). Changes in glial fibrillary acidic protein immunoreactivity in the rat facial nucleus following various types of nerve lesions. *Eur Arch Otorhinolaryngol, 253*(8), 475-480.

Laskin, D. L. (2009). Macrophages and inflammatory mediators in chemical toxicity: a battle of forces. *Chem Res Toxicol, 22*(8), 1376-1385.

Ledeboer, A., Brevé, J. J. P., Wierinckx, A., Van Der Jagt, S., Bristow, A. F., Leysen, J. E., . . . Van Dam, A.-M. (2002). Expression and regulation of interleukin-10 and interleukin-10 receptor in rat astroglial and microglial cells. *European Journal of Neuroscience, 16*(7), 1175-1185.

Lee, H., Brott, B. K., Kirkby, L. A., Adelson, J. D., Cheng, S., Feller, M. B., . . . Shatz, C. J. (2014). Synapse elimination and learning rules co-regulated by MHC class I H2-Db. *Nature, 509*(7499), 195-200.

Lewis, K. E., Rasmussen, A. L., Bennett, W., King, A., West, A. K., Chung, R. S., & Chuah, M. I. (2014). Microglia and motor neurons during disease progression in the SOD1G93A mouse model of amyotrophic lateral sclerosis: changes in arginase1 and inducible nitric oxide synthase. *J Neuroinflammation, 11*, 55.

Liao, L., Park, S. K., Xu, T., Vanderklish, P., & Yates, J. R., 3rd. (2008). Quantitative proteomic analysis of primary neurons reveals diverse changes in synaptic protein content in fmr1 knockout mice. *Proc Natl Acad Sci U S A, 105*(40), 15281-15286.

Liddelow, S. A., Guttenplan, K. A., Clarke, L. E., Bennett, F. C., Bohlen, C. J., Schirmer, L., . . . Barres, B. A. (2017). Neurotoxic reactive astrocytes are induced by activated microglia. *Nature, 541*(7638), 481-487.

Lidman, O., Fraidakis, M., Lycke, N., Olson, L., Olsson, T., & Piehl, F. (2002). Facial nerve lesion response; strain differences but no involvement of IFN-gamma, STAT4 or STAT6. *Neuroreport, 13*(13), 1589-1593.

Lieberman, A. R. (1971). The axon reaction: a review of the principal features of perikaryal responses to axon injury. *Int Rev Neurobiol, 14*, 49-124.

Lieberman, D. M., Jan, T. A., Ahmad, S. O., & Most, S. P. (2011). Effects of corticosteroids on functional recovery and neuron survival after facial nerve injury in mice. *Arch Facial Plast Surg, 13*(2), 117-124.

Lino, M. M., Schneider, C., & Caroni, P. (2002). Accumulation of SOD1 mutants in postnatal motoneurons does not cause motoneuron pathology or motoneuron disease. *J Neurosci, 22*(12), 4825-4832.

Liu, T., Clark, R. K., McDonnell, P. C., Young, P. R., White, R. F., Barone, F. C., & Feuerstein, G. Z. (1994). Tumor necrosis factor-alpha expression in ischemic neurons. *Stroke, 25*(7), 1481-1488.

Liu, Y., Zhou, L. J., Wang, J., Li, D., Ren, W. J., Peng, J., . . . Liu, X. G. (2017). TNF-alpha Differentially Regulates Synaptic Plasticity in the Hippocampus and Spinal Cord by Microglia-Dependent Mechanisms after Peripheral Nerve Injury. *J Neurosci, 37*(4), 871-881.

Liu, Z. Q., Bohatschek, M., Pfeffer, K., Bluethmann, H., & Raivich, G. (2005). Major histocompatibility complex (MHC2+) perivascular macrophages in the axotomized facial motor nucleus are regulated by receptors for interferon-gamma (IFNgamma) and tumor necrosis factor (TNF). *Neuroscience, 131*(2), 283-292.

Lobo-Silva, D., Carriche, G. M., Castro, A. G., Roque, S., & Saraiva, M. (2016). Balancing the immune response in the brain: IL-10 and its regulation. *J Neuroinflammation, 13*(1), 297.

Lu, C. H., Allen, K., Oei, F., Leoni, E., Kuhle, J., Tree, T., . . . Malaspina, A. (2016). Systemic inflammatory response and neuromuscular involvement in amyotrophic lateral sclerosis. *Neurol Neuroimmunol Neuroinflamm, 3*(4), e244.

Ma, S. F., Chen, Y. J., Zhang, J. X., Shen, L., Wang, R., Zhou, J. S., . . . Lu, H. Z. (2015). Adoptive transfer of M2 macrophages promotes locomotor recovery in adult rats after spinal cord injury. *Brain Behav Immun, 45*, 157-170.

Madan, R., Demircik, F., Surianarayanan, S., Allen, J. L., Divanovic, S., Trompette, A., . . . Karp, C. L. (2009). Nonredundant roles for B cell-derived IL-10 in immune counter-regulation. *J Immunol, 183*(4), 2312-2320.

Male, D. K., Pryce, G., & Hughes, C. C. (1987). Antigen presentation in brain: MHC induction on brain endothelium and astrocytes compared. *Immunology, 60*(3), 453-459.

Mariotti, R., Cristino, L., Bressan, C., Boscolo, S., & Bentivoglio, M. (2002). Altered reaction of facial motoneurons to axonal damage in the presymptomatic phase of a murine model of familial amyotrophic lateral sclerosis. *Neuroscience, 115*(2), 331-335.

Marshall, S. A., McClain, J. A., Kelso, M. L., Hopkins, D. M., Pauly, J. R., & Nixon, K. (2013). Microglial activation is not equivalent to neuroinflammation in alcohol-induced neurodegeneration: The importance of microglia phenotype. *Neurobiol Dis, 54*, 239-251.

Martinez-Muriana, A., Mancuso, R., Francos-Quijorna, I., Olmos-Alonso, A., Osta, R., Perry, V. H., . . . Lopez-Vales, R. (2016). CSF1R blockade slows the progression of amyotrophic lateral sclerosis by reducing microgliosis and invasion of macrophages into peripheral nerves. *Sci Rep, 6*, 25663.

Martinez, F. O., & Gordon, S. (2014). The M1 and M2 paradigm of macrophage activation: time for reassessment. *F1000Prime Rep, 6*, 13.

Masuda, T., Tsuda, M., Yoshinaga, R., Tozaki-Saitoh, H., Ozato, K., Tamura, T., & Inoue, K. (2012). IRF8 is a critical transcription factor for transforming microglia into a reactive phenotype. *Cell Rep, 1*(4), 334-340.

McCoy, M. K., & Tansey, M. G. (2008). TNF signaling inhibition in the CNS: implications for normal brain function and neurodegenerative disease. *J Neuroinflammation, 5*, 45.

McMahon, E. J., Bailey, S. L., & Miller, S. D. (2006). CNS dendritic cells: critical participants in CNS inflammation? *Neurochem Int, 49*(2), 195-203.

McPhail, L. T., McBride, C. B., McGraw, J., Steeves, J. D., & Tetzlaff, W. (2004). Axotomy abolishes NeuN expression in facial but not rubrospinal neurons. *Experimental Neurology, 185*(1), 182-190.

Mehta, P., Antao, V., Kaye, W., Sanchez, M., Williamson, D., Bryan, L., . . . Horton, K. (2014). Prevalence of amyotrophic lateral sclerosis - United States, 2010-2011. *MMWR Suppl, 63*(7), 1-14.

Meissner, F., Molawi, K., & Zychlinsky, A. (2010). Mutant superoxide dismutase 1-induced IL-1beta accelerates ALS pathogenesis. *Proc Natl Acad Sci U S A, 107*(29), 13046-13050.

Mentis, G. Z., Greensmith, L., & Vrbova, G. (1993). Motoneurons destined to die are rescued by blocking N-methyl-D-aspartate receptors by MK-801. *Neuroscience, 54*(2), 283-285.

Mesnard-Hoaglin, N. A., Xin, J., Haulcomb, M. M., Batka, R. J., Sanders, V. M., & Jones, K. J. (2014). SOD1(G93A) transgenic mouse CD4(+) T cells mediate

neuroprotection after facial nerve axotomy when removed from a suppressive peripheral microenvironment. *Brain Behav Immun, 40*, 55-60.
Mesnard, N. A., Alexander, T. D., Sanders, V. M., & Jones, K. J. (2010). Use of laser microdissection in the investigation of facial motoneuron and neuropil molecular phenotypes after peripheral axotomy. *Exp Neurol, 225*(1), 94-103.
Mesnard, N. A., Haulcomb, M. M., Tanzer, L., Sanders, V. M., & Jones, K. J. (2013). Delayed functional recovery in presymptomatic mSOD1 mice following facial nerve crush axotomy. *J Neurodegener Regen, 4*(1), 21-25.
Mesnard, N. A., Sanders, V. M., & Jones, K. J. (2011). Differential gene expression in the axotomized facial motor nucleus of presymptomatic SOD1 mice. *J Comp Neurol, 519*(17), 3488-3506.
Mesples, B., Plaisant, F., & Gressens, P. (2003). Effects of interleukin-10 on neonatal excitotoxic brain lesions in mice. *Developmental Brain Research, 141*(1-2), 25-32.
Min, K. J., Yang, M. S., Kim, S. U., Jou, I., & Joe, E. H. (2006). Astrocytes induce hemeoxygenase-1 expression in microglia: a feasible mechanism for preventing excessive brain inflammation. *J Neurosci, 26*(6), 1880-1887.
Moran, L. B., & Graeber, M. B. (2004). The facial nerve axotomy model. *Brain Res Brain Res Rev, 44*(2-3), 154-178.
Morganti, J. M., Riparip, L. K., & Rosi, S. (2016). Call Off the Dog(ma): M1/M2 Polarization Is Concurrent following Traumatic Brain Injury. *PLoS One, 11*(1), e0148001.
Moulignier, A., Moulonguet, A., Pialoux, G., & Rozenbaum, W. (2001). Reversible ALS-like disorder in HIV infection. *Neurology, 57*(6), 995-1001.
Mulle, J. G., Sharp, W. G., & Cubells, J. F. (2013). The gut microbiome: a new frontier in autism research. *Curr Psychiatry Rep, 15*(2), 337.
Mullen, R. J., Buck, C. R., & Smith, A. M. (1992). NeuN, a neuronal specific nuclear protein in vertebrates. *Development, 116*(1), 201-211.
Murray, P. J., Allen, J. E., Biswas, S. K., Fisher, E. A., Gilroy, D. W., Goerdt, S., . . . Wynn, T. A. (2014). Macrophage activation and polarization: nomenclature and experimental guidelines. *Immunity, 41*(1), 14-20.
Nardo, G., Trolese, M. C., de Vito, G., Cecchi, R., Riva, N., Dina, G., . . . Bendotti, C. (2016). Immune response in peripheral axons delays disease progression in SOD1G93A mice. *J Neuroinflammation, 13*(1), 261.
Noble, J., Munro, C. A., Prasad, V. S., & Midha, R. (1998). Analysis of upper and lower extremity peripheral nerve injuries in a population of patients with multiple injuries. *J Trauma, 45*(1), 116-122.
Olmstead, D. N., Mesnard-Hoaglin, N. A., Batka, R. J., Haulcomb, M. M., Miller, W. M., & Jones, K. J. (2015). Facial nerve axotomy in mice: a model to study motoneuron response to injury. *J Vis Exp*(96), e52382.
Olsson, T. P., Forsberg, I., & Kristensson, K. (1978). Uptake and retrograde axonal transport of horseradish peroxidase in regenerating facial motor neurons of the mouse. *J Neurocytol, 7*(3), 323-336.
Ooi, Y. Y., Dheen, S. T., & Tay, S. S. (2015). Paracrine effects of mesenchymal stem cells-conditioned medium on microglial cytokines expression and nitric oxide production. *Neuroimmunomodulation, 22*(4), 233-242.

Orrell, R. W. (2010). Motor neuron disease: systematic reviews of treatment for ALS and SMA. *Br Med Bull, 93*, 145-159.

Pandya, R. S., Zhu, H., Li, W., Bowser, R., Friedlander, R. M., & Wang, X. (2013). Therapeutic neuroprotective agents for amyotrophic lateral sclerosis. *Cell Mol Life Sci, 70*(24), 4729-4745.

Park, K. W., Lee, H. G., Jin, B. K., & Lee, Y. B. (2007). Interleukin-10 endogenously expressed in microglia prevents lipopolysaccharide-induced neurodegeneration in the rat cerebral cortex in vivo. *Exp Mol Med, 39*(6), 812-819.

Pascual, O., Ben Achour, S., Rostaing, P., Triller, A., & Bessis, A. (2012). Microglia activation triggers astrocyte-mediated modulation of excitatory neurotransmission. *Proc Natl Acad Sci U S A, 109*(4), E197-205.

Pfaffl, M. W. (2001). A new mathematical model for relative quantification in real-time RT-PCR. *Nucleic Acids Res, 29*(9), e45.

Plunkett, J. A., Yu, C. G., Easton, J. M., Bethea, J. R., & Yezierski, R. P. (2001). Effects of interleukin-10 (IL-10) on pain behavior and gene expression following excitotoxic spinal cord injury in the rat. *Exp Neurol, 168*(1), 144-154.

Pramatarova, A., Laganiere, J., Roussel, J., Brisebois, K., & Rouleau, G. A. (2001). Neuron-specific expression of mutant superoxide dismutase 1 in transgenic mice does not lead to motor impairment. *J Neurosci, 21*(10), 3369-3374.

Pryce, G., Male, D., & Sedgwick, J. (1989). Antigen presentation in brain: brain endothelial cells are poor stimulators of T-cell proliferation. *Immunology, 66*(2), 207-212.

Raivich, G. (2002). Cytotoxic Potential of Proinflammatory Cytokines: Combined Deletion of TNF Receptors TNFR1 and TNFR2 Prevents Motoneuron Cell Death after Facial Axotomy in Adult Mouse. *Experimental Neurology, 178*(2), 186-193.

Raivich, G., Jones, L. L., Kloss, C. U., Werner, A., Neumann, H., & Kreutzberg, G. W. (1998). Immune surveillance in the injured nervous system: T-lymphocytes invade the axotomized mouse facial motor nucleus and aggregate around sites of neuronal degeneration. *J Neurosci, 18*(15), 5804-5816.

Raivich, G., Moreno-Flores, M. T., Moller, J. C., & Kreutzberg, G. W. (1994). Inhibition of posttraumatic microglial proliferation in a genetic model of macrophage colony-stimulating factor deficiency in the mouse. *Eur J Neurosci, 6*(10), 1615-1618.

Ramprasad, M. P., Fischer, W., Witztum, J. L., Sambrano, G. R., Quehenberger, O., & Steinberg, D. (1995). The 94- to 97-kDa mouse macrophage membrane protein that recognizes oxidized low density lipoprotein and phosphatidylserine-rich liposomes is identical to macrosialin, the mouse homologue of human CD68. *Proc Natl Acad Sci U S A, 92*(21), 9580-9584.

Ransohoff, R. M., & Brown, M. A. (2012). Innate immunity in the central nervous system. *J Clin Invest, 122*(4), 1164-1171.

Ransohoff, R. M., Kivisakk, P., & Kidd, G. (2003). Three or more routes for leukocyte migration into the central nervous system. *Nat Rev Immunol, 3*(7), 569-581.

Raoul, C., Buhler, E., Sadeghi, C., Jacquier, A., Aebischer, P., Pettmann, B., . . . Haase, G. (2006). Chronic activation in presymptomatic amyotrophic lateral sclerosis (ALS) mice of a feedback loop involving Fas, Daxx, and FasL. *Proc Natl Acad Sci U S A, 103*(15), 6007-6012.

Raoul, C., Estevez, A. G., Nishimune, H., Cleveland, D. W., deLapeyriere, O., Henderson, C. E., . . . Pettmann, B. (2002). Motoneuron death triggered by a specific pathway downstream of Fas. potentiation by ALS-linked SOD1 mutations. *Neuron, 35*(6), 1067-1083.

Roers, A., Siewe, L., Strittmatter, E., Deckert, M., Schluter, D., Stenzel, W., . . . Muller, W. (2004). T cell-specific inactivation of the interleukin 10 gene in mice results in enhanced T cell responses but normal innate responses to lipopolysaccharide or skin irritation. *J Exp Med, 200*(10), 1289-1297.

Rothhammer, V., Mascanfroni, I. D., Bunse, L., Takenaka, M. C., Kenison, J. E., Mayo, L., . . . Quintana, F. J. (2016). Type I interferons and microbial metabolites of tryptophan modulate astrocyte activity and central nervous system inflammation via the aryl hydrocarbon receptor. *Nat Med, 22*(6), 586-597.

Round, J. L., & Mazmanian, S. K. (2009). The gut microbiota shapes intestinal immune responses during health and disease. *Nat Rev Immunol, 9*(5), 313-323.

Sadtler, K., Allen, B. W., Estrellas, K., Housseau, F., Pardoll, D. M., & Elisseeff, J. H. (2016). The Scaffold Immune Microenvironment: Biomaterial-Mediated Immune Polarization in Traumatic and Nontraumatic Applications. *Tissue Eng Part A*.

Saleh, I. A., Zesiewicz, T., Xie, Y., Sullivan, K. L., Miller, A. M., Kuzmin-Nichols, N., . . . Garbuzova-Davis, S. (2009). Evaluation of humoral immune response in adaptive immunity in ALS patients during disease progression. *J Neuroimmunol, 215*(1-2), 96-101.

Schiefer, J., Kampe, K., Dodt, H. U., Zieglgansberger, W., & Kreutzberg, G. W. (1999). Microglial motility in the rat facial nucleus following peripheral axotomy. *J Neurocytol, 28*(6), 439-453.

Schwenkgrub, J., Joniec-Maciejak, I., Sznejder-Pacholek, A., Wawer, A., Ciesielska, A., Bankiewicz, K., . . . Czlonkowski, A. (2013). Effect of human interleukin-10 on the expression of nitric oxide synthases in the MPTP-based model of Parkinson's disease. *Pharmacol Rep, 65*(1), 44-49.

Seddon, H. J. (1942). A Classification of Nerve Injuries. *Br Med J, 2*(4260), 237-239.

Serpe, C. J., Coers, S., Sanders, V. M., & Jones, K. J. (2003). CD4+ T, but not CD8+ or B, lymphocytes mediate facial motoneuron survival after facial nerve transection. *Brain, Behavior, and Immunity, 17*(5), 393-402.

Serpe, C. J., Kohm, A. P., Huppenbauer, C. B., Sanders, V. M., & Jones, K. J. (1999). Exacerbation of facial motoneuron loss after facial nerve transection in severe combined immunodeficient (scid) mice. *J Neurosci, 19*(11), RC7.

Serpe, C. J., Sanders, V. M., & Jones, K. J. (2000). Kinetics of facial motoneuron loss following facial nerve transection in severe combined immunodeficient mice. *J Neurosci Res, 62*(2), 273-278.

Serpe, C. J., Tetzlaff, J. E., Coers, S., Sanders, V. M., & Jones, K. J. (2002). Functional recovery after facial nerve crush is delayed in severe combined immunodeficient mice. *Brain Behav Immun, 16*(6), 808-812.

Sharma, K., Schmitt, S., Bergner, C. G., Tyanova, S., Kannaiyan, N., Manrique-Hoyos, N., . . . Simons, M. (2015). Cell type- and brain region-resolved mouse brain proteome. *Nat Neurosci, 18*(12), 1819-1831.

Sheean, R. K., Weston, R. H., Perera, N. D., D'Amico, A., Nutt, S. L., & Turner, B. J. (2015). Effect of thymic stimulation of CD4+ T cell expansion on disease onset and progression in mutant SOD1 mice. *J Neuroinflammation, 12*, 40.

Siqueira Mietto, B., Kroner, A., Girolami, E. I., Santos-Nogueira, E., Zhang, J., & David, S. (2015). Role of IL-10 in Resolution of Inflammation and Functional Recovery after Peripheral Nerve Injury. *J Neurosci, 35*(50), 16431-16442.

Smith, G. M., & Hale, J. H. (1997). Macrophage/Microglia regulation of astrocytic tenascin: synergistic action of transforming growth factor-beta and basic fibroblast growth factor. *J Neurosci, 17*(24), 9624-9633.

Sohda, M., Misumi, Y., & Oda, K. (2015). TNFalpha triggers release of extracellular vesicles containing TNFR1 and TRADD, which can modulate TNFalpha responses of the parental cells. *Arch Biochem Biophys, 587*, 31-37.

Spani, C., Suter, T., Derungs, R., Ferretti, M. T., Welt, T., Wirth, F., . . . Kulic, L. (2015). Reduced beta-amyloid pathology in an APP transgenic mouse model of Alzheimer's disease lacking functional B and T cells. *Acta Neuropathol Commun, 3*, 71.

Sta, M., Sylva-Steenland, R. M., Casula, M., de Jong, J. M., Troost, D., Aronica, E., & Baas, F. (2011). Innate and adaptive immunity in amyotrophic lateral sclerosis: evidence of complement activation. *Neurobiol Dis, 42*(3), 211-220.

Staff, N. P., & Appel, S. H. (2016). The immune system continues to knock at the ALS door. *Neuromuscul Disord, 26*(6), 335-336.

Streit, W. J., Hurley, S. D., McGraw, T. S., & Semple-Rowland, S. L. (2000). Comparative evaluation of cytokine profiles and reactive gliosis supports a critical role for interleukin-6 in neuron-glia signaling during regeneration. *J Neurosci Res, 61*(1), 10-20.

Streit, W. J., Semple-Rowland, S. L., Hurley, S. D., Miller, R. C., Popovich, P. G., & Stokes, B. T. (1998). Cytokine mRNA profiles in contused spinal cord and axotomized facial nucleus suggest a beneficial role for inflammation and gliosis. *Exp Neurol, 152*(1), 74-87.

Sun, J., Madan, R., Karp, C. L., & Braciale, T. J. (2009). Effector T cells control lung inflammation during acute influenza virus infection by producing IL-10. *Nat Med, 15*(3), 277-284.

Sunderland, S. (1951). A classification of peripheral nerve injuries producing loss of function. *Brain, 74*(4), 491-516.

Tada, S., Okuno, T., Hitoshi, Y., Yasui, T., Honorat, J. A., Takata, K., . . . Nakatsuji, Y. (2014). Partial suppression of M1 microglia by Janus kinase 2 inhibitor does not protect against neurodegeneration in animal models of amyotrophic lateral sclerosis. *J Neuroinflammation, 11*, 179.

Tam, W. Y., & Ma, C. H. (2014). Bipolar/rod-shaped microglia are proliferating microglia with distinct M1/M2 phenotypes. *Sci Rep, 4*, 7279.

Terrado, J., Monnier, D., Perrelet, D., Vesin, D., Jemelin, S., Buurman, W. A., . . . Garcia, I. (2000). Soluble TNF receptors partially protect injured motoneurons in the postnatal CNS. *Eur J Neurosci, 12*(9), 3443-3447.

Tetzlaff, W., Alexander, S. W., Miller, F. D., & Bisby, M. A. (1991). Response of facial and rubrospinal neurons to axotomy: changes in mRNA expression for cytoskeletal proteins and GAP-43. *J Neurosci, 11*(8), 2528-2544.

Tetzlaff, W., Bisby, M. A., & Kreutzberg, G. W. (1988a). Changes in cytoskeletal proteins in the rat facial nucleus following axotomy. *J Neurosci, 8*(9), 3181-3189.
Tetzlaff, W., Graeber, M. B., Bisby, M. A., & Kreutzberg, G. W. (1988b). Increased glial fibrillary acidic protein synthesis in astrocytes during retrograde reaction of the rat facial nucleus. *Glia, 1*(1), 90-95.
Tian, L., Ma, L., Kaarela, T., & Li, Z. (2012). Neuroimmune crosstalk in the central nervous system and its significance for neurological diseases. *J Neuroinflammation, 9*, 155.
Tong, X., Ao, Y., Faas, G. C., Nwaobi, S. E., Xu, J., Haustein, M. D., . . . Khakh, B. S. (2014). Astrocyte Kir4.1 ion channel deficits contribute to neuronal dysfunction in Huntington's disease model mice. *Nat Neurosci, 17*(5), 694-703.
Torvik, A., & Skjorten, F. (1971). Electron microscopic observations on nerve cell regeneration and degeneration after axon lesions. I. Changes in the nerve cell cytoplasm. *Acta Neuropathol, 17*(3), 248-264.
Tu, H., Juelich, T., Smith, E. M., Tyring, S. K., Rady, P. L., & Hughes, T. K. (2003). Evidence for endogenous interleukin-10 during nociception. *Journal of Neuroimmunology, 139*(1-2), 145-149.
Turner, M. R., Parton, M. J., & Leigh, P. N. (2001). Clinical trials in ALS: an overview. *Semin Neurol, 21*(2), 167-175.
Tyzack, G. E., Sitnikov, S., Barson, D., Adams-Carr, K. L., Lau, N. K., Kwok, J. C., . . . Lakatos, A. (2014). Astrocyte response to motor neuron injury promotes structural synaptic plasticity via STAT3-regulated TSP-1 expression. *Nat Commun, 5*, 4294.
Verderio, C., & Matteoli, M. (2001). ATP Mediates Calcium Signaling Between Astrocytes and Microglial Cells: Modulation by IFN- *The Journal of Immunology, 166*(10), 6383-6391.
Villacampa, N., Almolda, B., Vilella, A., Campbell, I. L., Gonzalez, B., & Castellano, B. (2015). Astrocyte-targeted production of IL-10 induces changes in microglial reactivity and reduces motor neuron death after facial nerve axotomy. *Glia, 63*(7), 1166-1184.
Wada, Y., Nakamachi, T., Endo, K., Seki, T., Ohtaki, H., Tsuchikawa, D., . . . Shioda, S. (2013). PACAP attenuates NMDA-induced retinal damage in association with modulation of the microglia/macrophage status into an acquired deactivation subtype. *J Mol Neurosci, 51*(2), 493-502.
Wainwright, D. A., Mesnard, N. A., Xin, J., Sanders, V. M., & Jones, K. J. (2009a). Effects of facial nerve axotomy on Th2-associated and Th1-associated chemokine mRNA expression in the facial motor nucleus of wild-type and presymptomatic SOD1 mice. *J Neurodegener Regen, 2*(1), 39-44.
Wainwright, D. A., Xin, J., Mesnard, N. A., Beahrs, T. R., Politis, C. M., Sanders, V. M., & Jones, K. J. (2009b). Exacerbation of facial motoneuron loss after facial nerve axotomy in CCR3-deficient mice. *ASN Neuro, 1*(5), e00024.
Wainwright, D. A., Xin, J., Mesnard, N. A., Politis, C. M., Sanders, V. M., & Jones, K. J. (2009c). Effects of facial nerve axotomy on Th2- and Th1-associated chemokine expression in the facial motor nucleus of wild-type and presymptomatic mSOD1 mice. *J Neuroimmunol, 216*(1-2), 66-75.

Wainwright, D. A., Xin, J., Sanders, V. M., & Jones, K. J. (2008). Differential actions of pituitary adenylyl cyclase-activating polypeptide and interferon gamma on Th2- and Th1-associated chemokine expression in cultured murine microglia. *J Neurodegener Regen, 1*(1), 31-34.

Wajant, H. (2002). The Fas signaling pathway: more than a paradigm. *Science, 296*(5573), 1635-1636.

Wajant, H., & Scheurich, P. (2011). TNFR1-induced activation of the classical NF-kappaB pathway. *FEBS J, 278*(6), 862-876.

Wang, L., Rouleau, D. M., & Beaumont, E. (2013). Most effective adjuvant treatments after surgery in peripheral nerve laceration: Systematic review of the literature on rodent models. *Restor Neurol Neurosci, 31*(3), 253-262.

Werdelin, L., Boysen, G., Jensen, T. S., & Mogensen, P. (1990). Immunosuppressive treatment of patients with amyotrophic lateral sclerosis. *Acta Neurol Scand, 82*(2), 132-134.

White, F. A., Sun, J., Waters, S. M., Ma, C., Ren, D., Ripsch, M., . . . Miller, R. J. (2005). Excitatory monocyte chemoattractant protein-1 signaling is up-regulated in sensory neurons after chronic compression of the dorsal root ganglion. *Proc Natl Acad Sci U S A, 102*(39), 14092-14097.

Wijesekera, L. C., & Leigh, P. N. (2009). Amyotrophic lateral sclerosis. *Orphanet J Rare Dis, 4*, 3.

Wolf, S. A., Steiner, B., Akpinarli, A., Kammertoens, T., Nassenstein, C., Braun, A., . . . Kempermann, G. (2009). CD4-positive T lymphocytes provide a neuroimmunological link in the control of adult hippocampal neurogenesis. *J Immunol, 182*(7), 3979-3984.

Xie, R. D., Villacampa, N., Almolda, B., González, B., Castellano, B., & Campbell, I. L. (2014). 202: Interferon regulator factor (IRF) 8 regulates the microglial response to neuronal injury. *Cytokine, 70*(1), 77.

Xin, J., Wainwright, D. A., Mesnard, N. A., Serpe, C. J., Sanders, V. M., & Jones, K. J. (2011). IL-10 within the CNS is necessary for CD4+ T cells to mediate neuroprotection. *Brain Behav Immun, 25*(5), 820-829.

Xin, J., Wainwright, D. A., Serpe, C. J., Sanders, V. M., & Jones, K. J. (2008). Phenotype of CD4+ T cell subsets that develop following mouse facial nerve axotomy. *Brain Behav Immun, 22*(4), 528-537.

Xue, J., Schmidt, S. V., Sander, J., Draffehn, A., Krebs, W., Quester, I., . . . Schultze, J. L. (2014). Transcriptome-based network analysis reveals a spectrum model of human macrophage activation. *Immunity, 40*(2), 274-288.

Yang, J. W., Rodrigo, R., Felipo, V., & Lubec, G. (2005). Proteome analysis of primary neurons and astrocytes from rat cerebellum. *J Proteome Res, 4*(3), 768-788.

Yang, Y., Vidensky, S., Jin, L., Jie, C., Lorenzini, I., Frankl, M., & Rothstein, J. D. (2011). Molecular comparison of GLT1+ and ALDH1L1+ astrocytes in vivo in astroglial reporter mice. *Glia, 59*(2), 200-207.

Yeh, T. Y., Wang, S. M., Tseng, G. F., & Liu, P. H. (2017). Differential regulation of glial reactions in the central facial tract and the facial nucleus after facial neurorrhaphy. *J Chem Neuroanat, 79*, 38-50.

Yoshihara, T., Ishigaki, S., Yamamoto, M., Liang, Y., Niwa, J., Takeuchi, H., . . . Sobue, G. (2002). Differential expression of inflammation- and apoptosis-related genes in

spinal cords of a mutant SOD1 transgenic mouse model of familial amyotrophic lateral sclerosis. *J Neurochem, 80*(1), 158-167.

Yu, L. R., Conrads, T. P., Uo, T., Kinoshita, Y., Morrison, R. S., Lucas, D. A., . . . Veenstra, T. D. (2004). Global analysis of the cortical neuron proteome. *Mol Cell Proteomics, 3*(9), 896-907.

Zamanian, J. L., Xu, L., Foo, L. C., Nouri, N., Zhou, L., Giffard, R. G., & Barres, B. A. (2012). Genomic analysis of reactive astrogliosis. *J Neurosci, 32*(18), 6391-6410.

Zhang, H., Sparks, J. B., Karyala, S. V., Settlage, R., & Luo, X. M. (2015). Host adaptive immunity alters gut microbiota. *ISME J, 9*(3), 770-781.

Zhang, Y., Chen, K., Sloan, S. A., Bennett, M. L., Scholze, A. R., O'Keeffe, S., . . . Wu, J. Q. (2014). An RNA-sequencing transcriptome and splicing database of glia, neurons, and vascular cells of the cerebral cortex. *J Neurosci, 34*(36), 11929-11947.

Zhang, Y. G., Wu, S., Yi, J., Xia, Y., Jin, D., Zhou, J., & Sun, J. (2017). Target Intestinal Microbiota to Alleviate Disease Progression in Amyotrophic Lateral Sclerosis. *Clin Ther*.

Zhou, K., Zhong, Q., Wang, Y. C., Xiong, X. Y., Meng, Z. Y., Zhao, T., . . . Yang, Q. W. (2016). Regulatory T cells ameliorate intracerebral hemorrhage-induced inflammatory injury by modulating microglia/macrophage polarization through the IL-10/GSK3beta/PTEN axis. *J Cereb Blood Flow Metab*.

Zhou, X., Rodriguez, W. I., Casillas, R. A., Ma, V., Tam, J., Hu, Z., . . . Waschek, J. A. (1999). Axotomy-induced changes in pituitary adenylate cyclase activating polypeptide (PACAP) and PACAP receptor gene expression in the adult rat facial motor nucleus. *J Neurosci Res, 57*(6), 953-961.

Zhou, Z., Peng, X., Insolera, R., Fink, D. J., & Mata, M. (2009). IL-10 promotes neuronal survival following spinal cord injury. *Exp Neurol, 220*(1), 183-190.

CURRICULUM VITAE

DEBORAH OLMSTEAD SETTER

EDUCATION

2011-Present	M.D., Indiana University School of Medicine, Indianapolis, IN
2011-2017	Ph.D., Anatomy and Cell Biology, Indiana University, Indianapolis, IN
2007-2011	B.S, Science Pre-Professional and Spanish Supplementary Major, *magna cum laude* University of Notre Dame, South Bend, IN

RESEARCH EXPERIENCE

2013-2017	Ph.D. dissertation research with Kathryn J. Jones, Ph.D. Indiana University School of Medicine, Indianapolis, IN Dissertation: Immunoregulation of the central response to peripheral nerve injury: motoneuron survival and relevance to ALS
2009-2011	Research Assistant, Robert V. Stahelin, Ph.D., University of Notre Dame, Notre Dame, IN.
Summer 2010	Undergraduate Research Experience for Prospective Physician-Scientists, Mervin Yoder, M.D., Indiana University School of Medicine, Indianapolis, IN
2008-2009	Research Assistant, A. Graham Lappin, Ph.D., University of Notre Dame, Notre Dame, IN

PUBLICATIONS

Manuscripts

1. **Olmstead DN**, NA Mesnard-Hoaglin, RJ Batka, MM Haulcomb, WM Miller, KJ Jones. Facial nerve axotomy in mice: a model to study motoneuron response to injury. Journal of Visualized Experiments, 2015.
2. **Olmstead, DN**, X Hua, P Osvath and AG Lappin. Stereoselectivity in electron-transfer reactions in chiral media. Dalton Trans., 2010, 39, 1375 – 1378.

Abstracts

1. **Setter DO,** EM Runge, NA Mesnard-Hoaglin, MM Haulcomb, RJ Batka, ND Schartz, VM Sanders, KJ Jones. Gene expression profile analysis of immunodeficient mice after WT or mSOD1 immunoreconsitution reveals differential motoneuron death mechanisms after facial nerve axotomy. Experimental Biology, Chicago, IL. (2017)
2. **Setter DO,** EM Runge, NA Mesnard-Hoaglin, MM Haulcomb, RJ Batka, ND Schartz, VM Sanders, KJ Jones. Analysis and comparison of WT and mSOD1G93A immune-mediated neuroprotection mechanisms in immunodeficient mice after facial nerve axotomy. Society for Neuroscience Annual Meeting, San Diego, CA. (2016)
3. **Setter DO,** EM Runge, NA Mesnard-Hoaglin, MM Haulcomb, RJ Batka, ND Schartz, VM Sanders, KJ Jones. Characterizing the roles of CD4+ T cells and interleukin-10 in immune-mediated neuroprotection after facial nerve axotomy. Federation of American Societies for Experimental Biology Summer

Conference on Translational Neuroimmunology: From Mechanisms to Therapeutics, Big Sky, MT. (2016)

4. **Olmstead DN,** NA Mesnard-Hoaglin, MM Haulcomb, RJ Batka, ND Schartz, VM Sanders, KJ Jones. Investigation of the neuroprotective actions of CD4+ T cells and interleukin-10 after facial nerve axotomy. Society for Neuroscience Annual Meeting, Chicago, IL. (2015)
5. **Olmstead DN,** VM Sanders, KJ Jones. Investigation of the role of CD4+ T cells and interleukin-10 in immune-mediated neuroprotection. American Physician Scientists Association Annual Meeting, Chicago, IL. (2015)
6. **Olmstead DN,** VM Sanders, KJ Jones. Investigation of the role of CD4+ T cells and interleukin-10 in immune-mediated neuroprotection. Experimental Biology, Boston, MA. (2015)
7. **Olmstead DN,** NA Mesnard-Hoaglin, MM Haulcomb, RJ Batka, ND Schartz, VM Sanders, KJ Jones. Dysregulated gene expression in the axotomized facial motor nucleus of RAG-2 KO mice: relevance to ALS. Society for Neuroscience Annual Meeting, Washington, DC. (2014)
8. **Olmstead DN,** MM Haulcomb, NA Mesnard-Hoaglin, RJ Batka, ND Schartz, VM Sanders, KJ Jones. Comparative analysis of gene expression response to facial nerve axotomy in mouse models of immunodeficiency and ALS. Indianapolis Chapter of the Society for Neuroscience Annual Meeting, Indianapolis, IN. (2014)
9. **Olmstead DN,** MM Haulcomb, NA Mesnard-Hoaglin, RJ Batka, ND Schartz, VM Sanders, KJ Jones. Comparative analysis of gene expression response to

facial nerve axotomy in mouse models of immunodeficiency and ALS. Indiana Clinical Translational Sciences Institute Annual Meeting, Indianapolis, IN. (2014)

10. **Olmstead DN,** MM Haulcomb, NA Mesnard-Hoaglin, RJ Batka, ND Schartz, VM Sanders, KJ Jones. Comparative analysis of gene expression response to facial nerve axotomy in mouse models of immunodeficiency and ALS. Midwest Motoneuron Consortium, Indianapolis, IN. (2014)
11. **Olmstead DN,** MM Haulcomb, NA Mesnard-Hoaglin, RJ Batka, ND Schartz, VM Sanders, KJ Jones. Comparative analysis of gene expression response to facial nerve axotomy in mouse models of immunodeficiency and ALS. National MD/PhD Student Conference, Keystone, CO. (2014)
12. **Olmstead DN,** MM Haulcomb, NA Mesnard-Hoaglin, RJ Batka, ND Schartz, VM Sanders, KJ Jones. Comparative analysis of gene expression response to facial nerve axotomy in mouse models of immunodeficiency and ALS. Federation of American Societies for Experimental Biology Summer Conference on Translational Neuroimmunology: From Mechanisms to Therapeutics, Big Sky, MT. (2014)
13. **Olmstead DN**, K Ward, CG Sudhahar, T Kutateladze, RV Stahelin. Elucidation of cPLA2α and C1P Binding Site. ASBMB Annual Meeting. Experimental Biology Conference, Washington D.C. (2011)
14. **Olmstead, DN**, P Osvath, AG Lappin. Mechanistic Investigation of the Reaction Between [IrCl6]2- and [Co(edta)]2-. University of Michigan Undergraduate Summer Research Symposium, Ann Arbor, MI. (2008)

ORAL PRESENTATIONS

1. **Setter DO**, KJ Jones. Characterizing the roles of CD4+ T cells and interleukin-10 in immune-mediated neuroprotection after facial nerve axotomy. Federation of American Societies for Experimental Biology Summer Conference on Translational Neuroimmunology: From Mechanisms to Therapeutics, Big Sky, MT. (2016)
2. **Olmstead DN**, KJ Jones. Immune-mediated neuroprotection: the role of CD4+ T cells and interleukin-10; relevance to amyotrophic lateral sclerosis. Regenerative Medicine seminar, IUSM, Indianapolis, IN. (2014)
3. **Olmstead DN**, KJ Jones. Using the facial nerve axotomy to study immune-mediated neuroprotection. Federation of American Societies for Experimental Biology Summer Conference on Translational Neuroimmunology: From Mechanisms to Therapeutics, Big Sky, MT. (2014)
4. **Olmstead DN**, RV Stahelin. Elucidation of $cPLA_2\alpha$ and C1P Binding Site. Notre Dame Undergraduate Research Symposium. University of Notre Dame, Notre Dame, IN. (2009)

POSTER PRESENTATIONS

1. **Setter DO,** EM Runge, NA Mesnard-Hoaglin, MM Haulcomb, RJ Batka, ND Schartz, VM Sanders, KJ Jones. Gene expression profile analysis of immunodeficient mice after WT or mSOD1 immunoreconsitution reveals differential motoneuron death mechanisms after facial nerve axotomy. Experimental Biology, Chicago, IL. (2017)

2. **Setter DO,** EM Runge, NA Mesnard-Hoaglin, MM Haulcomb, RJ Batka, ND Schartz, VM Sanders, KJ Jones. Analysis and comparison of WT and mSOD1G93A immune-mediated neuroprotection mechanisms in immunodeficient mice after facial nerve axotomy. Society for Neuroscience Annual Meeting, San Diego, CA. (2016)
3. **Setter DO,** EM Runge, NA Mesnard-Hoaglin, MM Haulcomb, RJ Batka, ND Schartz, VM Sanders, KJ Jones. Characterizing the roles of CD4+ T cells and interleukin-10 in immune-mediated neuroprotection after facial nerve axotomy. Federation of American Societies for Experimental Biology Summer Conference on Translational Neuroimmunology: From Mechanisms to Therapeutics, Big Sky, MT. (2016)
4. **Olmstead DN,** NA Mesnard-Hoaglin, MM Haulcomb, RJ Batka, ND Schartz, VM Sanders, KJ Jones. Investigation of the neuroprotective actions of CD4+ T cells and interleukin-10 after facial nerve axotomy. Society for Neuroscience Annual Meeting, Chicago, IL. (2015)
5. **Olmstead DN,** VM Sanders, KJ Jones. Investigation of the role of CD4+ T cells and interleukin-10 in immune-mediated neuroprotection. American Physician Scientists Association Annual Meeting, Chicago, IL. (2015)
6. **Olmstead DN,** VM Sanders, KJ Jones. Investigation of the role of CD4+ T cells and interleukin-10 in immune-mediated neuroprotection. Experimental Biology, Boston, MA. (2015)
7. **Olmstead DN,** NA Mesnard-Hoaglin, MM Haulcomb, RJ Batka, ND Schartz, VM Sanders, KJ Jones. Dysregulated gene expression in the axotomized facial

motor nucleus of RAG-2 KO mice: relevance to ALS. Society for Neuroscience Annual Meeting, Washington, DC. (2014)

8. **Olmstead DN,** MM Haulcomb, NA Mesnard-Hoaglin, RJ Batka, ND Schartz, VM Sanders, KJ Jones. Comparative analysis of gene expression response to facial nerve axotomy in mouse models of immunodeficiency and ALS. Indianapolis Chapter of the Society for Neuroscience Annual Meeting, Indianapolis, IN. (2014)
9. **Olmstead DN,** MM Haulcomb, NA Mesnard-Hoaglin, RJ Batka, ND Schartz, VM Sanders, KJ Jones. Comparative analysis of gene expression response to facial nerve axotomy in mouse models of immunodeficiency and ALS. Indiana Clinical Translational Sciences Institute Annual Meeting, Indianapolis, IN. (2014)
10. **Olmstead DN,** MM Haulcomb, NA Mesnard-Hoaglin, RJ Batka, ND Schartz, VM Sanders, KJ Jones. Comparative analysis of gene expression response to facial nerve axotomy in mouse models of immunodeficiency and ALS. Midwest Motoneuron Consortium, Indianapolis, IN. (2014)
11. **Olmstead DN,** MM Haulcomb, NA Mesnard-Hoaglin, RJ Batka, ND Schartz, VM Sanders, KJ Jones. Comparative analysis of gene expression response to facial nerve axotomy in mouse models of immunodeficiency and ALS. National MD/PhD Student Conference, Keystone, CO. (2014)
12. **Olmstead DN,** MM Haulcomb, NA Mesnard-Hoaglin, RJ Batka, ND Schartz, VM Sanders, KJ Jones. Comparative analysis of gene expression response to facial nerve axotomy in mouse models of immunodeficiency and ALS.

Federation of American Societies for Experimental Biology Summer Conference on Translational Neuroimmunology: From Mechanisms to Therapeutics, Big Sky, MT. (2014)

13. **Olmstead DN**, K Ward, CG Sudhahar, T Kutateladze, RV Stahelin. Elucidation of cPLA2α and C1P Binding Site. American Society of Biochemists and Molecular Biologists Annual Meeting. Experimental Biology Conference, Washington D.C. (2011)
14. **Olmstead DN**, P Osvath, AG Lappin. Mechanistic Investigation of the Reaction Between [IrCl6]2- and [Co(edta)]2-. Fall Undergraduate Research Symposium. University of Notre Dame, Notre Dame, IN. (2008)
15. **Olmstead DN**, P Osvath, AG Lappin. Mechanistic Investigation of the Reaction Between [IrCl6]2- and [Co(edta)]2-. University of Michigan Undergraduate Summer Research Symposium. University of Michigan, Ann Arbor, MI. (2008)

AWARDS & HONORS

2017	American Association of Anatomists Travel Award
2016	Graduate & Professional Educational Grant
2015	Christopher Hrvoj Travel Award
2015	American Physician Scientists Association Travel Award
2015	American Association of Anatomists Travel Award
2014	Educational Enhancement Grant
2014	Indiana University School of Medicine Travel Grant

2011	American Society of Biochemists and Molecular Biologists Honors Society
2011	Emil T. Hofman Scholarship Award, University of Notre Dame
2011	ASBMB Undergraduate Affiliate Network/Regional Meeting Travel Award
2011	University of Notre Dame College of Science Undergraduate Research Travel Award
2011	University of Notre Dame Center for Undergraduate Scholarly Engagement Travel Award
2007	Notre Dame Club of Indianapolis Scholarship

TEACHING EXPERIENCE

2013-2016	Teaching Assistant, Neuroscience and Clinical Neurology, Indiana University School of Medicine, Indianapolis, IN
2009-2011	Tutor, General Chemistry, Organic Chemistry, Vertebrate Physiology, University of Notre Dame, Notre Dame, IN

COMMUNITY SERVICE

2011-Present	Clinical Examiner and Spanish Language Interpreter, Indiana University School of Medicine Student Outreach Clinic

LEADERSHIP EXPERIENCE

2014-2017	Member, Board of Directors, Notre Dame Club of Indianapolis
2011-Present	Representative, Combined-Degree Student Council, Indiana University School of Medicine

2013-2015 President, Combined-Degree Student Council, Indiana University School of Medicine

2011-2016 President, Young Alumni, Notre Dame Club of Indianapolis

PROFESSIONAL MEMBERSHIPS

2014-Present American Associations of Anatomists

2013-Present Society for Neuroscience (SfN)

2011-Present American Medical Women's Association (AMWA)

2011-Present American Medical Association (AMA)

2013-2016 American Physician Scientists Association (APSA)

2009-2011 American Society for Biochemistry and Molecular Biology (ASBMB)